



International Conference on Nanotechnology and Smart  
Materials, Design Artificial Intelligence,  
Manufacturing and Engineering  
(ICNSMDAIME-21)

Vadodara, India

25<sup>th</sup> April, 2021

Institute for Scientific and Engineering Research

[www.iser.org.in](http://www.iser.org.in)

Publisher: ISER Explore

© Copyright 2021, ISER-International Conference, Vadodara, India

No part of this book can be reproduced in any form or by any means without prior written

Permission of the publisher.

This edition can be exported from Indian only by publisher

ISER-Explore

**Editorial:**

We cordially invite you to attend the International Conference on Nanotechnology and Smart Materials, Design Artificial Intelligence, Manufacturing and Engineering (ICNSMDAIME-21), which will be held in Vadodara, India on April 25<sup>th</sup>, 2021. The main objective of ICNSMDAIME-21 is to provide a platform for researchers, students, academicians as well as industrial professionals from all over the world to present their research results and development activities in Nanotechnology and Smart Materials, Design Artificial Intelligence, Manufacturing and Engineering. This conference provides opportunities for the delegates to exchange new ideas and experience face to face, to establish business or research relations and to find global partners for future collaboration.

These proceedings collect the up-to-date, comprehensive and worldwide state-of-art knowledge on Nanotechnology and Smart Materials, Design Artificial Intelligence, Manufacturing and Engineering. All accepted papers were subjected to strict peer-reviewing by 2-4 expert referees. The papers have been selected for these proceedings because of their quality and the relevance to the conference. We hope these proceedings will not only provide the readers a broad overview of the latest research results on Nanotechnology and Smart Materials, Design Artificial Intelligence, Manufacturing and Engineering but also provide the readers a valuable summary and reference in these fields.

The conference is supported by many universities and research institutes. Many professors played an important role in the successful holding of the conference, so we would like to take this opportunity to express our sincere gratitude and highest respects to them. They have worked very hard in reviewing papers and making valuable suggestions for the authors to improve their work. We also would like to express our gratitude to the external reviewers, for providing extra help in the review process, and to the authors for contributing their research result to the conference.

Since February 2021, the Organizing Committees have received more than 40 manuscript papers, and the papers cover all the aspects in Nanotechnology and Smart Materials, Design Artificial Intelligence, Manufacturing and Engineering. Finally, after review, about 10 papers were included to the proceedings of ICNSMDAIME-2021.

We would like to extend our appreciation to all participants in the conference for their great contribution to the success of International Conference 2021. We would like to thank the keynote and individual speakers and all participating authors for their hard work and time. We also sincerely appreciate the work by the technical program committee and all reviewers, whose contributions make this conference possible. We would like to extend our thanks to all the referees for their constructive comments on all papers; especially, we would like to thank to organizing committee for their hard work.

## **Acknowledgement**

ISER is hosting the International Conference on Nanotechnology and Smart Materials, Design Artificial Intelligence, Manufacturing and Engineering this year in month of April. International Conference on Nanotechnology and Smart Materials, Design Artificial Intelligence, Manufacturing and Engineering will provide a forum for students, professional engineers, academician, and scientist engaged in research and development to convene and present their latest scholarly work and application in the industry. The primary goal of the conference is to promote research and developmental activities in Nanotechnology and Smart Materials, Design Artificial Intelligence, Manufacturing and Engineering and to promote scientific information interchange between researchers, developers, engineers, students, and practitioners working in and around the world. The aim of the Conference is to provide a platform to the researchers and practitioners from both academia as well as industry to meet the share cutting-edge development in the field.

I express my hearty gratitude to all my Colleagues, Staffs, Professors, Reviewers and Members of organizing committee for their hearty and dedicated support to make this conference successful. I am also thankful to all our delegates for their pain staking effort to travel such a long distance to attain this conference.



**Dr. Chi-Yuang San**  
**Director**  
**Institute for Scientific and Engineering Research (ISER)**

# CONTENTS

<b>S.NO</b>	<b>TITLES AND AUTHORS</b>	<b>PAGE NO</b>
1.	Experimental investigation on Combustion, Performance and Emission characteristics Of a Plastic oil and B20 Pongamia Biodiesel as a substitute fuel in Diesel Engine ➤ <i>D. K. Ramesha</i> ➤ <i>G Prema Kumara</i> ➤ <i>Abhishek Jain C N</i> ➤ <i>Akash B</i> ➤ <i>Babu Reddy R,</i> ➤ <i>Kalappa M. Kammar</i>	1-5
2.	Performance Study of Stainless Steel Fin with and Without Cnt Coating ➤ <i>Mr. Shankara Murthy H M</i> ➤ <i>Mr. Krishna Kumar M</i> ➤ <i>Mr. Pranav K.V</i> ➤ <i>Mr. Roni T.Raju</i> ➤ <i>Mr. Sachin Vinod</i>	6-10
3.	Influence of Thermal Radiation on Mhd Boundary Layer Flow In A Newtonian Liquid With Temperature Dependent Properties Over An Exponential Stretching Sheet ➤ <i>A. S. Chethan</i> ➤ <i>G. N. Sekhar</i> ➤ <i>Annamma Abraham</i>	11-18
4.	Production and Characterization of Rice Husk Ash-Silicon Carbide ReinforcedAl1100 Aluminium Alloy Hybrid Composites ➤ <i>Ghanaraja S</i> ➤ <i>Gireesha B L</i> ➤ <i>Ravikumar K S</i> ➤ <i>Madhusudan B M</i>	19-23
5.	A Numerical Study on Flow Characteristics around Two Square Cylinders in Tandem Arrangement near A Moving Plane Wall ➤ <i>Rajendra S. Rajpoot</i> ➤ <i>S. Dhinakaran</i>	24-30
6.	An Experimental Study on Suppression of Vortex Shedding with Different Structural Configurations ➤ <i>Sanal M V</i> ➤ <i>Prof. Sunil A S</i>	31-35
7.	Monitoring of Elderly/Blind Patients Health Remotely Through Wearable Sensors ➤ <i>Nasreen Taj M.B</i> ➤ <i>Firoz Khan</i> ➤ <i>Imran Khan</i> ➤ <i>Sandeep Telkar R</i>	36-40

# CONTENTS

S.NO	TITLES AND AUTHORS	PAGE NO
8.	Detection and Identification of Head and Neck Cancer Using Hybrid Image Processing Technique ➤ <i>Imran Khan</i> ➤ <i>Firoz Khan</i> ➤ <i>Nasreen Taj M.B</i> ➤ <i>Sandeep Telkar R</i>	41-48
9.	A Survey on the Role of Emotions in Engineering, Medical and Psychology Domains ➤ <i>Imran Khan</i> ➤ <i>Dr.Mouneshachari S</i>	49-59
10.	Comparison of CNN and Contour Algorithm for Number Identification Using Hand Gesture Recognition ➤ <i>Adarsh Pathak</i> ➤ <i>Faraz Ahmed Khan</i>	60-64

# Experimental investigation on Combustion, Performance and Emission characteristics of a Plastic oil and B20 Pongamia Biodiesel as a substitute fuel in Diesel Engine

[<sup>1</sup>]D. K. Ramesha, [<sup>2</sup>]G Prema Kumara, [<sup>3</sup>]Abhishek Jain C N, [<sup>4</sup>]Akash B, [<sup>5</sup>]Babu Reddy R,  
[<sup>6</sup>]Kalappa M. Kammar

[<sup>1</sup>][<sup>3</sup>][<sup>4</sup>][<sup>5</sup>][<sup>6</sup>] University Visvesvaraya College of Engineering, Bangalore University, K. R. Circle, Bangalore, India  
[<sup>2</sup>]University of Victoria, EOW Building, Victoria, Canada

**Abstract:** --The thirst for fuel is steadily increasing as technology continues to open new areas of exploration. At the same time, the indiscriminate extraction of fossil fuels also may result in depletion of petroleum deposits. Diesel being the main transport fuel in India, finding suitable alternative to diesel in an urgent need. In this context, waste plastic solid is currently receiving renewed interest. Waste plastic oil is suitable for Compression Ignition engines and more attention is focused in India because of its potential to generate large-scale employment and relatively lower scale degradation. The present investigation was to study the effect of plastic oil blend with B20 Pongamia biodiesel on four strokes, single cylinder Direct Injection diesel engine. Experimental results show that performance characteristics were found to be comparable with diesel. The emission characteristics show that NOx emission levels are higher and other emissions like CO, HC are compatible with diesel modes of operation. Hence plastic oil can be used as substitute fuel in place of conventional diesel fuels  
**Keywords:** Diesel engine; poultry litter oil methyl ester; biodiesel; alumina nanoparticles; transesterification; ethanol; performance; combustion; emission.

**Keywords:** Plastic oil; Pongamia biodiesel; Performance; Emission; Combustion characteristics;

## I. INTRODUCTION

The Conventional mineral fuels such as petrol and diesel are fast depleting; the fuel reserve available now may not be sufficient to meet the demand or need of the near future. Besides the search of fuel for the future, pollution has increased to alarming levels due to overcrowding population of vehicles on roads. Diesel being the main transport fuel in India has imported about 202.1 million tons of crude oil (24% of its requirement) and petroleum products during the year 2015-2016 causing heavy burden on foreign exchange out go. To decrease the foreign exchange and contribute towards protection of earth from the threat of environmental degradation, bio fuels can be good alternative for diesel for most of the developing countries. The abundance of vegetable oils and ease of handling enables us to supplement existing conventional fuel to a great extent, if not as substitutes but as blended fossil fuels. Vegetable oils can be classified into two types one is edible oil and other being non-edible oil [2]. Since edible oils are in great demand for domestic consumption, the non-edible oil like Honge oil used as a substitute fuel due to following reasons. Biodiesels can be used in existing engine without any modification. The use of bio diesel in

conventional diesel engine results in substantial reduction of unburnt hydrocarbon, carbon monoxide and particulate matter [but NOx about 2% higher]. Biodiesel has almost no sulphur (0.05%), no aromatics and has about 10 % built in oxygen which helps in better combustion [1]. High viscosity, high flash and fire point and low volatility are main disadvantages of vegetable oils as alternative fuels in IC Engines. Transesterification process are carried out to remove impurities, reduce viscosity and to match most of properties closely with petroleum diesel properties [2].

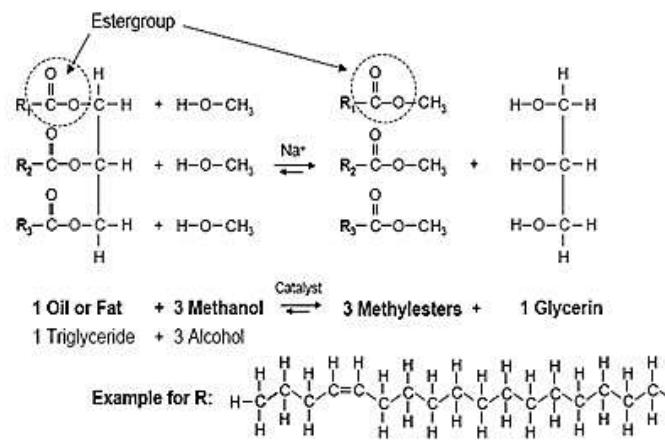
Waste plastics are indispensable materials in the modern world and application in the industrial field is continually increasing. More attention is focused in India because of its potential to large scale employment and relatively low environmental degradation [3]. The countries have to simultaneously address the issues of energy insecurity, increasing oil prices and large scale employment. The waste plastic oil is obtained from the process called Pyrolysis. Pyrolysis is the thermal decomposition of organic material at elevated temperatures, in the absence of gases such as air or oxygen. It is in this context a diesel was fuelled with waste plastic oil in present work. But it was found to be giving more NOx emissions [4]. The waste plastic oil is compared with petroleum products and found that it can also

be used as fuel in CI engine. Plastic oil is non-biodegradable and renewable oil [3]. A pilot level method of recycling waste plastic disposal in India produces Waste plastic oil of 25000 L/ day and one hectare of Honge plantation could yield 10 tons of seeds which can be used to convert to honge Oil.

## Nomenclature

BP	Brake Power
BTDC	Before Top Dead Centre
BTE	Brake Thermal Efficiency
HRR	Heat release rate
B20	20% biodiesel & 80% Diesel
CI	Compression Ignition
CO	Carbon monoxide
HOME	Honge Oil Methyl Ester
EGT	Exhaust Gas Temperature at Engine
IC	Internal combustion
NOx	Oxides of Nitrogen
ppm	Parts per million
UBHC	Unburnt hydrocarbons
WPO	Waste plastic oil

### 1.1 Transesterification



Transesterification, the chemical process of making biodiesel, refers to a reaction between an ester of one alcohol and a second alcohol to form an ester of the second alcohol and an alcohol from the original ester, as that of methyl acetate and ethyl alcohol to form ethyl acetate and methyl alcohol. Chemically, Transesterification means taking a triglyceride molecule or a complex fatty acid, neutralizing the free fatty acids, removing the glycerin and creating an alcohol ester. This is accomplished by mixing methanol with sodium hydroxide to make sodium

methoxide. This liquid is then mixed into vegetable oil. The entire mixture then settles. Glycerin is left on the bottom and methyl esters, or biodiesel, is left on top. The glycerin can be used to make soap and the methyl esters is washed and filtered. Transesterification of Honge oil is normally done with ethanol and sodium ethanolate serving as the catalyst.

Sodium ethanolate can be produced by reacting ethanol with sodium. Thus, with sodium ethanolate as the catalyst, ethanol is reacted with the algal oil (the triglyceride) to produce bio-diesel & glycerol. The end products of this reaction are hence biodiesel, sodium ethanolate and glycerol. The Honge oil after this trans-esterification process is usually referred to as Honge oil methyl ester. Figure 1 shows the chemical reaction of Transesterification of honge oil. The properties of honge biodiesel and are tabulated in Table 1

## II. EXPERIMENTAL SETUP

The experiments were conducted on a computerized diesel engine test rig shown in Figure 2. Kirloskar made single cylinder, 4-stroke, naturally aspirated direct injection, water cooled diesel engine of 10 HP rated power at 1500 rpm was directly coupled to an eddy current dynamometer (Table 2). The engine and the dynamometer were interfaced to a control panel which is connected to a digital computer. The computerized test rig was used for recording the test parameters.

The computerized test rig was used for recording the test parameters such as fuel flow rate, temperature, air flow rate, load etc. and for calculating the engine performance characteristics such as brake power, brake thermal efficiency, brake specific fuel consumption, volumetric efficiency etc. The calorific value and the density of the particular fuel were fed to the engine software for calculating the performance parameters. Similarly, combustion characteristics such as heat release rate, peak pressure, etc. were also calculated. Exhaust emissions such as NO<sub>x</sub>, UBHC, CO, and EGT were measured with a MRU make exhaust gas analyzer and smoke opacity using an AVL smoke meter.

The whole set of experiments were conducted at a compression ratio of 17.5:1 and injection timing of 27° BTDC. The tests were conducted at 20%, 40%, 60%, 80% and 100% of maximum load condition with Diesel, B20HOME, B20HOME +10WPO. This was done in order to obtain optimum results without over stressing the engine. The data recording was done after the experiment was carried out for three times to obtain a repeatability of values for each blend [5].

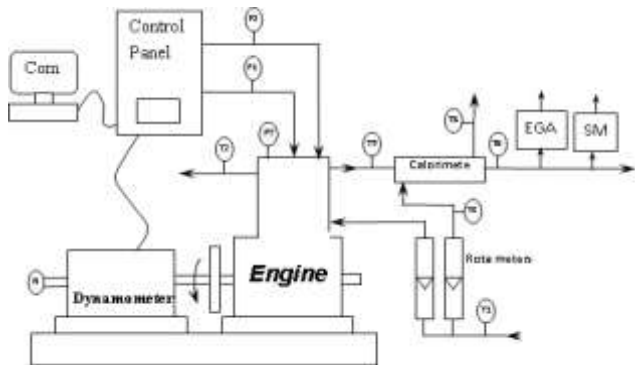


**Figure 2: Schematic Representation of the Experimental Setup.**

1. Water inlet to the calorimeter and engine ( $T_1^0\text{C}$ )
2. Water outlet from the engine jacket ( $T_2^0\text{C}$ )
3. Water outlet from the calorimeter ( $T_3^0\text{C}$ )
4. Exhaust gas inlet to the calorimeter ( $T_4^0\text{C}$ )
5. Exhaust gas outlet from the calorimeter ( $T_5^0\text{C}$ )
6. Atmospheric air temperature ( $T_6^0\text{C}$ )
7. Fuel flow
8. Pressure Transducer, EGA. Exhaust gas analyzer, SM. Smoke Meter.

**Table 1: Properties of Diesel, HOME and WPO**

Properties	Diesel	Pongamia Oil	HOME	WPO
Color	Orange	Yellowish Brown	Brown	Pale Black
Density ( $\text{kg/m}^3$ ) at	828	915	873	835
Specific Gravity at $40^\circ\text{C}$	0.828	0.909	0.873	0.835
Kinematic Viscosity (centi-strokes) at $40^\circ\text{C}$	3.78	42.78	5.46	2.52
Calorific Value (kJ/kg)	44030	37304	40210	44340
Iodine Value (gm I <sub>2</sub> /kg)	38.3	82.78	90	--
Saponification Value	Nil	179.55	90	--
Cetane number	55	42	--	51
Flash Point ( $^\circ\text{C}$ )	47	220	171	42
Fire Point ( $^\circ\text{C}$ )	63	243	184	45

**Table 2: Specification of Engine**

Make	Kirloskar
Speed	1500RPM
Compression Ratio	17.5:1
Cylinder Bore	87.5mm
Stroke	110mm
Connecting Rod Length	234mm
Cooling	Water Cooling
Orifice Diameter	20mm
Rated Power	3.5kW
Maximum Load	12KN
Injection Pressure	180 bar
No. of Cylinders	1

### III. RESULTS AND DISCUSSION

#### 3.1. Performance Analysis:

##### Brake Thermal Efficiency (BTE)

The variation of BTE with Load for different fuel blends and diesel is shown in Figure 3. Thermal Efficiency indicates how efficiently energy in the fuel is converted into mechanical output. As percentage of load increased, BTE of all fuels used increase due to increase in mechanical efficiency [11]. The mean BTE of B20 HOME is 21.4% and for Plastic blend is 21.41% which are nearest to that of 23.2% of Diesel. Hence the performance of Engine with Pongamia Biodiesel and Plastic oil blend is comparable to that of Diesel in terms of BTE.

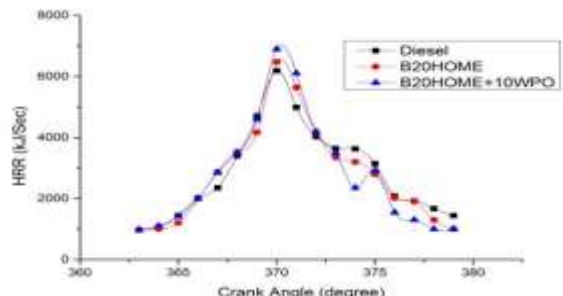


**Figure 3: Variation of BTE with**

#### 1.1. 3.2. Combustion Analysis

##### 1.2. Heat release Rate (HRR)

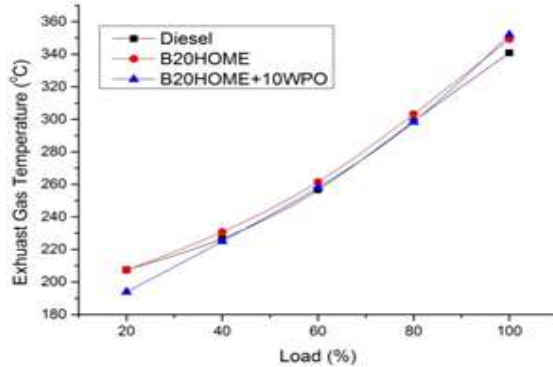
The comparison of heat release rate for B20 HOME-WPO blend, B20 HOME and Diesel fuel operation at full load is shown in Figure 4. Heat release diagram is a quantitative description of timely burning of fuel in engine. Because of vaporization of the fuel during ignition delay, a negative heat release rate is observed at the beginning and after the combustion is initiated, it becomes positive [14].

In general, during ignition delay, the fuel droplets spread over a wide area around fresh air to form the fuel-air mixture. Once the ignition delay is over, the premixed fuel-air mixture burns, releasing heat at a very rapid rate. The maximum value of HRR is shown by B20 HOME-WPO at 6900 kJ/sec whereas B20 HOME and Diesel showed 6480 kJ/sec and 6190 kJ/sec respectively. It is observed that B20 HOME-WPO showed greater HRR than Diesel by 11%.

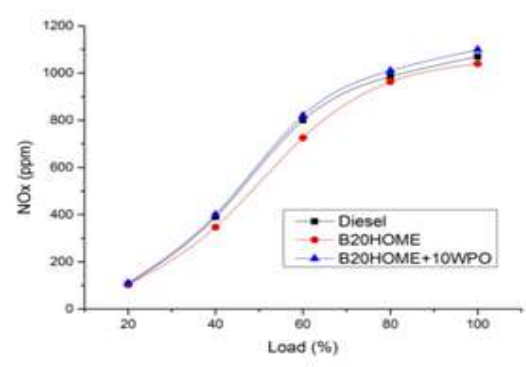
##### Peak Cylinder Pressure

Figure 5 shows the variation of peak pressure of different blends with load. The peak pressure increases steadily with

load, it is seen from the figure that the peak pressure of all blends is higher as compared to that of Diesel at all loads. At full load the B20HOME-10WPO showed more peak pressure than Diesel by 5%. The reason for this could be



**Figure 7: Variation of EGT with Load**



**Figure 8: Variation of NO<sub>x</sub> with Load**

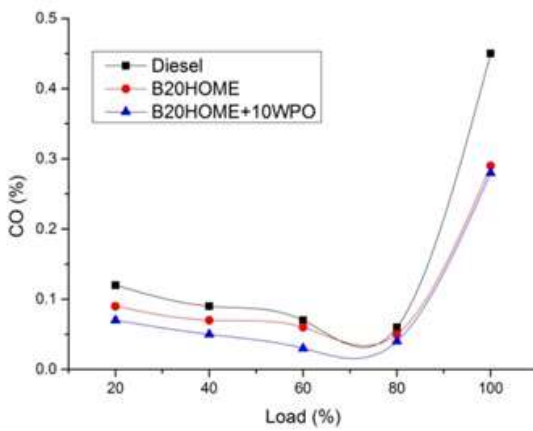


**Figure 9: Variation of CO with Load**

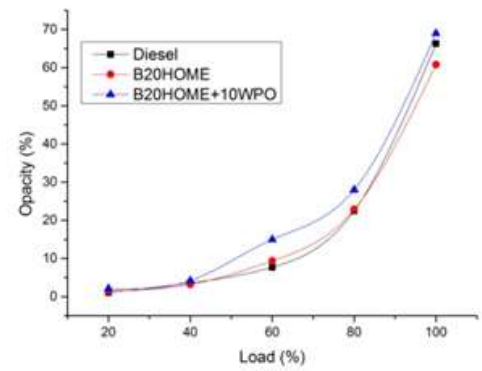


**Figure 10: Variation of Opacity**

#### **Smoke Opacity**

Smoke emission is nothing but solid soot particles suspended in exhaust gas. The Figure10 shows the variation of smoke with load for all fuels tested. It is observed from Figure that the smoke opacity of exhaust gas increases in the load for all blends. The smoke emission for blended fuels are high compared to that of the diesel. This is due to poor volatility, higher viscosity of blends. The molecule of blends being heavier also attributes to increase in smoke emission [8]

#### **IV. CONCLUSION**

The engine tests were conducted with Plastic oil and Pongamia oil blends for no load to full condition and the corresponding performance and combustion characteristics were studied in comparison with Diesel fuel. All the tests were conducted under the same conditions and repeated for three to four times to obtain consistent values. Pongamia oil blended with Waste plastic oil is determined for suitable replacement of conventional diesel. B20HOME-10WPO blend exhibits a higher cylinder peak pressure compare to diesel because of evaporation of WPO inside the cylinder by absorbing heat from combustion chamber. The heat release

rate with B20HOME-10WPO blend is higher compared to Diesel fuel due to better combustion. With the addition of WPO, NOx increases due to higher heat release and combustion temperature. Engine with B20HOME-10WPO blend results in better performance and can be used as replacement for diesel.

## REFERENCES

- [1]. M. Mani, G. Nagarajan, S. Sampath. An experimental investigation on a DI diesel engine using waste plastic oil with exhaust gas recirculation. *Fuel* 89 (2010) 1826-1832.
- [2]. M. Mani, G. Nagarajan, S. Sampath. Characteristic and effect of using waste plastic oil and diesel fuel blends in compression ignition engine. *Energy* 36 (2013) 212-219.
- [3]. M. Mani, G. Nagarajan. Influence of injection timing on performance, emission and combustion characteristic of a DI diesel engine running on waste plastic oil. *Energy* 34 (2009) 1617-1623.
- [4]. PrajwalTewari, EshankDoijode, N.R. Banapurmath, V.S. Yaliwal. Experimental investigation on a diesel fuelled with multiwall carbon nanotubes blended biodiesel fuels. *ICESTD* 2013, Feb 2013, ISSN 2250-2459
- [5]. S.H. Park, S.H. Yoon, C.S. Lee, Effect of the temperature variation on properties of biodiesel and Biodiesel–ethanol blends fuels, *Oil & Gas Science and Technology* 63 (6) (2008) 737–745
- [6]. D K Ramesh, Rajiv K T, Rajiv Simhasan, Manjunath N and Prithvish M Gowda A Study on Performance Combustion and Emission Evaluation of Corn oil as Substitute fuel in a CI Engine, *Journal of The Institutions of Engineers India Ser. C DOI* 10.1007/s40032-012-0030-4.
- [7]. Vedaraman N, Puhan S, Nagarajan G, Velappan KC. Preparation of palm oil biodiesel and effect of various additives on NOx emission reduction in B20 : an experimental study. *Int J Green Energy* 2011; 8:383-97.
- [8]. Balusamy T, Marappan R. Performance evaluation of a direct injection diesel engine with blends of *Thevetiaperuviana* seed oil and diesel. *J SciInd Res* 2007; 66:1035-40.
- [9]. Behcet R. Performance and emission study of waste anchovy fish Biodiesel in a diesel engine. *Fuel Process Technol* 2011; 92:1187-94.
- [10]. Lin CY, Lin HA. Engine performance an emission characteristics of a three phase emulsion of biodiesel produce by peroxidation. *Fuel Process Technol* 2007; 88:35-41.
- [11]. Godiganur S, Murthy CS, Reddy RP. Performance and emission characteristics of Kirloskar HA394 diesel engine operated on fish oil methyl esters. *Renew energy* 2010; 35:355-9.
- [12]. Lin CY, Li RJ. . Engine performance emission characteristics of marine fish oil produced from the discarded parts of marine fish. *Fuel Process Technol* 2009; 90:883-8.
- [13]. Jayasinghe P, Hawboldt K. A review of bio-oils from waste biomass; focus on fish processing waste .*Renew Sust Energy Rev* 2012;60:798-821.
- [14]. Qi DH, Geng LM, Chen H, Bian YZH, Liu J, Ren XCH. Combustion and performance evaluation of a Diesel engine fuelled with biodiesel produce from soybean crude oil. *Renew Energy* 2009; 34:2706-13.

# Performance Study of Stainless Steel Fin with and Without Cnt Coating

[<sup>1</sup>] Mr. Shankara Murthy H M, [<sup>2</sup>] Mr. Krishna Kumar M., [<sup>3</sup>] Mr. Pranav K.V, [<sup>4</sup>] Mr. Roni T.Raju, [<sup>5</sup>] Mr. Sachin Vinod,

[<sup>1</sup>] Assistant Professor, [<sup>2, 3, 4, 5</sup>] UG Student

[<sup>1</sup>][<sup>2</sup>][<sup>3</sup>][<sup>4</sup>][<sup>5</sup>] Dept of Mechanical Engineering, Srinivas Institute of Technology, Mangaluru, Karnataka, India

**Abstract:** --Fins are used to remove the excess heat from the systems and to transfer it to the surroundings. Hence, there is a need to increase the thermal efficiency of the fin in order to achieve the maximum heat transfer. The work includes the enhancement of the heat transfer rate of stainless steel-304 fin with and without carbon nanotube coating. The heat transfer rate due to the natural as well as forced convection is studied. Various types of fin profiles were tested under natural and forced convection. As rectangular profile fins abstract higher air velocity as compared to any other profile fin, it is chosen for the study. The dip coating method is adopted for coating the stainless steel fin section and Rockwell hardness test is carried out to check the uniformity in the coating. In this work, the various parameters such as temperature distribution, thermal conductivity, and convective heat transfer coefficient are studied at different heat inputs. The experimental results shows that thermal conductivity of stainless steel (AISI SS-304) fin is increased by 21% with CNT coating and also convective heat transfer coefficient of the coated fin increases by 9%.

**Keywords:** Carbon Nanotubes, Heat transfer coefficient, Dip coating, CNT coating.

NOMENCLATURE	
A	Surface area of the rectangular fin in m <sup>2</sup>
V	Voltage in Volts
I	Current in Amps
K	Thermal conductivity in W/mK
h	Heat transfer coefficient in W/m <sup>2</sup> .K
Q	Heat input in Watts
T <sub>a</sub>	Ambient temperature in °C
T <sub>b</sub>	Base temperature in °C
T <sub>s</sub>	Surface temperature in °C
ABBREVIATION	
CNT	Carbon Nano-Tube
SWCNTs	Single Wall Carbon Nanotubes
MWCNT	Multi Wall Carbon Nanotubes
CFD	Computational Fluid Dynamics
MEMS	Micro Electro-Mechanical Systems
NEMS	Nano Electro-Mechanical Systems

## I. INTRODUCTION

Fins are surfaces that extend from an object to increase the rate of heat transfer to the environment by increasing convection. The amount of conduction, convection, or radiation of an object determines the amount of heat it transfers.

Increasing the temperature gradient between the object and the environment, increasing the convection heat transfer coefficient, or increasing the surface area of the object increases the heat transfer.

There are different types of fins and they are: Rectangular fins, Elliptical fins, Triangular fins,

Disc/annular fins, Pin fins, Tapered fins and Radial plate fins.

There are many factors which influence the heat transfer rate of a fin and they are

- Effect of number of fins and thickness of fins
- Effect of material and climatic condition
- Effect of perforations, notches and varying geometry

The heat transfer is an important process for the removal of excess heat from the system that removes heat to the surroundings. Fins find wider applications in the industries, computer chips, and in bikes. Fins are also subjected to natural as well as forced convection. Normally, in bikes, engines may be air cooled or liquid cooled depending upon the requirements. Air cooled engines depend on their air flow in the surfaces external to the engine cylinders and to remove the necessary heat. The amount of the heat dissipated depends upon the mass flow rate, temperature difference between cylinder and air and the thermal conductivity of the material. Air cooled engines uses the fins for the removal of the heat from the engines. Air-cooled engines are better adapted to extremely cold as well as hot environmental weather temperatures. It can see air-cooled engines starting and running in freezing conditions that seized water-cooled engines and continue working when water-cooled ones start producing steam jets, thus making it an immense popularity. Air-cooled engines have an advantage compared to the liquid cooled engine from a thermodynamic point of view, due to higher operating temperature. The worst problem is air-cooled aircraft engines have the effect of the Shock cooling, it happens

when the airplane entered in a dive after climbing or level flight with throttle opened, with the engine under no load condition while the airplane dives generating lesser heat, and the flow of air that cools the engine will be increased, a catastrophic engine failure may result because of the engine having different temperatures at different locations, and thus different thermal expansions. In such conditions the engine may seize, and if any sudden change or imbalance in the relation between heat produced by the engine and heat dissipated by cooling may occur, it will result in an increased wear of engine, so as a consequences, considering the thermal expansion at different parts of the engine, liquid-cooled engines will be more stable and uniform working temperatures.

Also, in the spark ignition engines cooling must be satisfactorily to avoid any kind of pre-ignition and the knock. In short, cooling is important because it is an equalization of the internal temperature to prevent the local over heating as well as to remove the excess junk heat so as to operate the engine in practically maintaining conditions.

Therefore, there is a need to increase the efficiency of the air cooled engines (fins) in order to have the performance of the engines consistently and effectively.

The profiles of the fins mainly used in the bikes are:

- Rectangular profiles: As this is the simplest geometry, the cross section of the fins will be in rectangular shape.
- Trapezoidal profiles: Fins will be in trapezoidal in nature, also provide greater surface for the heat transfer.

The carbon nanotubes are allotropes of the carbon having length-to-diameter ratio of upto 132,000,000:1. It has very good thermal properties and it can be used in heat transfer applications due to its very large surface area.

Among various potential candidates for future MEMS/NEMS applications the carbon nanotubes have a unique position. Their remarkable properties, such as the great strength, light weight, special electronic structures and also high stability, make carbon nanotubes the ideal material for a wide range of applications. Because of the bright future for carbon nanotubes, a great deal of effort has been devoted to understanding and also characterizing their properties since the discovery of multi-walled carbon nanotubes by Ijima in 1991 and of single-walled nanotubes by Ijima et al and Bethunes et al.in 1993.

The high thermal conductivity of single wall carbon nanotubes (SWCNT's) makes them necessary for thermal applications. To illustrate, in magnetic field aligned films of SWCNT's, a value of 250 W/mK has been measured at room temperature (M.C. Llaguno, J. Hone) et al. For single tubes, theoretical calculations of the thermal conductivity give even higher values of about 10,000 W/mK. In addition, the unique structure of carbon nanotubes allows for the study of low-dimensional phonons.

Specifically, the cylindrical geometry of a tube enforces periodic boundary conditions on the circumferential wave vector, resulting in the formation of 1D phonon called the 'sub bands' which is analogous to the electronic sub bands. In an isolated SWCNT, there are four acoustic phonon modes, with the first optical sub band which contributes an energy of a few mega electron Volt [10]. In heat capacity measurements, the quantized phonon spectrum was observed as a deviation from linear behavior at around 8 Kelvin [7] which corresponds to a first sub band energy of 4 Mega electron Volt. Similarly, the thermal conductivity of nanotubes should exhibit a linear T-dependence at low T and then a nonlinear trend above a crossover temperature that is directly related to the sub band splitting. Previous measurements [7] indeed show a linear thermal conductivity at low T, with an upturn to a higher slope, is consistent with this picture. However, the temperature of this is much higher than would be expected from the band structure derived from heat capacity measurements. In addition, the behavior of the phonon scattering time at t is unknown. Therefore it is not possible to conclude with certainty from a single measurement that the observed low-T linear thermal conductivity is due to 1D phonon quantization. To help determine whether the linear thermal conductivity of bulk SWCNTs at low Temperature is due to quantization effects, we have investigated the diameter dependence of thermal conductivity on several bulk samples with different average tube diameters. Because the energy splitting between 1D sub bands varies inversely with the radius, we expect that the crossover from linear to non-linear thermal conductivity should occur at higher temperatures in tubes with smaller radius. The data show increasing crossover temperature with decreasing diameter. In addition, an effect of annealing on thermal conductivity has been observed.

The single walled carbon nanotubes have the thermal conductivity in the range of 3200 w/mk in room temperature in axial directions and acts as insulators in the radial directions. The temperature stability of carbon nanotubes is 2800°C in vacuum and 750°C in air (sujith Kumar et al.2012; prabhu and vinayagan, 2011; senthil Kumar nanda kumar et al. 2013).

The extended surface can be coated with these highly conductive and convective materials. The experiment results by J nagarani et al. (2013) showed that the heat transfer due to this coating increases by an amount of 19% by conduction and 9% by convection in an elliptical fin.

## **II. RELATED WORKS**

shinde sunil kumar et.al [1] studied analysis of the heat transfer of various fins profiles through forced convection. They observed that the air flow velocity in abstraction with rectangular profile is higher as compared to all the profiles. Due to this, rectangular fins have higher heat

transfer coefficient than any other profiles. The analysis had done through the experiment as well as CFD software and results are compared. They concluded that the rectangular fins have maximum amount of heat transfer than any other profiles in forced convection.

J.nagarani. K et al. [2] has presented the work on the stainless steel-304 fin with and without carbon nanotube coatings (MWCNT). They observed that the heat transfer rate due to this coating increases with an amount of 21% by conduction and 7% by convection through the natural convections in the coated fins. They concluded that thermal conductivity considerably increases for the coated fin and there was a considerable improvement in efficiency and effectiveness for the coated fin.

SSujith kumar et al.[3] presented the heat transfer enhancement by carbon nanotube coating, this work deals on the experimental investigation on the heat transfer and pressure drop characteristics of CNT coating on a stainless steel substrate in a rectangular macro-channel with water as the working fluid. The uniform coatings were tested under the Rockwell hardness tester. The experiments were conducted under both laminar and turbulent flow conditions with Reynolds number varying from 500°-2600°. The experimental heat transfer coefficient has increased significantly in the case of coated plate. The conclusions obtained are the use of CNT coatings on the surface enhances the heat flux when compared to an uncoated surface. This is mainly due to the enhancement in surface area and the increase in the roughness on the surface causing local turbulence.

### **III. PRESENT WORK**

In this work, the fins of the Hero Honda motorcycle are taken as the standard and its dimension is measured for the study. Vernier calipers are used to get the accurate dimensions of the fin. The heat transfer analysis is done for both natural and forced convection. SWCNT is used for the fin coating to enhance the rate of heat transfer from hot surface.

SWCNT in the powdered form is collected with 75% purity. The SWCNT is diluted in the cholorosulphonic acid (virgina a Davis, Nicholas g Parra et al. 2009) for getting into dispersed form and epoxy-818 is used as the binder (sujith Kumar et al.2013). Since the carbon nanotube would not adhere directly to stainless steel. The dip coating method is used, as it is the fastest and the simple way of coating the stainless steel. A sample test piece of the same material is taken for trials in order to calculate the time required in dipping and its uniformity is checked. The coating is done and it is kept at 150°C for 6 hours for getting a stable coating surfaces. The Rockwell hardness test is carried out to check the uniformity in coating. Then, the

time required is calculated and then the coating is done on the stainless steel fin.

### **IV. EXPERIMENTAL SETUP**

The experimental setup has a rectangular fin sections. Its base is connected to the Electrical heater to heat the base of the test section for conduction of the experiment. The voltmeter and ammeters are used to measure voltage and current readings for calculating the heat input. The dimmer stat is used for the voltage regulation. The K-type thermocouples are mounted to measure the temperature accurately at 6 different locations of the test fin section. A digital temperature indicator is used to measure the temperature at 6 different locations.



**Fig 1: Experimental setup**

### **V. FIN ANALYSIS**

#### **Heat input:**

$$Q = V \cdot I \text{ in Watts.}$$

Where, V = Voltage in volts.

I = Current in amps.

#### **Heat transfer coefficient:**

$$h = \frac{Q}{A(T_s - T_a)}$$

Where, h = convective heat transfer coefficient in W/m²K.

A = Area in m².

T<sub>s</sub> = Surface Temperature in °C.

T<sub>a</sub> = Ambient Temperature in °C.

#### **Efficiency of the fin:**

$$\eta = \frac{\tanh(mL)}{mL}$$

(Assuming that tip of the fin insulated).

#### *Effectiveness of the fin:*

$$\varepsilon = \frac{Q_{fin}}{Q_{max}}$$

Error estimation in temperature measurement of thermocouples:

$$\frac{T_t - T_\infty}{T_0 - T_\infty} = \frac{1}{Cosh(mL)}$$

## VI. RESULTS AND DISCUSSION

In this work, the AISI SS-304 rectangular fin has been studied with and without SWCNT coating. Fig 2 demonstrates the experimental temperature distribution for the coated and non coated fins for different heat input values. It shows that the drop in the temperature values for the different Nano-coated AISI SS-304 fin. This decrease in temperature is because of the CNT coating, and its thermal properties. The CNTs expose added surface for heat transfer. A similar type of the work has done by the J.nagarani, mayilsami et al. (2013) for SS fin and the same effect was discussed.

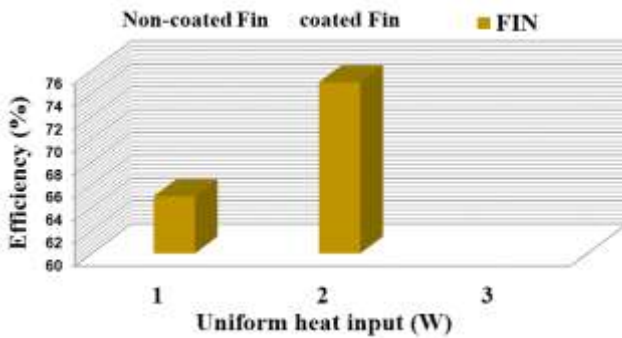


Fig 2: Efficiency v/s heat input for the coated and non coated fin.

These values are used to find out the parameters for the instance for the convective heat transfer and the shaped tube efficiency. The Fig 3. Shows the heat input with respect to the thermal conductivity for the rectangular fin with and without SWNT coating.

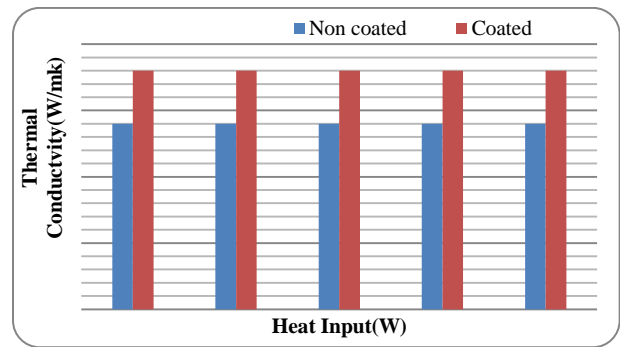


Fig 3: Thermal conductivity for the coated and non coated fins for different heat input values.

The thermal conductivity was increased due to the higher withstand temperature of the SWCNTs. The increase in the thermal conductivity routinely increases the heat transfer rate. For any heat inputs the value of the thermal conductivity of the coated and noncoated fins remains constant as shown in the above plot.

A considerable increase in the convective heat transfer coefficient from 7% to 14% for different heat input values are observed for the coated fins. The coating of SWCNTs on the surface results in increase in the convective heat transfer and increase in the area of the contact. The reason for the increase in the heat transfer rate is due to the increase in the surface area of the vertically aligned CNT will act as Nano fins.

## VII. CONCLUSION

The convective heat transfer coefficient, efficiency, effectiveness were calculated for the coated and non coated rectangular fin. The following observations were made:

- The thermal conductivity increases for the Nano-coated fin.
- For different heat inputs, there was a significant drop in the surface temperature for the CNT coated fin.
- The convective heat transfer is higher for the CNT coated fin, due to the increase in the surface area of the CNT.
- There was a considerable improvement in the thermal efficiency and the effectiveness of the nano coated fin.

## REFERENCES

- [1] J. Nagarani., K. Mayilsamy., VP. Venkataramana Murthy., "Heat transfer enhancement of the AISI stainless steel 304 elliptical annular fin coated with the carbon nanotube" International journal of Ambient energy: Vol.37,No 1, December 2013,pp.55-63.

- [2] Shindesandip.,Shindesunilkumar.,Nitingokhale.,  
“Numerical and experimental analysis of heat transfer through various types of fin profiles by forced convection”, International Journal of Engineering Research & Technology (IJERT), Vol.2 Issue7, July 2013, pp.32-37.
- [3] Sujithkumar., Suresh.,Rajiv k.,”Heat transfer enhancement by nano structured carbon nanotube coating” International Journal of Scientific & Engineering Research, Vol.3 Issue 6, march 2013, pp.185-200.
- [4] Vinaya Kumara U M., Mr. Krishnamurthy K.N., Akash Deep B N.,“Experimental Analysis of Rectangular Fin Arrays with Continuous Fin and Interrupted Fins Using Natural and Forced Convection” International journal of innovative research in science, Engineering and technology,Vol.5,Issue6,January 2016,pp.85-95.
- [5] Virginia A., Davis A., Nicholas G., Parra-Vasquez Micah., J.Green., Pradeep K. Rai., “True solutions of single-walled carbon nanotubes for assembly into macroscopic materials” Nature nanotechnology, page 830-834,issue4,November 2009,page55-63.
- [6] “Engineering heat and mass transfer”,R.C sachdeva, Third edition, New age international publications
- [7] NANO: The essentials-understanding nanoscience and nanotechnology,T pradeep,Tata McGraw hill india,2007edition.
- [8] “Nanotechnology”,Richard booker&earl Boysen,Wiley India Pvt.Ltd,2007edition.
- [9] N. Singh, V. Sathyamurthy, W. Peterson, J. Arendt and D. Banerjee, “Flow boiling enhancement on a horizontal heater using carbon nanotubes coatings”, International Journal of Heat and Fluid Flow, issue 31, 201-207, 2010.
- [10] Senthilkumar, R., S. Prabhu, and M. Cheralathan. “Experimental Investigation on Carbon Nano Tubes Coated Brass. Rectangular Extended Surfaces.” Applied Thermal Engineering, may 2013, issue 50, vol 5, pp.1361–1368

# Influence of Thermal Radiation on Mhd Boundary Layer Flow In A Newtonian Liquid With Temperature Dependent Properties Over An Exponential Stretching Sheet

[<sup>1</sup>] A. S. Chethan, [<sup>2</sup>] G. N. Sekhar, [<sup>3</sup>] Annamma Abraham

[<sup>1</sup>], [<sup>3</sup>] BMS Institute of Technology & Management, [<sup>2</sup>] BMS College of Engineering

**Abstract:** --The paper presents a study of a forced flow and heat transfer of an electrically conducting Newtonian fluid in the presence of a magnetic field due to an exponentially stretching sheet. Thermal radiation term is incorporated in the temperature equation. The governing coupled, non-linear, partial differential equations are converted into coupled, non-linear, ordinary differential equations by a similarity transformation and are solved numerically using shooting method. The influence of various parameters such as the Prandtl number, Chandrasekhar number, variable viscosity parameter, heat source (sink) parameter, radiation parameter and suction/injection on velocity and temperature profiles are presented and discussed.

**Index Terms**— Stretching sheet, Variable viscosity, Shooting Method, Heat source.

## I. INTRODUCTION

Flows due to a continuously moving surface are encountered in several important engineering applications .viz, in the polymer processing unit of a chemical engineering plant, annealing of copper wires, glass fiber and drawing of plastic films. Sakiadis [1-3] initiated the theoretical study of these applications by considering the boundary layer flow over a continuous solid surface moving with constant speed. This problem was extended by Erickson et al. [4] to the case where the transverse velocity at the moving surface is non-zero with heat and mass transfer in the boundary layer accounted for.

Crane [5] studied the steady two-dimensional boundary layer flow caused by the stretching sheet, which moves in its own plane with a velocity which varies linearly with the axial distance. There after various aspects of the above boundary layer problem on continuous moving surface were considered by many researchers (Vleggar [6], Gupta and Gupta [7], Grubka and Bobba [8], Chen and Char [9] and Siddheshwar et al. [10]).

Many metallurgical processes involve the cooling of continuous strips or filaments by drawing them through a quiescent fluid. During this process of drawing the strips are sometimes stretched. The properties of final product depend on the rate of cooling. Pavlov [11] examined the flow of an electrically conducting fluid caused solely by the stretching of an elastic sheet in the presence of a uniform magnetic field. Chakrabarti and Gupta [12] considered the flow and heat transfer of an electrically conducting fluid past a porous

stretching sheet. Anderson [13] presented an analytical solution of the magnetohydrodynamic flow using a similarity transformation for the velocity and temperature fields. In all the above mentioned studies the physical properties of the ambient fluid were assumed to be constants. However, it is well known that these physical properties of the ambient fluid

may change with temperature (Herwig and Wickern [14], Takhar et al. [15], Pop et al. [16], Subhash Abel et al. [17], Pantokratoras [18], Ali [19], Andersson and Aaresth [20], Prasad et al. [21], Sekhar and Chethan [22]).

Magyari and Keller [23] studied the heat and mass transfer on the boundary layer flow due to an exponentially stretching surface. Elbashbeshy [24] added new dimension to the study on exponentially stretching surface. Partha et al. [25] have examined the mixed convection flow and heat transfer from an exponentially stretching vertical surface in quiescent liquid using a similarity solution. Heat and mass transfer in a viscoelastic boundary layer flow over an exponentially stretching sheet were investigated by Khan and Sanjayanand [26-27]. Sajid and Hayat [28] considered the influence of thermal radiation on the boundary layer flow due to an exponentially stretching sheet. Sekhar and Chethan [29] analyzed the flow and heat transfer due to an exponentially stretching continuous surface in the presence of Boussinesq-Stokes suspension. Later various investigations were made on the stretching sheet problems in different directions ([30]-[39]).

Suction/injection of a fluid through the bounding surface can significantly change the flow field. In general, suction tends to increase the skin friction whereas injection acts in the opposite manner. The process of suction/injection has also its importance in many engineering activities such as in the design of thrust bearing and radial diffusers, and thermal oil recovery. Suction is applied to chemical processes to remove reactants. Blowing is used to add reactants, cool the surface, prevent corrosion or scaling and reduce the drag.

The radiative effects have important applications in physics and engineering. The radiation heat transfer effects on different flows are very important in space technology and high temperature processes. Thermal radiation effects play an important role in controlling heat transfer in polymer processing industry where the quality of the final product depends on the heat controlling factors to some extent. In the present work, we study the MHD boundary layer flow and heat transfer characteristics of a Newtonian fluid past an exponentially stretching sheet, when viscosity is a function of temperature and in the presence of thermal radiation.

## II. MATHEMATICAL FORMULATION

We consider a steady, two-dimensional boundary layer flow of an incompressible, weakly electrically conducting Newtonian fluid due to a stretching sheet. The liquid is at rest and the motion is affected by pulling the sheet at both ends with equal force parallel to the sheet and with speed  $u$ , which varies exponentially with the distance  $x$  from the origin.

The boundary layer equations governing the flow and heat transfer in a Newtonian fluid over a stretching sheet, assuming that the viscous dissipation is negligible, are

$$\frac{\partial u}{\partial x} + \frac{\partial v}{\partial y} = 0, \quad (1.1)$$

$$u \frac{\partial u}{\partial x} + v \frac{\partial u}{\partial y} = \frac{\partial}{\partial y} \left\{ \frac{\mu(t)}{\rho} \frac{\partial u}{\partial y} \right\} - \frac{\mu_m^2 \sigma H_0^2}{\rho} u, \quad (1.2)$$

$$u \frac{\partial t}{\partial x} + v \frac{\partial t}{\partial y} = \frac{k}{\rho C_p} \frac{\partial^2 t}{\partial y^2} + Q_s (t - t_\infty) - \frac{1}{\rho C_p} \frac{\partial q_r}{\partial y}, \quad (1.3)$$

Here  $u$  and  $v$  are the components of the liquid velocity in the  $x$  and  $y$  directions, respectively,  $t$  is the temperature of the sheet,  $t_\infty$  is the temperature of the fluid far away from the sheet,  $\mu$  is the dynamic viscosity,  $\mu_m$  is the magnetic permeability,  $H_0$  is the applied magnetic field,  $\rho$  is the density,  $\sigma$  is the electric conductivity of the fluid,  $k$  is the thermal conductivity,  $C_p$  is the specific heat at constant pressure,  $Q_s$  is the heat source coefficient and  $q_r$  is the radiative heat flux.

The coefficient of viscosity is assumed to be a reciprocal function of temperature and it is of the form

$$\mu(t) = \frac{\mu_\infty}{1 + \delta(t - t_\infty)}$$

If  $\frac{1}{\mu}$  is expanded in Taylor's series about  $t = t_\infty$  then the scalar appearing in the above expression can be written as

$$\delta = \left[ \frac{\partial}{\partial t} \left( \frac{1}{\mu} \right) \right]_{t=t_\infty}.$$

Here  $\mu_\infty$  is the coefficient of viscosity far away from the sheet.

Using Rosseland approximation for radiation we can write

$$q_r = -\frac{4\sigma^*}{3k^*} \frac{\partial t^4}{\partial y}$$

The following boundary conditions are used.

$$u = U_w(x) = U_0 e^{\frac{2x}{L}}, \quad v = v_c, \quad \begin{cases} t = t_w = t_\infty + Ae^{\frac{x}{L}} & \text{in PEST case} \\ -k \left( \frac{\partial t}{\partial y} \right)_w = De^{\frac{3x}{2L}} & \text{in PEHF case} \end{cases} \quad \text{at } y=0, \quad (1.4)$$

$u \rightarrow 0, t \rightarrow t_\infty$  as  $y \rightarrow \infty$ .

$$t_w - t_\infty = \begin{cases} Ae^{\frac{x}{L}} & \text{in PEST case} \\ \frac{DL}{k\sqrt{Re}} e^{\frac{x}{2L}} & \text{in PEHF case} \end{cases}$$

where  $t_w$  is the temperature of the sheet,  $U_0$  is the reference velocity and  $L$  is the reference length.

We now make the equations and boundary conditions dimensionless using the following definition:

$$(x, y) = \frac{(x, y \sqrt{Re})}{L}, \quad (u, v, V_c) = \frac{(u, v \sqrt{Re}, v_c \sqrt{Re})}{U_0}, \quad T = \frac{t - t_\infty}{\Delta t} \quad (1.5)$$

where  $Re = \frac{U_0 L}{v}$  is the Reynolds number and  $\Delta t = t_w - t_\infty$  is the sheet-liquid temperature difference.

The boundary layer equations (1.1) - (1.3) on using Eq. (1.5) take the following form.

$$\frac{\partial U}{\partial X} + \frac{\partial V}{\partial Y} = 0, \quad (1.6)$$

$$U \frac{\partial U}{\partial X} + V \frac{\partial V}{\partial Y} = -\frac{V}{(1+VT)^2} \frac{\partial T}{\partial Y} \frac{\partial U}{\partial Y} + \frac{1}{(1+VT)} \frac{\partial^2 U}{\partial Y^2} - QU, \quad (1.7)$$

$$U \frac{\partial T}{\partial X} + V \frac{\partial T}{\partial Y} + U T = \frac{1}{Pr} \left( 1 + \frac{4}{3} R \right) \frac{\partial^2 T}{\partial Y^2} + H_s T, \quad (1.8)$$

where

$V = \delta \Delta t$  is the variable viscosity parameter,

$Q = \frac{\mu_m^2 \sigma H_0^2}{\alpha}$  is the Chandrasekhar number,

$R = \frac{4 \sigma^* T_\infty^3}{k^* K}$  is the radiation parameter,

$Pr = \frac{\mu C_p}{k}$  is the Prandtl number and

$H_s = \frac{Q_s}{\alpha}$  is the heat source (sink) parameter.

The boundary conditions (1.4) take the form

$$U = e^X, V = V_c, \begin{cases} T = 1 & \text{in PEST} \\ \frac{\partial T}{\partial Y} = -e^X & \text{in PEHF} \end{cases} \quad \text{at } Y = 0, \quad (1.9)$$

$U \rightarrow 0, T \rightarrow 0$  as  $Y \rightarrow \infty$ .

We introduce the stream function  $\psi(X, Y)$  as

$$U = \frac{\partial \psi}{\partial Y}, \quad V = -\frac{\partial \psi}{\partial X}, \quad (1.10)$$

Using Eq. (1.10), the boundary layer equations Eqs. (1.7) and (1.8) can be written as

$$\begin{aligned} (1+VT) \frac{\partial^3 \psi}{\partial Y^3} - V \frac{\partial T}{\partial Y} \frac{\partial^2 \psi}{\partial Y^2} + (1+VT)^2 \frac{\partial \psi}{\partial X} \frac{\partial^2 \psi}{\partial Y^2} - (1+VT)^2 \frac{\partial \psi}{\partial Y} \frac{\partial^2 \psi}{\partial X \partial Y} \\ - (1+VT)^2 Q \frac{\partial \psi}{\partial Y} = 0, \end{aligned} \quad (1.11)$$

$$\frac{\partial \psi}{\partial Y} \frac{\partial T}{\partial X} - \frac{\partial \psi}{\partial X} \frac{\partial T}{\partial Y} + U T = \frac{1}{Pr} \left( 1 + \frac{4}{3} R \right) \frac{\partial^2 T}{\partial Y^2} + H_s T. \quad (1.12)$$

The corresponding boundary conditions in terms of the stream function can be written as

$$\frac{\partial \psi}{\partial Y} = e^X, \quad \begin{cases} \frac{\partial \psi}{\partial X} = -V_c & \text{in PEST} \\ \frac{\partial T}{\partial Y} = -e^X & \text{in PEHF} \end{cases} \quad \text{at } Y = 0, \quad (1.13)$$

$\frac{\partial \psi}{\partial Y} \rightarrow 0, T \rightarrow 0$  as  $Y \rightarrow \infty$ .

The following similarity transformation will now be used on Eqs. (2.11) and (2.12).

$$\begin{aligned} \psi(x, \eta) &= f(\eta) e^x, \\ T(X, Y) &= \begin{cases} \theta(\eta) & \text{in PEST case} \\ \phi(\eta) & \text{in PEHF case} \end{cases}, \\ \eta &= Y e^X. \end{aligned} \quad (1.14)$$

Using the transformations given by Eq. (1.14) in Eq. (1.11) and (1.12), we get the following boundary value problems.

### (ii) PEHF:

$$(1+V\Phi) f''' - V\Phi' f'' + (1+V\Phi)^2 \left( f f'' - 2f'^2 - Q_x f' \right) = 0, \quad (1.18)$$

$$\left( 1 + \frac{4}{3} R \right) \phi'' + Pr(f\phi' - f'\phi) + Pr H_{sx} \phi = 0, \quad (1.19)$$

$$\begin{aligned} f(0) &= -V_{cx}, \quad f'(0) = 1, \quad \Phi'(0) = -1, \\ f'(\infty) &\rightarrow 0, \quad \Phi(\infty) \rightarrow 0. \end{aligned} \quad (1.20)$$

where  $V_{cx} = \frac{V_c}{e^X}$  is the local suction/injection parameter,  $Q_x = \frac{Q}{e^{2X}}$  is the local Chandrasekhar number and  $H_{sx} = \frac{Q_s L}{U_0 e^{2X}}$  is the local heat source (sink) parameter.

Here, primes denote the differentiation with respect to  $\eta$ .

### III. METHOD OF SOLUTION

The boundary value problems due to an exponential stretching sheet are solved numerically by shooting method. We adopt the shooting method with Runge-Kutta-Fehlberg-45 scheme to solve the boundary value problems in PEST and PEHF cases mentioned in the previous section. The coupled non-linear Eqs. (1.15) and (1.16) in the PEST case are transformed to a system of five first order differential equations as follows:

$$\begin{aligned} \frac{df_0}{dY} &= f_1, \\ \frac{df_1}{dY} &= f_2, \\ \frac{df_2}{dY} &= \frac{V\theta_1}{(1+V\theta_0)} f_2 + (1+V\theta_0)(f_0 f_2 + 2f_1^2 + Q_x f_1), \\ \frac{d\theta_0}{dY} &= \theta_1, \\ \frac{d\theta_1}{dY} &= \frac{Pr f_1 \theta_0 - Pr f_0 \theta_1 - Pr H_{sx} \theta_0}{\left( 1 + \frac{4}{3} R \right)}. \end{aligned} \quad (1.21)$$

Subsequently the boundary conditions in Eq. (1.17) take the form

$$\begin{aligned} f_0(0) &= -V_{cx}, \quad f_1(0) = 1, \quad f_1(\infty) \rightarrow 0, \\ \theta_0(0) &= 1, \quad \theta_0(\infty) \rightarrow 0. \end{aligned} \quad (1.22)$$

Here  $f_0 = f(\eta)$  and  $\theta_0 = \theta(\eta)$ .

Aforementioned boundary value problem is converted into an initial value problem by choosing the values of  $f_2(0)$  and  $\theta_1(0)$  appropriately. Resulting initial value problem is integrated using the fourth order Runge-Kutta method. Newton-Raphson method is implemented to correct the guess values of  $f_2(0)$  and  $\theta_1(0)$ . In solving equations (1.21) subjected to boundary conditions (1.22) the appropriate ‘ $\infty$ ’ is determined through the actual computation. Same procedure is adopted to solve the boundary layer equations in PEHF case.

#### IV. RESULTS AND DISCUSSION

The hydromagnetic boundary layer flow and heat transfer in a weakly electrically conducting Newtonian fluid past an exponentially stretching sheet with temperature dependent viscosity and thermal radiation are investigated. Numerical solution of the problem is obtained by shooting method.

Figures 1 - 3 are the plots of horizontal and transverse velocities for various values of variable viscosity parameter ( $V$ ), suction/injection parameter ( $V_{cx}$ ) and Chandrasekhar number ( $Q_x$ ).

The effect of variable viscosity parameter  $V$  on the velocity profiles  $f(\eta)$  and  $f'(\eta)$  with  $\eta$  is depicted in Fig. 1. It is observed the both the horizontal and transverse velocity profiles decreases with increasing values of  $V$ .

Figure 2 presents the effects of suction or injection on the horizontal and transverse velocity. With the increasing values of  $V_{cx}$ , the horizontal velocity increases. i. e. suction ( $V_{cx} < 0$ ) causes to decrease the velocity of the fluid in the boundary layer region. This is because in case of suction, the heated fluid is pushed towards the wall where the buoyancy forces act to retard the fluid due to high influence of the viscosity. The same principle operates but in opposite direction in case of injection ( $V_{cx} > 0$ ). Figure 3 show the effect of Chandrasekhar number  $Q_x$  on the velocity profiles above the sheet. An increase in  $Q_x$  is seen to decrease both velocity components at any point above the sheet. This is because of the retarding effects of the Lorentz force set forth by the magnetic field.

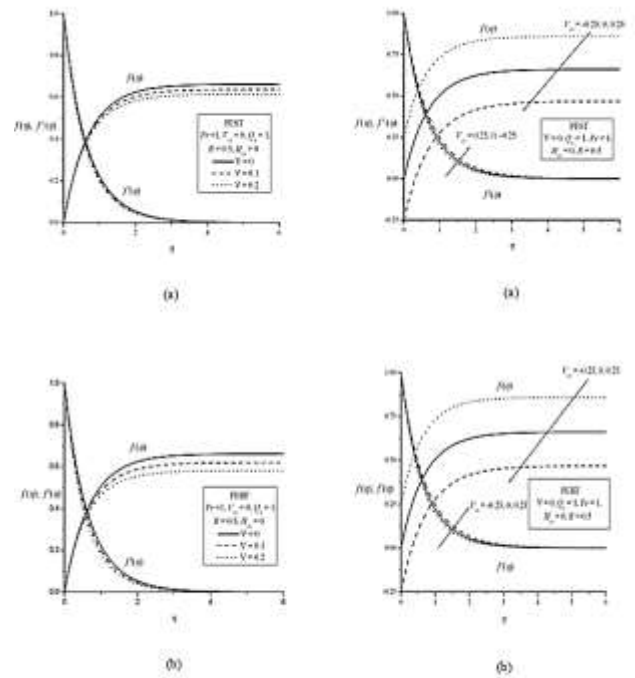


Figure 1: Plot of velocity for different values of variable viscosity parameter  $V$  in PEST and PEHF cases.

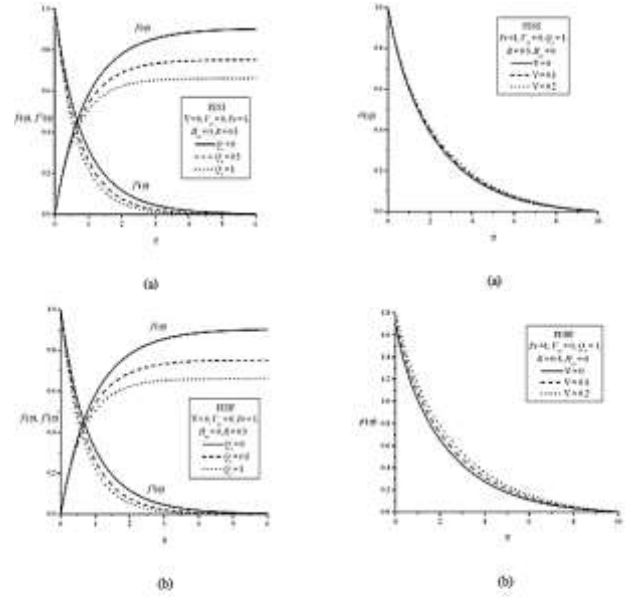
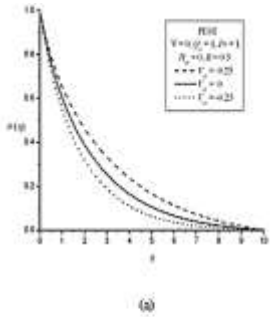


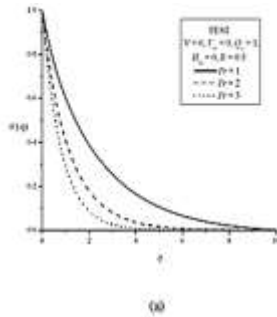
Figure 2: Plot of velocity for different values of suction/injection parameter  $V_{cx}$  in PEST and PEHF cases.

Figures 4 and 5 demonstrate the effect of variable viscosity parameter  $V$  and suction/injection parameter  $V_{cx}$  on the temperature distribution. The effect of  $V$  and injection is to increase the thermal boundary layer thickness whereas suction reduces it.

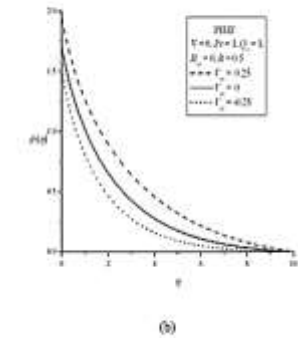
# Influence of Thermal Radiation on Mhd Boundary Layer Flow In A Newtonian Liquid With Temperature Dependent Properties Over An Exponential Stretching Sheet



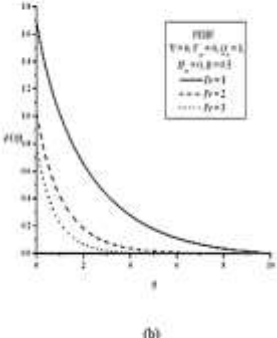
(a)



(b)



(a)

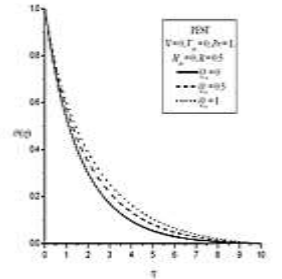


(b)

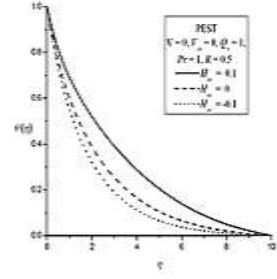
Figure 5: Plot of temperature for different values of suction/injection parameter in PEST and PEHF cases.

Figure 6: Plot of velocity for different values of Prandtl number in PEST and PEHF cases.

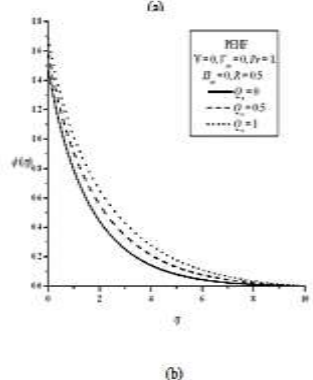
The effect of Prandtl number  $Pr$  on the temperature field is shown in Fig. 6. It is noticed that the temperature decreases with the increasing value of Prandtl number because thermal boundary layer decreases due to increase in  $Pr$ .



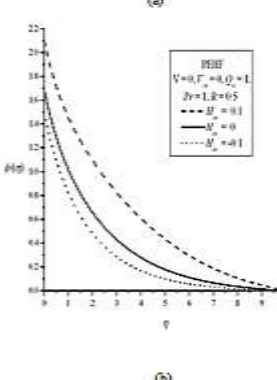
(a)



(b)



(a)



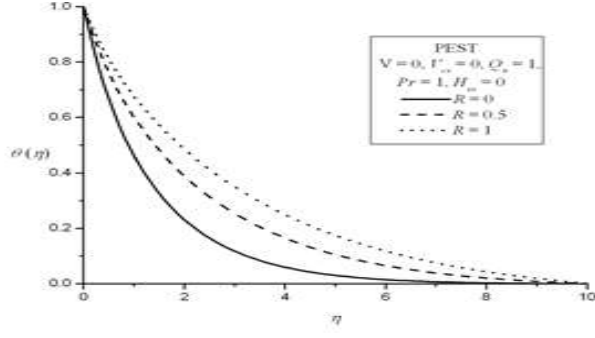
(b)

Figure 7: Plot of velocity for different values of Chandrasekhar number in PEST and PEHF cases.

Figure 8: Plot of velocity for different values of heat source/sink parameter in PEST and PEHF cases.

The effect of Chandrasekhar number  $Qx$  on temperature profiles are shown in Fig. 7. It is noticed that the effect of  $Qx$  is to increase the temperature in the boundary layer. This is because of the fact that the introduction of transverse magnetic field to an electrically conducting fluid gives rise to a resistive type of force known as Lorentz force. This force has the tendency to slow down the motion of the fluid in the boundary layer and to increase the temperature profile. Also, the effect of increasing values of Prandtl number is decrease the temperature distribution in the flow region.

It is observed that the effect of heat source in the boundary layer generates energy which causes the temperature to increase, while the presence of heat sink in the boundary layer absorbs the energy which causes the temperature to decrease. These behaviors are seen in Fig. 8.



(a)

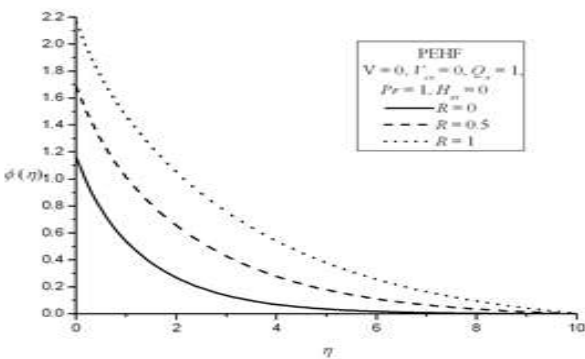


Figure 9 shows the variation of temperature with  $\eta$  for various values of radiation parameter  $R$ . It is clear that thermal radiation  $R$  enhances the temperature in the thermal boundary layer region. The increase in radiation parameter means of release of heat energy from the flow region and so the fluid temperature decreases as the thermal boundary layer thickness becomes thinner.

In order to validate our results, we have compared the skin friction rate of heat transfer in the absence of variable

viscosity , suction/injection Chandrasekhar number and heat source/sink parameter ( $H_{sx}=0$ ) with the published results and found them to be in good agreement (see Table 1.1 and 1.2).

Table 1.1: Comparison of values of skin friction  $-f''(0)$  for various values of  $V_{cx}$  with  $V = Q_x = H_{sx} = R = 0$  in case of exponential stretching.

$V_{cx}$	$-f''(0)$	
	Elbashbeshy (2001)	Present study
0	1.28181	1.281816
-0.2	1.37889	1.378894
-0.4	1.4839	1.484389
-0.6	1.59824	1.598242

Table 1.2: Comparison of values  $-\theta'(0)$  for various values of Prandtl number and radiation parameter with  $V = Q_x = H_{sx} = R = 0$  in case of exponential stretching.

Pr	R	$-\theta'(0)$				
		Magyari and Keller (2001)	Bidin and Nazar 2009	Ishak 2011	Mukho-padhyay 2013	Present study
1	0	0.9548	0.9547	0.9548	0.9547	0.9548
2			1.4714		1.4714	1.4715
2	0.5		1.0735		1.0734	1.0735
	1		0.8627		0.8626	0.8627
	0.5		1.3807		1.3807	1.3807
3	1		1.1214		1.1214	1.1214

#### IV. CONCLUSIONS

- Increasing values of variable viscosity parameter V reduces the velocity.
- The effect of variable viscosity parameter V is to increase the temperature in the boundary layer.
- The temperature in the boundary layer decreases (increases) due to suction (injection).
- The effect of Prandtl number Pr is to decrease the thermal boundary layer thickness.
- The heat source parameter  $H_{sx}$  increases the heat transfer in both PEST and PEHF cases and the opposite is observed in the case of a sink.
- Thermal boundary layer thickness increases with the increase in the radiation parameter.

#### REFERENCES

- [1]. B. C. Sakiadis, "Boundary-layer behavior on continuous solid surfaces I: The boundary layer on a equations for two dimensional and axisymmetric flow," AIChE J, vol.7, pp. 26-28, 1961a.
- [2]. B.C. Sakiadis, "Boundary-layer behavior on continuous solid surfaces II: The boundary layer on a continuous flat surface," AIChE J, vol. 7, pp. 221-225, 1961b.
- [3]. B. C. Sakiadis, "Boundary-layer behavior on continuous solid surfaces III: The boundary layer on a continuous cylindrical surface," AIChE J, vol. 7, pp. 467-472, 1961c.
- [4]. L. E. Erickson, L. T. Fan, and V. G. Fox, "Heat and mass transfer on a moving continuous flat plate with suction or injection," Ind. Engng. Chem. Fund., vol. 5, pp. 19-25, 1969.
- [5]. L. J. Crane, "Flow past a stretching plate," ZAMP, vol. 21, pp. 645-647, 1970.
- [6]. J. Vleggar, "Laminar boundary layer behavior on continuous accelerating surfaces," Chem. Eng. Sci., vol. 32, pp. 1517-1525, 1977.
- [7]. P. S. Gupta, and A. A. Gupta, "Heat and mass transfer on a stretching sheet with suction or blowing," Can. J. Chem. Engg., vol. 55, pp. 744-746, 1977.
- [8]. L. J. Grubka, and K. M. Bobba, "Heat transfer characteristics of a continuous stretching surface with variable temperature," ASME J. Heat Transfer, vol. 107, pp. 248-250, 1985.
- [9]. C. K. Chen, and M. I. Char, "Heat transfer of a continuous stretching surface with suction or blowing," J. Math. Anal.Appl., vol. 135, pp. 568-580, 1988.
- [10]. P. G. Siddheshwar, and U. S. Mahabaleshwar, "Effects of radiation and heat source on MHD flow of a viscoelastic liquid and heat transfer over a stretching sheet," Int. J. Nonlinear Mech., vol. 40, pp. 807-820, 2005.
- [11]. K. B. Pavlov, "Magneto hydro dynamic flow of an incompressible viscous fluid caused by deformation of a plane surface," MagnitanayaGidrodinamika (USSR), vol. 4, pp. 146-147, 1974.
- [12]. A. Chakrabarti, and A.S. Gupta, "Hydrodynamic flow and heat transfer over a stretching sheet," Quart. Appl. Math., vol. 37, pp. 73-78, 1979.
- [13]. H. I. Anderson, "MHD flow of a viscoelastic fluid past a stretching surface," Acta Mech., vol. 95, pp. 227-230, 1992.
- [14]. H. Herwig, and G. Wickern, "The effect of variable properties on laminar boundary layer flow," WärmeStoffubert, vol. 20, pp. 47-57, 1986.

## Influence of Thermal Radiation on Mhd Boundary Layer Flow In A Newtonian Liquid With Temperature Dependent Properties Over An Exponential Stretching Sheet

---

- [15]. H. S. Takhar, S. Nitu, and I. Pop, "Boundary layer flow due to a moving plate: variable fluid properties," *Acta. Mech.*, vol. 90, pp. 37-42, 1991.
- [16]. I. Pop, R. S. R. Gorla, and M. Rashidi, "The effect of variable viscosity on flow and heat transfer to a continuous moving flat plate," *Int. J. Eng. Sci.*, 30, pp. 1-6, 1992.
- [17]. M. Subhash Abel, S. K. Khan, and K. V. Prasad, "Study of viscoelastic fluid flow and heat transfer over a stretching sheet with variable fluid viscosity," *Int. J. Non-Linear Mech.*, vol. 27, pp. 81-88, 2002.
- [18]. A. Pantokratoras, "A further results on the variable viscosity on the flow and heat transfer to continuous moving flat plate," *Int. J. Eng. Sci.*, vol. 42, pp. 1891-1896, 2004.
- [19]. M. E. Ali, "The effect of variable viscosity on mixed convection heat transfer along a vertical moving surface," *Int. J. Thermal Sci.*, vol. 45, pp. 60-69, 2006.
- [20]. H. I. Andersson, and J. B. Aarseth, "Sakiadis flow with variable fluid properties: revisited," *Int. J. Eng. Sci.*, vol. 45, pp. 554-561, 2007.
- [21]. K. V. Prasad, Dulal Pal, and P. S. Datti, "MHD power law fluid flow and heat transfer over non-isothermal stretching sheet," *Comm. Non-Linear Sci. Numer. Simulat.*, vol. 14, pp. 2178-2189, 2009.
- [22]. G. N. Sekhar, and A. S. Chethan, "Heat transfer in a stretching sheet problem in electrically conducting Newtonian liquids with temperature dependent viscosity," Proceedings of the ASME 2010 International Mechanical Engineering Congress & Exposition IMECE2010, November 12-18, 2010, British Colombia, Vancouver, Canada, ISBN 978-07918-3891-4, order No. 1858DV.
- [23]. E. Magyari, and B. Keller, "Heat and mass transfer in the boundary layers on an exponentially stretching continuous surface," *Journal of Physics D: Applied Physics*, vol. 32, pp. 577-585, 2000.
- [24]. E. M. A. Elbashbeshy, "Heat transfer over an exponentially stretching continuous surface with suction," *Arch. Mech.*, vol. 53(6), pp. 643-651, 2001.
- [25]. M. K. Partha, P. V. S. N. Murthy, and G. P. Rajashekhar, "Effect of viscous dissipation on the mixed convection heat transfer from an exponentially stretching surface," *Heat Mass Transfer*, vol. 41, pp. 360-366, 2005.
- [26]. S. K. Khan, and E. Sanjayanand, "Viscoelastic boundary layer flow and heat transfer over an exponential stretching sheet," *Int. J. Heat and Mass Transfer*, vol. 48, pp. 534-542, 2005.
- [27]. E. Sanjayanand, and S. K. Khan, "On the heat and mass transfer in a viscoelastic boundary layer flow over an exponentially stretching sheet," *Int. J. Therm. Sci.*, vol. 45, pp. 819-828, 2006.
- [28]. M. Sajid, and T. Hayat, "Influence of thermal radiation on the boundary layer flow due to an exponentially stretching sheet," *Int. Comm. Heat Mass Transfer*, vol. 35, pp. 347-356, 2008.
- [29]. G. N. Sekhar, and A. S. Chethan, "Flow and heat transfer of an exponential stretching sheet in Boussinesq-Stokes suspension," *Int. J. Mathematical Archive*, vol. 3(5), pp. 1978-1984, 2012.
- [30]. R. Cortell, "Radiation effects in the Blasius flow," *Applied Mathematics and Computation*, vol. 198, pp. 333-338, 2008.
- [31]. M. A. El-Aziz, "Radiation effect on the flow and heat transfer over an unsteady stretching sheet," *International Communications in Heat and Mass Transfer*, vol. 36, pp. 521-524, 2009.
- [32]. A. Ishak, "Radiation effects on the flow and heat transfer over a moving plate in a parallel stream," *Chinese Physics Letters*, vol. 26, 034701, 2009.
- [33]. A. Ishak, "MHD boundary layer flow due to an exponentially stretching sheet with radiation effect," *SainsMalaysiana*, vol. 40, pp. 391-395, 2011.
- [34]. S. Mukhopadhyay, "Slip effects on MHD boundary layer flow over an exponentially stretching sheet with suction/blowing and thermal radiation," *Ain Shams Engineering Journal*, vol. 4, pp. 485-491, 2013.
- [35]. A. S. Chethan, and G. N. Sekhar, "Flow and heat transfer of quadratic stretching sheet in a Boussinesq-Stokes suspension," *International Journal of Applied Mechanics and Engineering*, vol. 16(4), pp. 1109-1128, 2011.
- [36]. A. S. Chethan, and G. N. Sekhar, "Flow and heat transfer of an exponential stretching sheet in a Boussinesq-Stokes suspension," *International Journal of Mathematical Archive*, vol. 3(5), pp. 1978-1984, 2012.
- [37]. Pradeep G Siddheshwar, G. N. Sekhar, and A. S. Chethan, "MHD flow and heat transfer of an exponential stretching sheet in Boussinesq-Stokes suspension," *Journal of Applied Fluid Mechanics*, vol. 7(1), pp. 169-176, 2014.
- [38]. Pradeep G Siddheshwar, G. N. Sekhar, and A. S. Chethan, "Flow and heat transfer in a Newtonian liquid with temperature dependent properties over an

- exponential stretching sheet," Journal of Applied Fluid Mechanics, vol. 7(2), pp. 367-374, 2014.
- [39]. A. S. Chethan, G. N. Sekhar, and Pradeep G Siddheshwar, "Flow and heat transfer of an exponential stretching sheet in a viscoelastic liquid with Navier slip boundary condition," Journal of Applied Fluid Mechanics, vol. 8(2), pp. 223-229, 2015.

# Production and Characterization of Rice Husk Ash-Silicon Carbide Reinforced Al11100 Aluminium Alloy Hybrid Composites

[<sup>1</sup>] Ghanaraja S, [<sup>2</sup>] Gireesha B L, [<sup>3</sup>] Ravikumar K S, [<sup>4</sup>] Madhusudan B M

[<sup>1</sup>] P.E.S College of Engg., Dept. of Mechanical Engg., Mandya, India ,

[<sup>2</sup>] Malla Reddy Engg college and Management Science, Dept. of Mechanical Engg, Hyderabad, India

[<sup>3</sup>] Maharaja Institute of Technology, Dept. of Mechanical Engg., Mysore, India.

[<sup>4</sup>] GSSSIETW, Dept. of Mechanical Engg., Mysore, India

**Abstract:** --Aluminums Matrix Composites (AMCS) are light weight, high-strength materials with potential applications in areas such as automobiles, aerospace, defence, engineering and other industries. Stir casting route is the most promising one for synthesizing discontinuous reinforcement aluminium matrix composites because of its relative simplicity and easy adaptability with all shape casting process used in metal casting industry. The objective of developing aluminium alloy based metal matrix hybrid composites using stir casting is to study their mechanical properties. Hybridization of metal matrix composites is the introduction of more than one type/kind, size and shape of reinforcement during processing of composites. The advantages of one type of reinforcement could complement with what are lacking in the other. As a consequence, a balance in cost and performance can be achieved through proper material design. The liquid metallurgy route (stir casting technique) was successfully adopted in the preparation of aluminium alloy, magnesium (3 wt%) is added to achieve good wettability and hybrid composites containing 3, 6, 9, 12 and 15 wt% of SiC particles and constant 3 wt% of rice husk ash. There is an effort to understand the microstructure study of the cast hybrid composites including particle distribution and defects like porosity in order to correlate with the observed mechanical properties measured in terms of hardness and tensile properties.

**Index Terms**— AMCS, Al 1100; Hybrid composite; Rice Husk Ash; SiC

## I. INTRODUCTION

Many of our modern day technology require materials with unusual combinations of properties that cannot be met by the conventional metal alloys, ceramics and polymeric materials. This is especially true for materials that are needed for aerospace, underwater and transportation applications. During the past few years, material design has shifted emphasis to pursue light weight, environment friendliness, low cost, quality, higher service temperature, higher elastic modulus, improved wear resistance and performance [1-5]. Hybridization of metal matrix composites is the introduction of more than one type/kind, size and shape of reinforcement during processing of composites. It is carried out to obtain synergistic properties of different reinforcements and matrix used, which may not be realized in monolithic alloy or in conventional monocomposites [6-9]. Hybridization of monocomposites with second reinforcement i.e. introduction of more than one reinforcements simultaneously during processing, can be carried out by most of the conventional monocomposites fabrication techniques [10]. The primary composite processing techniques, such as, stir casting, infiltration process, spray deposition process, in-situ and powder metallurgy techniques can be used [11].

Stir casting route is the most promising one for synthesizing discontinuous reinforcement aluminium matrix composites because of its relative simplicity and easy adaptability with all shape casting process used in metal casting industry. This method involves producing a melt of the selected matrix material, followed by the introduction of the reinforcing materials in to the melt and obtaining a suitable dispersion through stirring [12]. Hybridization of metal matrix composites is carried out to obtain synergistic properties of different reinforcements and matrix used, which may not be realized in monolithic alloy or in conventional monocomposites [13-17].

The present study involves synthesis of hybrid composites by adding constant wt% of rice husk ash and different wt% of silicon carbide particles in to molten aluminium alloy during stirring. The objective of developing hybrid composites in this study by stir casting is to study their potential applications in structural components and the mechanical properties of these composites is, therefore, essential for the present study. There is an effort to understand the microstructure of the composites including particle distribution and defects like porosity, in order to correlate with the observed mechanical properties measured in terms of hardness and tensile properties.

## II. EXPERIMENTAL METHODOLOGY

Al 1100 of 99.674% purity and commercial magnesium of 99.92% purity is used as the matrix for the synthesis of particle reinforced metal matrix composites. The molten Al 1100 was alloyed with magnesium since it promotes wetting between the molten alloy and the oxide particles. Silicon Carbide (SiC) of average size 25-30  $\mu\text{m}$  and Rice Husk Ash (RHA) of average size 0.5-5 $\mu\text{m}$  are used as the reinforcements.

### A. Stir Casting and Its Experimental Setup

About 700 g of commercially pure Al 1100 was melted and superheated to a desired processing temperature in a clay-graphite crucible inside the muffle furnace. Before any addition, the surface of the melt was cleaned by skimming. The weighed amount of powders was added into molten Al 1100 at a processing temperature of 900°C and the rate of addition of particles was controlled at an approximate rate 6-8 g/min. A coated mechanical stirrer was used to disperse the rice husk ash and SiC particles in the melt. The speed of the stirrer was kept constant at 300 rpm. A non-contact type speed sensor was used to measure the stirring speed. The temperature of the melt was measured by using a digital temperature indicator connected to a chromel-alumel thermocouple. During stirring, the temperature of the slurry was maintained within  $\pm 10^\circ\text{C}$  of the processing temperature. A magnesium lump of 3 wt% was wrapped by aluminium foil and plunged into the melt-particle slurry after the addition of rice husk ash and SiC particles. When the desired time of the stirring elapsed, reduce the stirrer speed. After completion of processing steps, the graphite stopper at the bottom of the crucible is removed by using the lever to pour the melt-particle slurry into split type graphite coated and preheated permanent steel mould. The mould is kept right below the graphite stopper, the mould containing that cast ingot is allowed to cool in air, in order to achieve better uniformity in distribution of the particles throughout the casting.

**Table 1: Nominal composition of the hybrid composite**

DESIGNATION OF HYBRID COMPOSITE	MAGNESIUM (WT%)	RICE HUSK ASH (WT%)	SILICON CARBIDE (WT%)
AM	3	0	0
AMRS3	3	3	3
AMRS6	3	3	6
AMRS9	3	3	9
AMRS12	3	3	12

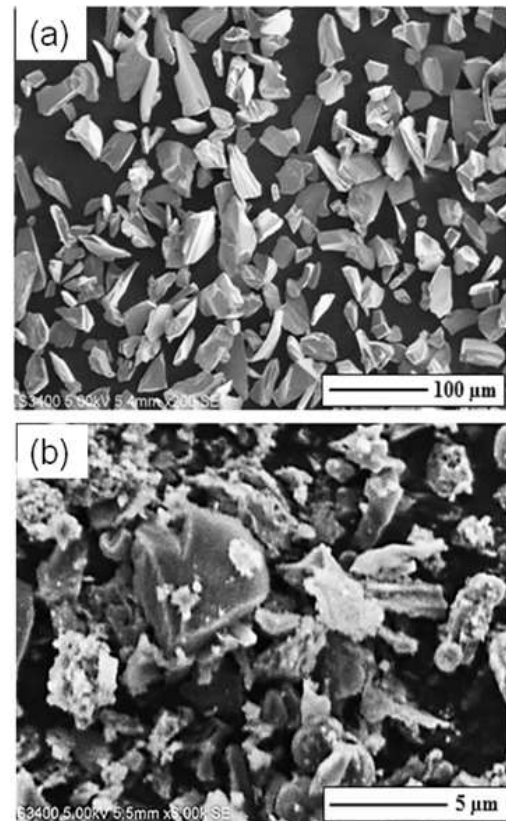
Different hybrid composites have been synthesized by adding silicon carbide and rice husk ash powders as given in

Table 1 and these hybrid composites have been designated by using the letters AM to indicate Al 1100-Mg (3 wt%) alloy followed by a letter R indicates rice husk ash powder (3 wt% constant in all hybrid composites). The fourth digit S indicates silicon carbide powder, followed by the number indicating the wt% of SiC powder added.

## III. RESULTS AND DISCUSSIONS

### A. Morphology of SiC and Rice Husk Ash

The size and particle shape of the SiC (average size 25  $\mu\text{m}$  – 30  $\mu\text{m}$ ) and RHA (average size 0.5  $\mu\text{m}$  – 5  $\mu\text{m}$ ) particles in the powder has been observed under SEM and the results are shown in Figure 1 (a) and (b) respectively, it is also observed that smaller and longer particles are irregular in shape.



**Fig 1: SEM micrograph showing size and shape of the a) silicon carbide powder and b) RHA Powder used in the synthesis of Al1100 (Mg)-SiC-RHA hybrid composites**

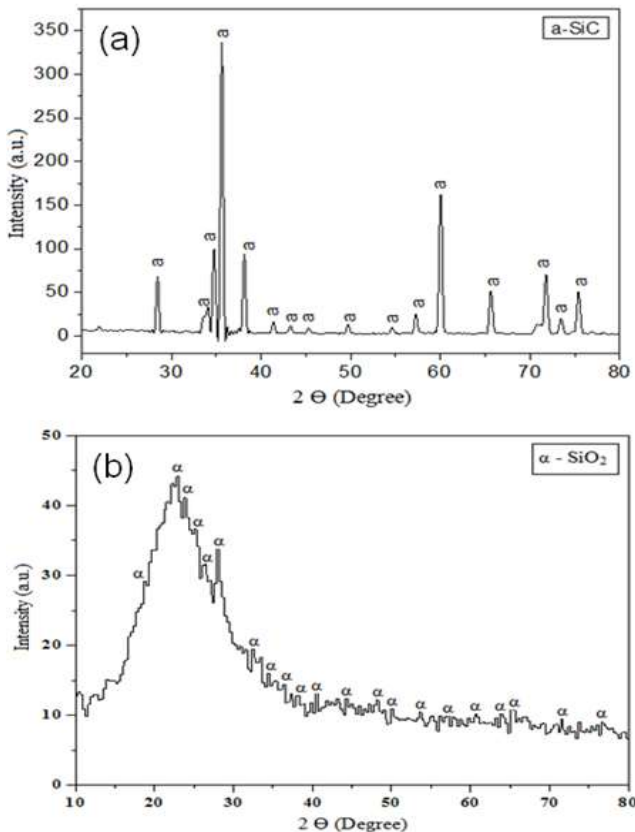


**Fig 2: XRD pattern of a) Silicon Carbide particles and b) Rice husk ash used in the synthesis of Al1100 (Mg)-SiC-RHA hybrid composites**

The SiC and RHA powder has been examined for their X-ray diffraction (XRD) pattern using X-ray diffractometer in the two theta range of 10-80° and 5-80° respectively, using CuKα radiation target and nickel filter, step size and dwell time were suitably adjusted. This was used for identification of various phases with the help of inorganic JCPDS (joint committee on powder diffraction standards) x-ray diffraction data card which shows the SiC and RHA particles are fairly pure.

#### B. Microstructure Studies on Hybrid Composites

Figure 3 shows SEM micrographs of different hybrid cast composites (a) AMRS3, (b) AMRS6, (c) AMRS9, (d) AMRS12 and (e) AMRS15 respectively, which reveals similar phase but their weight fraction varies depending upon the amount of rice husk ash and silicon carbide particles additions. The hybrid composite AMRS15 has more distributed phase than AMRS3. In general, porosity (dark spots not clearly visible due to uneven surface) in the

composites increases with increasing in addition of rice husk ash and silicon carbide particles. This is often attributed to attachment of particles with bubble during processing. This attachment takes place during particle transfer by stirring. It may also happen during solidification as the dissolved gases start nucleating on the heterogeneous surface of particles. Often these bubbles are not able to float out rapidly due to increased density because of attached particles and get entrapped during solidification, enhancing porosity in cast composites. Thus, porosity increases with increasing addition of Silicon Carbide and Rice husk ash (constant 3 wt%) particles in cast hybrid composites.

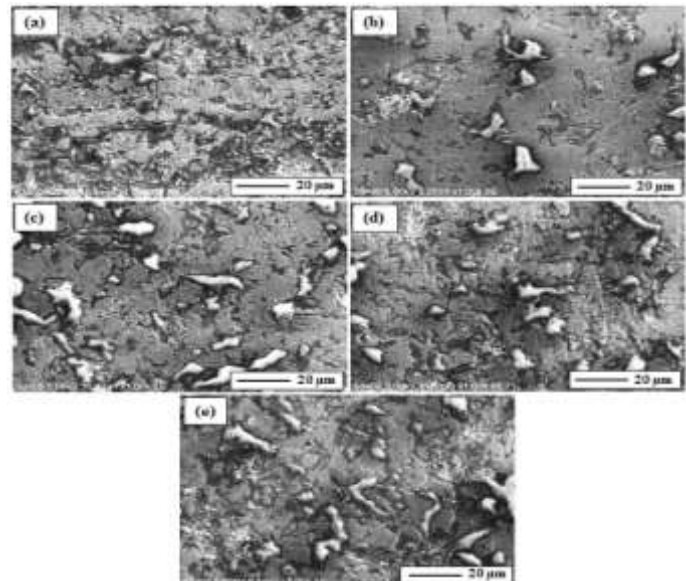


**Fig 3: SEM micrographs of different hybrid cast composites developed by constant 3 wt% of Rice husk ash and increasing wt% of SiC particles designated as (a) AMRS3, (b) AMRS6, (c) AMRS9, (d) AMRS12, and (e) AMRS15 respectively**

The particle distribution in the hybrid composites, developed by the addition of Rice husk ash (3 wt% constant) and silicon carbide particles, shows almost individual particles and no significant clustering in hybrid composites AMRS3 and AMRS6 respectively. As the weight percentage of Silicon Carbide particles increases beyond 9 wt% significant clustering of particles is observed.

#### C. Hardness of Hybrid Composites

The hardness of the cast hybrid composites increases with increasing addition of silicon carbide particles to the base alloy up to 9 wt% of silicon carbide particles. The hardness decreases for AMRS12 and AMRS15 may be due to

increased porosity and poor interface bonding between matrix and reinforcement particles as observed in Figure 4.

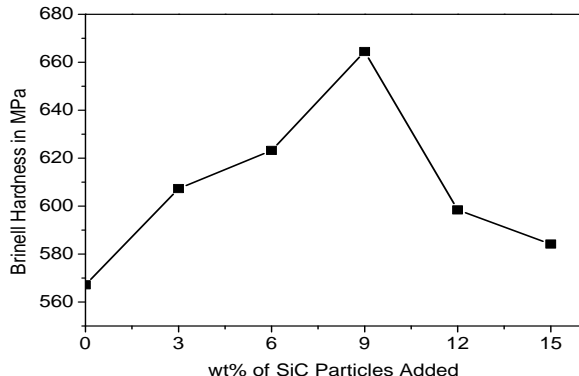


**Fig 4:** Variation of average Brinell hardness in cast hybrid composites developed by constant 3 wt% of Rice husk ash and 3, 6, 9, 12 and 15 wt% of SiC particles designated as AM, AMRS3, AMRS6, AMRS9, AMRS12 and AMRS15 respectively

#### D. Tensile Properties of Hybrid Composites

The variation of yield strength, tensile strength and percentage of elongation in the cast hybrid composites developed by addition of 3, 6, 9, 12 and 15 wt% of SiC and keeping rice husk ash 3 wt% constant is as shown in Figure 5.

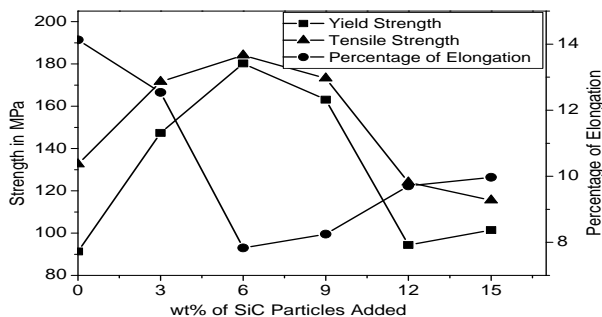


**Fig 5:** Variation of yield strength, tensile strength and percentage elongation in composites developed by by addition of RHA and SiC powder

In the composites percentage of elongation decreases with increase in wt% of SiC powder addition up to 6 wt% of SiC particles, further increasing in addition of SiC powder shows improvement in the percentage elongation. The tensile strength increases with increasing the addition of SiC particles up to 6 wt% in the cast composites, tensile strength decreases with further increase in wt% of SiC particles. The yield strength increases with increasing the addition of SiC particles up to 6 wt% in cast composites,

yield strength decreases with further increase in wt% of SiC particles.

#### IV. CONCLUSION

Cast composites have been synthesized by addition of the desired amount of silicon carbide and rice husk ash particles in to the molten Al 1100-Mg alloy followed by stir casting in permanent mould. The influence of increasing the wt% of SiC particles addition (3 wt% Rice husk ash kept constant) on evolution of cast microstructure and their impact on the mechanical properties of the resulting hybrid composites has been investigated.

1. The liquid metallurgy route (stir casting technique) was successfully adopted in the preparation of hybrid composites containing 3, 6, 9, 12 and 15 wt% of SiC particles and constant 3 wt% of rice husk ash.
2. XRD and SEM/EDAX analysis shows the SiC particles are fairly pure and the shape of the SiC particles are irregular and sharp edged. The Rice husk ash was amorphous form and irregular in shape.
3. The microstructure of the hybrid composite shows that particles are mostly occurring individually although there are some clusters of two or three particles observed at composite with higher content of SiC.
4. The hardness of the cast hybrid composite increases with increasing the addition of SiC up to 9 wt% (constant 3 wt% of rice husk ash) and thereafter hardness decreases.
5. There is increasing yield strength and tensile strength in hybrid composite developed with increasing addition of SiC powder up to 6 wt% (constant 3 wt% of Rice husk ash) beyond this addition impairs yield strength and tensile strength.
6. The cast hybrid composite developed from 6 wt% of SiC particles and 3 wt% rice husk ash exhibited good yield strength of 180.2 MPa, tensile strength of 184.1 MPa and percentage elongation of 5.63.

#### REFERENCES

- [1] Aakash Kumar and Prabhutosh Kumar, "A review on the mechanical properties, tribological behavior and the microstructural characterization of Aluminium metal matrix composites (AMMCs)", International Journal of Scientific & Engineering Research, Vol 6, pp.1234-1245, 2015.
- [2] Ankit Mittal and Ramnarayan Muni, "Fabrication and characterization of Mechanical Properties of Al-RHA-Cu Hybrid Metal Matrix Composites", International Journal of Current Engineering and Technology, Vol 3, pp.1779-1783, 2013.

## Production and Characterization of Rice Husk Ash-Silicon Carbide Reinforced Al1100 Aluminium Alloy Hybrid Composites

---

- [3] Hanamantrygouda and Shivakumar, "Effect of Forging condition on Mechanical Properties of Al/SiC Metal Matrix Composites", Vol 4, Issue 05, International Journal of Engineering Research & Technology, pp.567-571, 2015.
- [4] Velliyangiri, Muralidharan, M. Ranjith, G. Ranjithkumar and M. Sheik Alavutheen, "International Journal of Intellectual Advancements and Research in Engineering Computations", pp.192-199, 2015.
- [5] RabindraBehera, S. Das, D. Chatterjee and G. Sutradhar, "Forgeability and Machinability of Stir Cast Aluminum Alloy Metal Matrix Composites", Journal of Minerals & Materials Characterization & Engineering, Vol 10, N, pp.923-939, 2011.
- [6] K.K. Alaneme and T.M. Adewale, "Influence of Rice Husk Ash-Silicon Carbide Weight Ratios on the Mechanical behaviour of Al-Mg-Si Alloy Matrix Hybrid Composites", Tribology in Industry, Vol 35, pp.163-172, 2013.
- [7] Dr. Haydar A. H. Al-Ethari and Israa Adnan Njem, "Effect of Graphite on mechanical and machining properties of Al-base hybrid composite", International Journal of Mechanical Engineering and Technology, Vol 5, Issue 4, pp. 61-71, 2014.
- [8] MahendraBoopathi, "Evaluating the physical properties of Aluminium 2024 in the presence of Fly ash, Silicon Carbide and its combinations", International Journal of Engineering Research and General Science Vol 2, Issue 6, pp. 792-796, 2013.
- [9] Navin and Deivasigamani, "Material characterization of Aluminium hybrid composite for clutch plate", International Journal of Research in Engineering and Technology, Vol 4, pp. 297-303, 2015.
- [10] J. AllwynKingslyGladston, N. Mohamed Sheriff, I. Dinaharan and J. David Raja Selvam, "Production and characterization of rich husk ash particulate reinforced Al6061 Aluminum alloy composites by compocasting", Transaction of Nonferrous Metal Society, China, pp.683-691, 2014.
- [11] S. Charles and V.P. Arunachalan, "Property analysis and mathematical modeling of machining properties of Aluminum alloy hybrid (Al alloy/SiC/fly ash) composites produced by liquid metallurgy and powder metallurgy techniques", Indian Journal of Engineering and Materials Sciences, Vol 11, pp. 473-480, 2014, 2014.
- [12] S.D.Saravanan and M.Senthilkumar, "Mechanical Behavior of Aluminum (AlSi10Mg)-RHA Composite", International Journal of Engineering and Technology, Vol 5, pp.4834-4840.
- [13] Jyothi and Bharath Kumar, "Comparison of mechanical properties of Al-5% Si alloy reinforced with Cow dung ash and Rice husk ash", International Journal of Latest Research in Engineering and Technology , Vol 1, Issue 4, pp. 55-58, 2015.
- [14] A.P.S.V.R. Subrahmanyam, G. Narsaraju and B. SrinivasaRao, "Effect of Rice Husk ash and Fly ash reinforcements on Microstructure and Mechanical properties of Aluminium alloy (Al-Si-10Mg) Matrix Composites", International Journal of Advanced Science and Technology, Vol 76, pp. 1-8, 2015.
- [15] Md AI Mehedi, K. M. H. Bhadhon and Prof. Dr. M.N. Haque, "Tribological characteristics of Aluminium matrix hybrid composites reinforced with SiC and Al<sub>2</sub>O<sub>3</sub>", International Journal of Innovative Research in Science, Engineering and Technology, Vol 4, Issue 8, pp. 7253-7259, 2011.
- [16] Dora Siva Prasad, ChintadaShoba and NalluRamanainah, "Investigations on mechanical properties of Aluminium hybrid composite", Materials Research and Technology, Vol 3, pp. 379-85, 2014.
- [17] K.K. Alaneme, B.O. Ademilua and M.O. Bodunrin, "Mechanical Properties and Corrosion Behaviour of Aluminium Hybrid Composites Reinforced with Silicon Carbide and Bamboo Leaf Ash", Tribology in Industry, Vol 35, pp. 25-35, 2014.

# A Numerical Study on Flow Characteristics around Two Square Cylinders in Tandem Arrangement near A Moving Plane Wall

<sup>[1]</sup>Rajendra S. Rajpoot, <sup>[2]</sup>S. Dhinakaran

<sup>[1][2]</sup>The Centre for Fluids Dynamics, Department of Mechanical Engineering, Indian Institute of Technology Indore, Madhya Pradesh, India

**Abstract:** --Numerical simulations are performed for fluid flow around two square cylinders in tandem arrangement near a moving wall at Reynolds number ( $Re$ ) = 100 (based on the height of the cylinder,  $D$ ). The influence of moving wall with cylinder-to-wall gap ratio ( $G/D$ ) = 0.5 and longitudinal inter-spacing ratio ( $S/D$ ) = 0.5 to 8.0 on the unsteady force dynamics are examined. The governing equations are solved using a finite volume method based on SIMPLE algorithm. Primary aim of this study is to highlight the wall proximity effects on the force and wake dynamics, where the flow instability occurs due to mutual interaction of the vorticity field of two bluff bodies brought near a wall. Flow characteristics are presented by streamlines, vorticity contours, lift and drag coefficient and Strouhal number, and the same are compared with the single cylinder case (cylinder placed near a moving wall). The results show that the global flow quantities are found to be large for the upstream cylinder relative to the downstream and onset of vortex shedding is seen at  $G/D$  = 0.5 and  $S/D$  = 4.0. Trends of the present results are compared with the available literature, and a fair agreement is found. Many applications such as fuel saving intelligent transport system in automobiles and pipelines near the seabed can be associated with current study.

**Keywords:** Moving plane wall, Strouhal number, Tandem cylinder, Wake dynamics.

## I. INTRODUCTION

Over the past few decades, flow around bluff bodies placed near a moving plane wall and its wake interactions through the wall has been subject of fundamental interest. This phenomenon aid better understanding of this flow scenario particularly in intelligent transport systems of fuel saving in automobiles, sea-bed pipelines under water with rough terrain ground, underwater navigation system, submarines or mining vehicles near a bed, freight train and conveyors in food processing can be cited [1-11]. Basically, early experimentations and numerical studies show that flow pattern behind the square or circular cylinder is greatly altered by proximity effects of a stationary or moving wall are not only governed by Reynolds number ( $Re$ ) but also by some other factors. In unsteady case, flow past bluff bodies is influenced by flow separation, reattachment and the unsteady vortex formation in the wake region [12]. Durao et al. [13] studied flow around a square cross section cylinder placed near a channel wall. They observed that vortex shedding can be suppressed when bluff bodies approach the ground, likewise, various parameters such as Reynolds number ( $Re$ ), aspect ratio, blockage ratio of channel, turbulence intensity and wall boundary layer thickness affects the flow. Bearman et al. [14] have reviewed the aspects of bluff body aerodynamics that are pertinent to the understanding of vehicle flows. They concluded that effects on the lift are

often sensitive to both ground proximity and ground representation whereas drag has limited to proximity only. Hence, several parameters are essential to understand the flow physics of wall proximity, wake dynamic and structural stability of bluff body. Zdravkovich et al. [15, 16] found that more than one bluff body are placed side-by-side; in tandem or staggered arrangements, they reported that resulting forces and frequency of vortex shedding may be differ from the flow past a single bluff body at same Reynolds number. In addition to this, flow becomes complex in tandem arrangements due to the existence of two bodies and their reciprocal effect on the flow pattern as a consequence of their relative spacing and position from the ground. Wake dynamics is still not completely understood due to the presence many influencing factors as discussed above. The onset and cessation of vortex shedding can be recognized in flow over a tandem bodies and it may significantly affect various flow characteristics and life of the structure. The present study is to exemplify the mechanisms of the moving ground effect. Whereas, most of the earlier studies were conducted for tandem or staggered arrangement near a fixed ground or unconfined case of bluff bodies, and they are reviewed below.

### A. Previous work

Some studies are available to investigate the wake dynamics and aerodynamic performance of square cylinders

in tandem arrangement. Etminan et al. [17] studied the unconfined flow around tandem square cylinders in the flow regimes,  $Re = 1 - 200$  and fixed longitudinal inter-spacing ratio ( $S/D$ ) = 5. They predicted the three different onset values of flow separation and observed that level of the force variation on the downstream cylinder is larger than the upstream cylinder. The fluctuating lift force acting on the upstream cylinder is strictly influenced by the phase of the flow pattern of the downstream cylinder. Chatterjee et al. [18] performed numerical investigation in the range  $50 \leq Re \leq 150$  with varying  $S/D$  from 1 to 10. They revealed that critical spacing (the minimum gap between the walls of the cylinders, if the gap less than the critical spacing ( $S/D$ )<sub>cr</sub>, vortex shedding does not occur from the upstream cylinder) decreases as the Reynolds number increases i.e. for  $Re = 100$  and 150, ( $S/D$ )<sub>cr</sub> are reported 4 - 5 and 3 - 4, respectively. Sohankar et al. [19] studied the flow characteristics for  $Re$  from 1 to 200,  $S/D = 5$  and fixed Prandtl number ( $Pr$ ) 0.71. They found that force fluctuations on the downstream cylinder is larger and relatively sharp variation in the global parameters at  $Re = 55 - 60$  due to the diversity in flow structure space between the cylinders. Bhattacharyya et al. [20] studied the wall-induced vortices play a major role on flow characteristic for tandem arrangement near a wall. Vortex shedding starts at  $Re$  beyond 125 for all values of  $S/D$ .

Limited information is available for the flow past a square cylinder placed parallel to a moving plane wall which moves at the same speed of the far field. Arnal et al. [3] studied the vortex shedding from a bluff body adjacent to a plane sliding wall, in the study three cases are investigated which correspond to flow past a square rib in a free stream, flow past a rib on a fixed wall and flow past a rib on a sliding wall. They concluded that due to presence of a wall it affects the stability of the flow and the type of vortex shedding. The presence of the wall increases the critical  $Re$  also reduce the Strouhal number ( $St$ ) at which vortex shedding occurred. Dhinakaran et al. [21] performed the numerical investigation at  $Re = 100$  and  $G/D$  from 0.1 to 4. They reveals that when  $G/D < 1$ , the twin vortex shedding pattern change completely into single row of negative vortices and ultimately the flow becomes steady, when  $G/D < 0.3$ . The coefficient of lift ( $CL$ ) and drag ( $CD$ ) of the cylinder found higher as compared to that of an isolated cylinder and  $St$  increased linearly with decreased in  $G/D$  from 4 to 1. At  $G/D = 0.3$ , vortex shedding get suppressed. Bhattacharyya et al. [22] found that a weak shear layer of negative vorticity directed by the moving wall due to the vortex shedding behind the cylinder. The frequency of vortex shedding reduces with the reduction in wall to cylinder gap height ratio ( $G/D$ ). Lift and drag experienced by the cylinder does not very much at large Reynolds number and also cylinder experienced downwards lift. In addition of this Kim et al. [23] performed the experimental study for flow characteristics of a square

cylinder with moving ground system at higher Reynolds number.

### B. Objective of this study

Objective of the present work is to study the wake dynamics and wall proximity effect on frequency of vortex shedding at  $Re = 100$  of different value of  $S/D$  and at fixed  $G/D$ . In view of the applications and inspiring flow phenomenon, an organized study is to reveal the flow characteristics past tandem square cylinders placed near a moving wall. Authors' believe that there is no numerical study available for the flow past square cylinders arranged in tandem and placed near a moving plane wall with no-slip boundary at  $Re = 100$ . This work fills the literature gap and is of significant relevance to applications like fuel saving in automobiles, mining vehicles near sea -bed etc.

## II. MATHEMATICAL FORMULATION

### Problem description

As shown in Fig. 1 (a), two fixed identical square cylinders with height,  $D$ , are kept in tandem arrangement placed near a plane wall which is moving same as the velocity of far field,  $U_\infty$ . The distance between the lowest extremity of the cylinder and the wall is defined as 'G' and longitudinal inter-spacing distance between the two cylinders defined as 'S'. Gap ratio ( $G/D$ ) is fixed = 0.5. Longitudinal inter-spacing ratio ( $S/D$ ) varied as 0.5, 1.0, 2.0, 3.0, 4.0, 6.0 and 8.0.

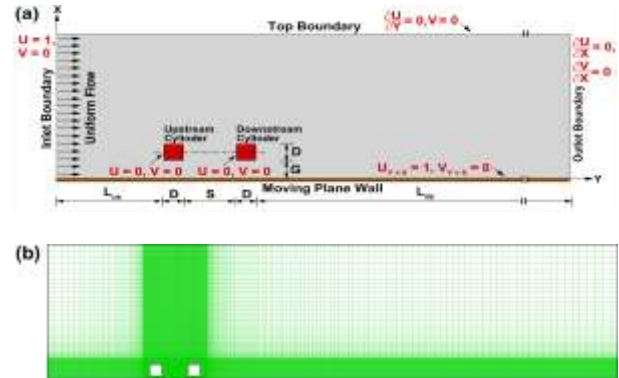


**Fig.1.** (a) Computational domain for uniform flow around the tandem square cylinders placed near a moving wall with its co-ordinate system; (b) Structured non-uniform mesh distribution in the vicinity of the plane moving wall of mesh elements clustered around a cylinder and the cylinder-to-wall gap ratio ( $G/D$ ) = 0.5 with longitudinal inter-spacing ratio ( $S/D$ ) = 2.0.

### Governing equations

The dimensionless form of the governing equation for 2D, laminar, incompressible flow from tandem square cylinder is given as:

Continuity equation:

$$\frac{\partial U}{\partial X} + \frac{\partial V}{\partial Y} = 0 \quad (1)$$

Momentum equation:

$$\frac{\partial U}{\partial \tau} + U \frac{\partial U}{\partial X} + V \frac{\partial U}{\partial Y} = - \frac{\partial P}{\partial X} + \frac{1}{Re} \left( \frac{\partial^2 U}{\partial X^2} + \frac{\partial^2 U}{\partial Y^2} \right) \quad (2)$$

$$\frac{\partial V}{\partial \tau} + U \frac{\partial V}{\partial X} + V \frac{\partial V}{\partial Y} = - \frac{\partial P}{\partial Y} + \frac{1}{Re} \left( \frac{\partial^2 V}{\partial X^2} + \frac{\partial^2 V}{\partial Y^2} \right) \quad (3)$$

The following characteristic scales are introduced to non-dimensionalize the governing equations:

$$X = \frac{x}{D}, Y = \frac{y}{D}, \tau = \frac{tU_\infty}{D}, P = \frac{p}{\rho U_\infty^2}, U = \frac{u}{U_\infty}, V = \frac{v}{U_\infty}$$

Where, ‘x’ and ‘X’ represents the horizontal coordinate, ‘y’ and ‘Y’ presents the vertical coordinate, ‘u’ and ‘U’ represents the x-components of velocity, ‘v’ and ‘V’ represents the y-component of velocity, ‘p’ and ‘P’ represents the pressure and ‘t’ and ‘τ’ represents the time. Here, small letter stands for the dimensional form of the quantity similarly same capital letter stands for the dimensionless form of the quantity. ‘ $U_\infty$ ’ represents the far field value of velocity at inlet and ‘ρ’ represents the fluid density. The dimensionless variable  $Re = \rho U_\infty D / \mu$ , is the Reynold number; ‘μ’ is the viscosity of fluid.

### C. Boundary condition

Following are the condition applied at various boundaries in order to solve the flow problem computationally. As shown in Fig.1. (a) At the inlet boundary a uniform flow profile is assumed. i.e.,  $U_\infty = 1, V = 0$ . At the top boundary symmetry boundary condition is applied. On moving plane wall, which moves at the same speed of the far field and no slip condition is applied on the surface. i.e.,  $U_{(Y=0)} = 1, V_{(Y=0)} = 0$ . At the outlet boundary, pressure outlet condition is applied and on the tandem cylinders surface no-slip condition are applied i.e.,  $U = 0, V = 0$ .

## III. NUMERICAL DETAILS

The numerical simulations are performed by utilizing the commercial CFD package ANSYS FLUENT [24]. It based on a control volume technique to solve the partial governing differential equations in a collocated grid system. The pressure based numerical scheme preferred, which solves the sequentially discretized governing equations. The two-dimensional, transient laminar viscous model with double precision selected. A QUICK scheme selected for spatial discretization. The pressure correction based iterative SIMPLE [25] algorithm used for solving the governing equation with boundary conditions, see in Fig. 1 (a), which are discussed previously. The PRESTO interpolation technique utilizes to interpolate the face

pressure from the cell center values and the second-order implicit scheme is used for time derivatives discretization. Iterations at each time step (~ 0.025) continue until the divergence-free velocity filed is obtained. The convergence criteria for the inner (time step) iterations are set as  $10^{-6}$  for discretized governing equations.

### A. Size of Computational domain, grid structure, grid dependence

A rectangular computational domain is shown in Fig. 1 (a). In order to minimize the influence of boundary effect the height of top lateral boundary, distance of the inlet and outlet boundary of domain are exclusive large far away from bluff bodies. The domain independence test is conducted in order to find out the suitable distance, the inlet boundary lies at a distance ( $L_{us}$ ) is 8D from the front surface of the upstream cylinder, distance of the top lateral boundary from the wall is 10D and the outlet boundary lies at from the rear surface of downstream cylinder ( $L_{ds}$ ) is 50D. The influence of  $L_{ds}$  on the mean drag coefficient of the cylinder is tested for three values of  $L_{ds}$ ; 45D, 50D and 55D. The value of  $L_{ds} = 50D$  has been found to be the optimum and used for this study. As shown in see Fig. 1 (b), a structured and non-uniform grid is used in the computational domain. The grid is sufficiently fine near the cylinders surface and the moving wall to capture the fine details of the flow, and course elsewhere. Following grids are used to test and assess the grid independent solution; 1200X350, 1225X700, and 1250X700. Grid 1225X700 found optimum with element size 0.005. For the sake of brevity, details of grid independence study are not presented here.

### B. Code validation

Code validation is performed in the present study. The configuration of a square cylinder near moving wall is validated with the numerical works by Dhinakaran [21] and Bhattacharyya and Maiti [22]. While, the cross-flow across square cylinders arranged in tandem is validated with the numerical attempt by Chatterjee and Mondal [18]. Acceptable variations are identified in the present results in comparison to the literature, as the maximum percentage error is reported to be 2.01%. For the purpose of brevity, any further details on code validation are skipped here.

## IV. RESULTS AND DISCUSSION

Flow around a tandem square cylinder placed near a plane wall has been considered in this study. Square cylinders of height, D, placed at fixed height, G, from the wall with different inter-spacing, S, has been investigated numerically. The following are the parameters that affect the flow field given by.

- Reynolds Number (Re): 100 (based on the height of the cylinder, D).
- Gap ratio (G/D) from the moving plane wall: 0.5
- Inter-spacing ratio (S/D): 0.5, 1, 2, 3, 4, 6, and 8.

### A. Instantaneous vorticity pattern

Instantaneous vorticity contours that grow from the tandem cylinder surfaces in the presence of a moving wall are shown in Fig. 2 at G/D = 0.5 with varying S/D = 0.5 to 8.0. Here, negative vorticity that corresponds to clockwise rotation is presented by dashed lines while the positive vorticity that correspond to anti-clockwise rotation is presented by solid lines. When single square cylinder is kept near to the moving wall at fixed G/D = 0.5, strong negative and positive vortices appear in the wake that resembles the single row vortex shedding. In order to ensure no slip, this negative wall vorticity in the gap between wall and tandem cylinders arises to suppress the tangential velocity component the wall. In case of tandem cylinders, at S/D = 0.5 wake zone is no longer same as single cylinder vorticity but still strong negative and positive vortices appear and positive vorticity from the bottom surface of cylinders starts to interact with the boundary layer negative vorticity of the wall. Tandem bodies behave as single bluff body vortex shedding occurs at cylinders. The wake is dominated mainly by the negative vortices shed from the top surface of the cylinder. At S/D = 1.0 to 3.0, steady wake formed behind the cylinder due to mutual interaction of shear layer of both the cylinder. The shedding mechanism from the upstream cylinder occurs in close conjugation with the shear layer growth on the downstream cylinder. The positive vortex that is evolving from the bottom surface of both the cylinders gets stretched when it interacts with the negative vorticity formed on the moving wall which slows the roll up process. Further increase the S/D from 3.0, a transition from a steady to an unsteady wake reported and onset of vortex shedding appears at S/D = 4.0. The positive and negative shear layers formed along the top and bottom surface of the cylinder. These negative vortices coalesce with the positive shear layer formed at the bottom surface of the cylinder and the vortices get stretched, resulting in a single row of vortices same as the single cylinder case. At S/D = 8.0, vorticity pattern of upstream cylinder similar to single cylinder vorticity patterns for the same boundary conditions means that existence of downstream cylinder not much influenced the flow patterns of upstream cylinder.

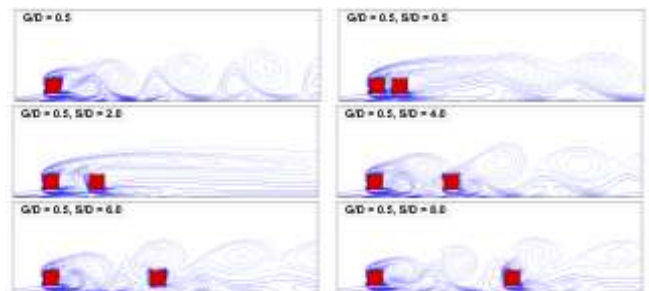


**Fig.2. Instantaneous vorticity contours at  $Re = 100$  for flow around square cylinders placed at fixed gap ratio ( $G/D = 0.5$ ) from the plane wall with varying longitudinal inter-spacing ratio ( $S/D$ ) at non-dimensional time,  $tU_{\infty}D = 300$ .**

### B. Streamlines patterns

Contours of instantaneous streamlines flow past tandem square cylinders placed near a plane moving wall are depicted in Fig. 3. At  $Re = 100$ , due dominated inertial forces as to viscous forces, flow separate from the cylinder surface at the upstream edge and reattached to downstream region of the cylinder. At  $S/D = 0.5$ , tandem bodies behaves as single bluff body and common wake appears with small two recirculation bubble. For  $S/D = 2.0$ , asymmetry wake formed with clear reattachment of flow and quasi steady flow is reported. In the region,  $2.0 < S/D < 3.0$  due to the presence of moving wall steady recirculating eddies are seen as vortex shedding is completely suppressed due to small longitudinal inter-spacing distance between the cylinders and mutual interaction of phase of flow. As same case of free stream flow across tandem cylinders, similar flow like regime proximity interference, intermediate wake interference, co-shedding regime identified in this study. Wake region is notably influenced by the proximity of the cylinder as well as  $S/D$  and presence of moving wall.

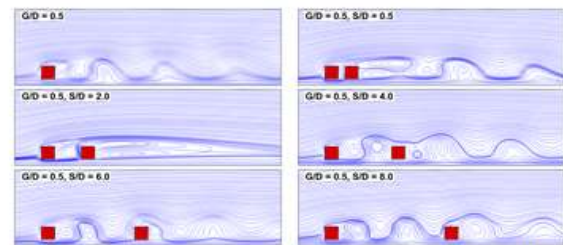


**Fig.3. Instantaneous streamline contours at  $Re = 100$  for flow around square cylinders placed at fixed gap ratio ( $G/D = 0.5$ ) from the plane wall with varying longitudinal inter-spacing ratio ( $S/D$ ) at non-dimensional time,  $tU_{\infty}D = 300$ .**

### C. Distribution of pressure coefficient on the cylinder surface ( $\bar{C}_p$ )

The variation of time averaged pressure coefficient ( $\bar{C}_p$ ) on the surface of the square cylinder is shown in Fig.4 at fixed  $G/D = 0.5$  for upstream cylinder and downstream

cylinder. The pressure distribution strongly depends on the separation ratio of the two cylinders and the moving plane wall boundary same a flow past a single cylinder case near a wall. As depicted in Fig.4 (a), the pressure coefficient shows a significant change along the bottom half of front face (AB) but this is less sensitive for varying S/D as compare to the other faces. Along the bottom face (BC), the pressure coefficient is negative with a peak suction occurring at the upstream corner of the bottom surface and this maximum for S/D = 0.6. As the separation ratio is increased the pressure coefficient increases towards the positive values along this face. It implies the difference between the pressure at the top and bottom surface of the cylinder contributes more to the total lift coefficient of the cylinder as reported at S/D > 4. Along the rear face (CD) increasing the separation ratio results in decrease in pressure coefficient due to formation of wake. Same variation observed for top surface (DA) of the cylinder due to separation of flow. As depicted in Fig.4 (b), the pressure coefficient shows a remarkable change along the bottom half of front face (EF) with variation of S/D. As increasing the S/D variation in  $\bar{C}_p$  reaching towards the single cylinder values. Along the bottom face (FG), the pressure coefficient is negative at the upstream corner of the bottom surface for all S/D except for S/D = 0.6. Distinct variation is reported for top surface (HE) of the cylinder due to flow separation and reattachment of the flow form the upstream cylinder.

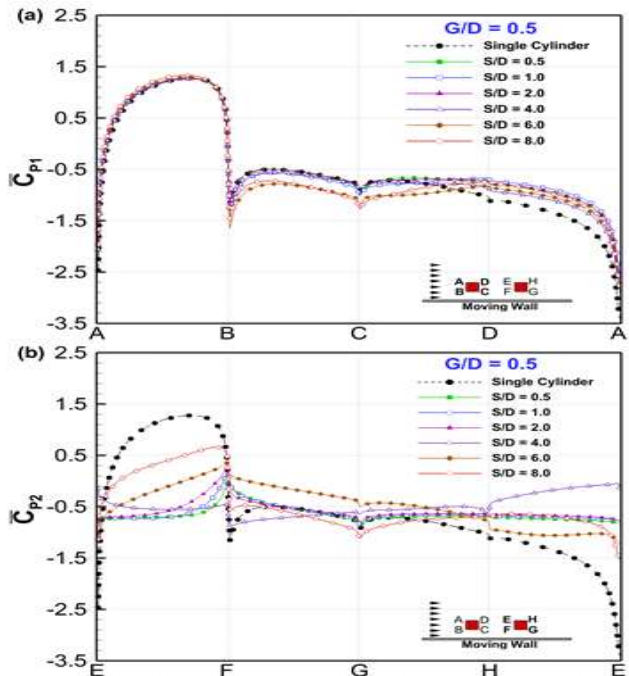


Fig. 4. Distribution of time averaged pressure coefficient ( $\bar{C}_p$ ) on the surface of the square cylinders at gap ratio ( $G/D$ ) = 0.5, near a stationary plane wall as a function of longitudinal inter-spacing ratio ( $S/D$ ), subscript '1' and '2' stand for upstream and downstream cylinder, respectively.

#### D. Time Averaged lift coefficient ( $\bar{C}_L$ )

As Fig. 5 (b) present the variation of times averaged lift coefficient  $\bar{C}_{L1}$  and  $\bar{C}_{L2}$  show the variation at  $Re = 100$  for different  $S/D$ . The Value of  $\bar{C}_L$  high for upstream cylinder and strongly dependent on  $S/D$ . As expected, lift coefficient of upstream cylinder more as compare to downstream cylinder. It is also observed that, the lift coefficient increases as increasing in  $S/D$ . It happens due to the increase in pressure along the bottom face of the cylinder. The proximity to the wall induces an increasing effect in the lift coefficient. At higher value of  $S/D$ , the values of lift coefficients approaches towards value of the single cylinder due to less influence of the downstream cylinder on upstream one.

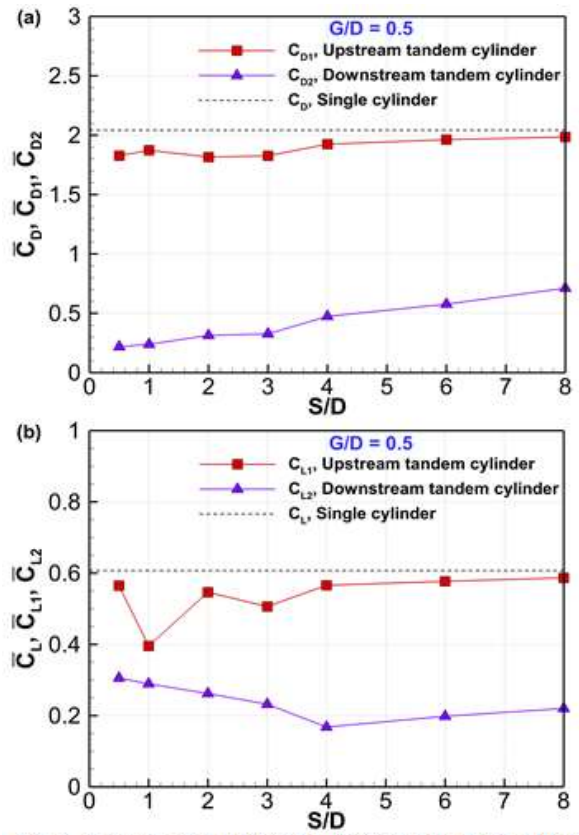


Fig. 5. A comparison between upstream and downstream cylinder time averaged drag ( $\bar{C}_D$ ) and lift ( $\bar{C}_L$ ) coefficient at  $Re = 100$  and gap ratio ( $G/D$ ) = 0.5 at different longitudinal inter-spacing ratio ( $S/D$ ). Dashed lines denote the single cylinder counterpart at  $G/D = 0.5$ .

#### E. Time Averaged lift coefficient ( $\bar{C}_D$ )

As Fig. 5 (a) present the variation times averaged drag coefficient  $\bar{C}_{D1}$  and  $\bar{C}_{D2}$  show the variation at  $Re = 100$  for different  $S/D$ . Drag coefficients are higher for upstream cylinder as compare to the downstream one and strongly dependent on  $S/D$ . It is also observed that, the drag coefficients increased as increases the  $S/D$  ratio for both

cylinders. The influence of S/D on drag coefficients is higher as compare to single cylinder case. Same as lift coefficient behavior value of drag coefficients approached towards value of the single cylinder at increase S/D.

#### F. Streamwise mean gap velocity profile

As shown in Fig. 6 the mean gap velocity profiles in x - direction obtained in the tandem configuration compared with the same G/D and compared with single cylinder case. It presents the variation of the mean gap velocity ( $U_M$ ) for downstream cylinders in the gap between the cylinder,  $y/(G/D) = 1$ , and the moving wall,  $y/(G/D) = 0$ , for varying S/D. The shape of UM velocity profile observed as inverted 'C' type. It started from the same as moving wall than velocity sharp change in the velocity is known as the inflection point crosses and finally it reached gradually to the no slip velocity condition on bottom wall of upstream or downstream cylinder. As increases, the value of the local maximum velocity decreases as the cylinder is brought closer to the moving wall. Minimum peak of mean gap velocity observed at  $S/D = 0.5$  and maximum at  $S/D = 8.0$  more close to single cylinder velocity profile. In overall, the jet action observed between the cylinders is increased due to the presence of moving wall.

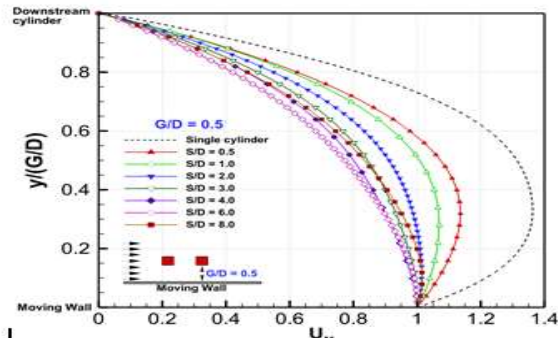


Fig. 6. Streamwise mean gap velocity ( $U_M$ ) for downstream cylinder of tandem arrangement at  $Re = 100$  and cylinder to gap ratio ( $G/D$ ) = 0.5 with different longitudinal inter-spacing ratio ( $S/D$ ).

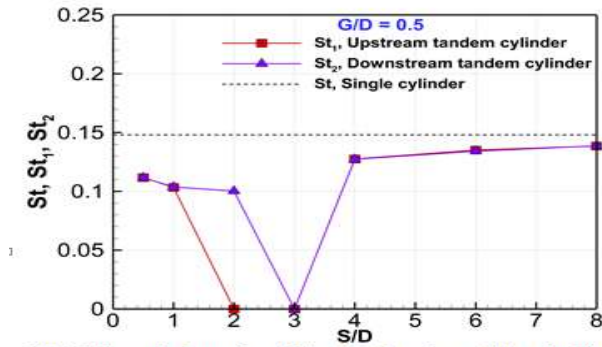


Fig. 7. Strouhal number ( $St$ ) as a function of longitudinal inter-spacing ratio ( $S/D$ ) for the flow around tandem square cylinders near a moving wall.

#### G. Strouhal Number ( $St$ )

The Strouhal Number ( $St$ ) is a non-dimensional parameter to analyzing oscillating unsteady fluid flow dynamics. Fig. 7 presents the variation of  $St$  of the downstream cylinder with varying  $S/D$  at fixed  $G/D$ . In proximity interference regime vortex shedding get suppressed from the upstream cylinder and tandem bodies behaves a single body because of vortex shedding occurs behind the rear cylinder. In intermediate wake interference regime intermittent vortex shedding can be observed between the separations. In case of co-shedding regime vortex shedding can be occurs from both the cylinders. These regimes can be identified as follows:  $0.5 \leq S/D \leq 1$  is proximity interference,  $2 \leq S/D \leq 3$  is intermediate wake interference and  $S/D \geq 4.0$  is co-shedding regime. When cylinder kept near a wall the intermediate (wake interference) regime exhibits much lower values of  $St$  than in the proximity interference and co-shedding regimes same as free stream tandem cylinder case. The presence of the moving wall accelerates the onset of co-shedding as  $S/D \geq 4$  sudden increments reported in  $St$ .

## V. SUMMARY AND CONCLUSIONS

In the present study, flow over tandem square cylinders in the vicinity of a moving plane wall has been investigated for understanding the wake dynamics behind a fixed cylinder at a gap ratio,  $G/D = 0.5$  and  $Re = 100$ . The longitudinal inter-spacing ratio,  $S/D$  is varied from 0.5 to 8.0. The plane wall is moving with the same velocity as far field. Numerical simulations have been performed based on finite volume method, by using the SIMPLE algorithm. A dimensionless time step size of 0.025 is used in this computation. The convergence criteria for the inner (time step) iterations are set as 10-6 for discretized governing equations. Some of the important conclusions are presented as follows:

- i. The flow is unsteady and periodic for  $0.5 \leq S/D \leq 1.0$  and  $4.0 \leq S/D \leq 8.0$ . Presence of a moving wall hastens the onset of vortex shedding. Single-row vortices are observed for  $4.0 \leq S/D \leq 8.0$ . At  $S/D = 2.0$ , where the flow remains quasi-steady, and for  $S/D = 3.0$  the vortex shedding is suppressed.
- ii. Average lift coefficient of the upstream cylinder ( $\bar{CL}_1$ ) is higher compared to the average lift coefficient of the downstream ( $\bar{CL}_2$ ) cylinder for all  $S/D$  values.
- iii. Drag coefficient ( $\bar{CD}_1$ ) of the downstream cylinder is higher than that of the upstream cylinder drag coefficient ( $\bar{CD}_2$ ) as  $S/D$  is increased. It is found that, the flow interactions of upstream and downstream cylinders in presence of the moving wall results in higher force fluctuations for the downstream cylinder compared the upstream one.
- iv. Average pressure coefficient ( $\bar{C}_p$ ) along the surface of upstream and downstream cylinders show a significant

- change as S/D is decreased. The Strouhal number (St) increases gradually as S/D is incremented from 4.0 to 8.0.
- v. A comparison of the results for single and tandem cylinders with same boundary condition shows that, as S/D is increased, values of global parameters for upstream cylinder approaches the single cylinder case.

## REFERENCES

- [1] J. E. D’Souza, R. K. Jaiman, and C. K. Mak, “Dynamics of tandem cylinders in the vicinity of a plane moving wall,” *Computers & Fluids*, vol. 124, pp. 117–135, Jan. 2016.
- [2] A. Rao, M. C. Thompson, T. Leweke, and K. Hourigan, “Dynamics and stability of the wake behind tandem cylinders sliding along a wall,” *Journal of Fluid Mechanics*, vol. 722, pp. 291–316, Mar. 2013.
- [3] M. Arnal, D. Goering, J. Humphrey, Vortex shedding from a bluff body adjacent to a plane sliding wall, 354 *Journal of fluids engineering* 113 (3) (1991) 384–398.
- [4] G. Bosch, M. Kappler, and W. Rodi, “Experiments on the flow past a square cylinder placed near a wall,” *Experimental Thermal and Fluid Science*, vol. 13, no. 3, pp. 292–305, Oct. 1996.
- [5] F. Alfieri, M. K. Tiwari, A. Renfer, T. Brunschwiler, B. Michel, and D. Poulikakos, “Computational modeling of vortex shedding in water cooling of 3D integrated electronics,” *International Journal of Heat and Fluid Flow*, vol. 44, pp. 745–755, Dec. 2013.
- [6] A. R. Bath, “Deep Sea Mining Technology: Recent Developments and Future Projects,” *Offshore Technology Conference*, 1989.
- [7] P. Hoagland, S. Beaulieu, M. A. Tivey, R. G. Eggert, C. German, L. Glowka, and J. Lin, “Deep-sea mining of seafloor massive sulfides,” *Marine Policy*, vol. 34, no. 3, pp. 728–732, May 2010.
- [8] S. Watkins and G. Vino, “The effect of vehicle spacing on the aerodynamics of a representative car shape,” *Journal of Wind Engineering and Industrial Aerodynamics*, vol. 96, no. 6–7, pp. 1232–1239, Jun. 2008.
- [9] Fred Browand and Charles Radovich, “Experimental Measurement of the Flow Field of Heavy Trucks,” May 2005.
- [10] N. Barry, D. Burton, J. Sheridan, M. Thompson, N. A. Brown, Flow field interactions between two tandem 369 cyclists, *Experiments in Fluids* 57 (12) (2016) 181.
- [11] Fred Browand and Charles Radovich, “Experimental Measurement of the Flow Field of Heavy Trucks,” May 2005.
- [12] T. Kim, B. Lee, Y. Park, D. Lee, and D. Lee, “The Study on a Vortex Shedding around Square Cylinders near a Wall,” 41st Aerospace Sciences Meeting and Exhibit, Jan. 2003.
- [13] D. F. G. Durao, P. S. T. Gouveia, and J. C. F. Pereira, “Velocity characteristics of the flow around a square cross section cylinder placed near a channel wall,” *Experiments in Fluids*, vol. 11, no. 6, Oct. 1991.
- [14] P. W. Bearman, “Review—Bluff Body Flows Applicable to Vehicle Aerodynamics,” *Journal of Fluids Engineering*, vol. 102, no. 3, p. 265, 1980.
- [15] M. M. Zdravkovich, “Flow induced oscillations of two interfering circular cylinders,” *Journal of Sound and Vibration*, vol. 101, no. 4, pp. 511–521, Aug. 1985.
- [16] M. M. Zdravkovich and P. W. Bearman, “Flow Around Circular Cylinders—Volume 1: Fundamentals,” *Journal of Fluids Engineering*, vol. 120, no. 1, p. 216, 1998.
- [17] A. Etminan, M. Moosavi, and N. Ghaedsharifi, “Determination of flow configurations and fluid forces acting on two tandem square cylinders in cross-flow and its wake patterns,” *International Journal of Mechanics*, 5, pp. 63–74, 2011.
- [18] D. Chatterjee and B. Mondal, “Forced Convection Heat Transfer from Tandem Square Cylinders for Various Spacing Ratios,” *Numerical Heat Transfer, Part A: Applications*, vol. 61, no. 5, pp. 381–400, Mar. 2012.
- [19] A. Sohankar and A. Etminan, “Forced-convection heat transfer from tandem square cylinders in cross flow at low Reynolds numbers,” *International Journal for Numerical Methods in Fluids*, vol. 60, no. 7, pp. 733–751, Jul. 2009.
- [20] S. Bhattacharyya and S. Dhinakaran, “Vortex shedding in shear flow past tandem square cylinders in the vicinity of a plane wall,” *Journal of Fluids and Structures*, vol. 24, no. 3, pp. 400–417, Apr. 2008.
- [21] S. Dhinakaran, “Heat transport from a bluff body near a moving wall at Re=100,” *International Journal of Heat and Mass Transfer*, vol. 54, no. 25–26, pp. 5444–5458, Dec. 2011.
- [22] S. Bhattacharyya and D. K. Maiti, “Vortex shedding from a square cylinder in presence of a moving wall,” *International Journal for Numerical Methods in Fluids*, vol. 48, no. 9, pp. 985–1000, 2005.
- [23] T.Y. Kim, J.H. Rho, Y.C. Ku, J.Y. Kim, Y.P. Kohama, and D.H. Lee, “An Experimental study for flow characteristics of a Square Cylinder with Moving Ground System,” CWE2006, Yokohama, pp.661–664, 2006.
- [24] Ansys Fluent, “14.0: Theory guide, Ansys,” Inc., Canonsburg, PA, 2011.
- [25] S. Patankar, “Numerical heat transfer and fluid flow,” CRC press, 1980.

# An Experimental Study on Suppression of Vortex Shedding with Different Structural Configurations

<sup>[1]</sup> Sanal M V, <sup>[2]</sup> Prof. Sunil A S

<sup>[1]</sup> P G Scholar, GEC Thrissur, India

<sup>[2]</sup> Associate Professor in Mechanical Engineering, GEC Thrissur, India

**Abstract**— The flow phenomena around bluff bodies or non-streamlined bodies in fluids are always of some engineering importance. Most of the engineering structures like buildings, bridges etc. can be considered as bluff bodies as far as the air or water flow in which the structure is being situated, is considered. This paper aims at the study of vortex induced vibration and suppression of the VIV on some common models of structures which can be considered, of having some engineering importance. The main parameter associated with the VIV formation is the Strouhal number (St.) which is the non-dimensional frequency of vortex shedding. The VIV was captured by using Fieldpaq Dynamic Signal Analyzer which has frequency ranges from 0 Hz to 40 kHz. The cylinders with varying number of fins and splitter plate length are tested. The methods to control VIV can be classified into three as active, passive or compound method. The passive method, would give some structural modifications on the model and considered to reduce the VIV formation. On the other hand, Among these, the active and compound methods are costlier compared to the passive method. Therefore on an economic point of view the engineers are keen to develop more and more methods to suppress the VIV effectively with a lesser cost i.e., by employing the passive method. My study is on employing the model with straight fins.

**Index Terms** — bluff bodies, vortex induced vibration, vortex shedding

## I. INTRODUCTION

In recent years, the flow around the bluff body has one of the subject of interest to engineers because of its engineering importance. Researcher's attention were on the control of vortex shedding behavior behind the bluff body which cause the flow-induced vibration and acoustic noise, and also resonance by increasing the mean lift and drag fluctuations. For prevent the problems due to the vortex shedding, there are two main flow control techniques: active control and passive control. Active control which is based on applying some external energy to the flow field while the passive control techniques control the vortex shedding by changing or modifying the shape of the bluff body or by attaching additional devices to the flow. Some of passive control techniques are Splitter plates, small rods, base bleed, roughness elements and helical wires.

Bearman (1984)[1] wrote a comprehensive review on the mechanism of vortex shedding from bluff bodies. He explains that the formation of a vortex-street wake is a mutual interaction between two separating shear layers is a key factor .It is find by Gerrard that a vortex continues to grow, fed by circulation from its connected shear layer, it is enough to draw the opposite shear layer across the near wake and also the approach of oppositely signed vorticity, in sufficient concentration, which cuts off further supply of

circulation to the growing vortex, which is then shed and moves off downstream."

S. Ozono (1999)[2] conduct numerical study on flow Control of vortex shedding by a splitter plate that are asymmetrically arranged downstream of a cylinder and he find the Suppression of vortex shedding is possible when the splitter plates were arranged asymmetrically also Length of splitter plate did not have much effect on flow structure.

In the paper put forward by D Sumner[3], an extensive study of the Reynolds number effect for the aerodynamic force would also be beneficial, similar to what has been conducted for the strouhal numbers. For side by side cylinders there is general lack of aerodynamic force measurements in particular the mean lift force, over a range of Reynolds number, compared to the other two basic configurations

Lee Kee Quen et al. (2003) [4]presented a paper on Investigation of the effectiveness of helical strakes in suppressing VIV of flexible riser and find out that the Experimentally Studies effectiveness of strakes by varying the height (h) and pitch (p) Effective configuration : $p=10D, h=0.10D$  (considering hydrodynamic forces)

Zachary J. Taylor (2012)[5] worked on Effects of leading edge geometry on the vortex shedding frequency is an

elongated bluff body at high Reynolds numbers and summarizes that Results show that the linear decrease in the shedding frequency of nearly about 40% as the leading edge separation angle is increased from  $0^\circ$ – $90^\circ$ .

### Components And Description

The instrument and component that are used in the experimental study are given below

- Water channel
- FieldpaqDynamic Signal Analyzer
- Collecting tank with water level measuring scale
- Hook gauge
- Pitot tube

### II. EXPERIMENTAL SET UP

The experiment in the present study were performed in fluid mechanics laboratory of department of mechanical engineering. The Experiments were performed in two steps: Dye visualization experiments and vibration analyzing experiments. description of apparatuses used in the experiment is given below.

#### Facility

Tests were carried out in a recirculating water channel with a test section 0.25m wide, 0.30m deep and 4.5m long, as seen in Fig.1. Side walls and bottom of the section were made of glass mounted on a steel frame for flow visualization. This is particularly useful for test conditions with very low Reynolds number.



Fig:1 .water channel

The baffles are provided in the flow field in order to stabilize the accelerated fluid and flow of fluid can controlled by valves provided on the inlet pipe. The inclination of water channel can be also adjusted by hand wheel mechanism. A movable platform with height gage is provided on the top of water channel for measuring the height of domain of flow. All experiments presented in this

work were conducted at the test section of the water channel.

Fieldpaq Dynamic Signal Analyzer is used as vibration meter for getting vibration of geometry model due to the vortex shedding .the frequency of this is called as vortex shedding frequency

The optional Vibration Meter software on the Fieldpaq allows you to measure four The Vibration Meter software also has built in ISO 10816-3 Standard for checking vibration severity. The user may also import his own severity standard if desired.

### III. VISUALIZATION OF VORTEX SHEDDING

Flow visualization produced by photographing particles travelling in water current is shown in Fig.2 As the free stream approaches the cylinder the flow splits around the body. Viscous boundary layers will develop from the front stagnation point while the flow remains attached to the walls. It is within the boundary layer that fluid viscous forces are playing a important role. The geometry of the body generates an adverse pressure gradient that, acting on the viscous prole of the boundary layer, will cause the flow to separate from the wall at the separation points on each side.

The visualization is done in this experiment by NIKONE DSLR CAMERA and also by using the die in the flow. For different velocity of flow the vortex shedding phenomenon was observed and some image are given below.



Fig 2: vortex shedding visualization

### IV. EXPERIMENT AND TABULATION

The experiment was conducted in water channel installed in fluid mechanics lab. The procedure for doing the experiment was make the constant velocity for all geometry models by adjusting the inlet valve and depth of flow. Then note the reading like time and vibration frequency etc. the experimental values and obtained graphs are given below.

**Experiment with a circular cylinder fitted with rectangular fins**



**Fig:2 Cylinder with rectangular fins**

**V. EXPERIMENT WITH A CIRCULAR BARE CYLINDER**

sentence punctuation follows the brackets [2]. Multiple references [2], [3] are each numbered with separate brackets [1]–[3]. When citing a section in a book, please give the relevant page numbers [2]. In sentences, refer simply to the

Depth Of flow	Water height	velocity	Reynolds number	Strouhal frequency	St.
9.42	0.56	0.3215	3855.06	8.80	0.2737
8.54	0.47	0.3037	3412.36	8.02	0.2641
8.13	0.45	0.2971	3338.20	7.80	0.2625
7.44	0.36	0.2657	3067.98	6.67	0.2510
6.92	0.30	0.2626	2725.84	6.10	0.2323
6.65	0.28	0.2344	2633.71	5.23	0.2231

**Table 1:experiment for bare cylinder**

**CIRCULAR CYLINDER FITTED WITH TWO FINS**

**Dimension : D = 10 mm, H = .0.2D**

Flow velocity(m/s)	Reynolds Number	Strouhal frequency	Strouhal number (St.)	% reduction (St.)
0.2971	3338.20	7.65	0.2575	1.9

**Table 2**

**CIRCULAR CYLINDER FITTED WITH THREE FINS**

**Dimension : D = 10 mm, H = .0.2D**

Flow velocity(m/s)	Reynolds Number	Strouhal frequency	Strouhal number (St.)	% reduction (St.)
0.2971	3338.20	7.12	0.2396	8.70

**Table 3**

**CIRCULAR CYLINDER FITTED WITH FOUR FINS**  
**Dimension : D = 10 mm, H = .0.2D**

Flow velocity(m/s)	Reynolds Number	Strouhal frequency	Strouhal number (St.)	% reduction (St.)
0.2971	3338.20	6.78	0.2282	13.06

**Table 4**

**CIRCULAR CYLINDER FITTED WITH FIVE FINS**  
**Dimension : D = 10 mm, H = .0.2D**

Flow velocity(m/s)	Reynolds Number	Strouhal frequency	Strouhal number (St.)	% reduction (St.)
0.2971	3338.20	4.75	0.1598	39.09

**Table 5**

**CIRCULAR CYLINDER FITTED WITH SIX FINS**  
**Dimension : D = 10 mm, H = .0.2D**

Flow velocity(m/s)	Reynolds Number	Strouhal frequency	Strouhal number (St.)	% reduction (St.)
0.2971	3338.20	4.88	0.1643	38.57

**Table 6**

**VI. RESULTS AND DISCUSSION**

Strouhal number v/s Reynolds number.

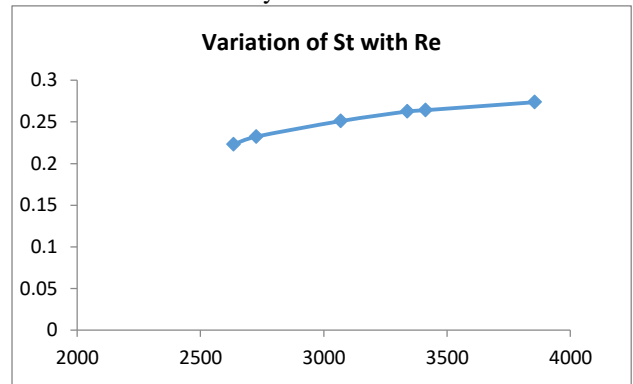


**Fig 3:variation of St with Re**

The graph shows the variation of Reynolds number with strouhal number and which indicated that The characteristics of the flow around a cylinder placed near a plane boundary are governed mainly by the Reynolds number and geometric shape of the body and also the gap. As the velocity increases, the Reynolds number increases , but the VIV frequency also increases with increase in flow velocity.

### Variation of St. with frequency

As the value of velocity (or Reynolds number) increases, the Strouhal number St also increases. This is because of the fact that increased flow velocity will produce more and more disturbances on the cylinder, so the induced vortex shedding frequency will also be high. But the variation in the velocity is small, as compared to the corresponding variation in the value of frequency. So as a result the corresponding value of Strouhal number will also be high, as compared to the value of St for low Reynolds number (ie, flow velocity).

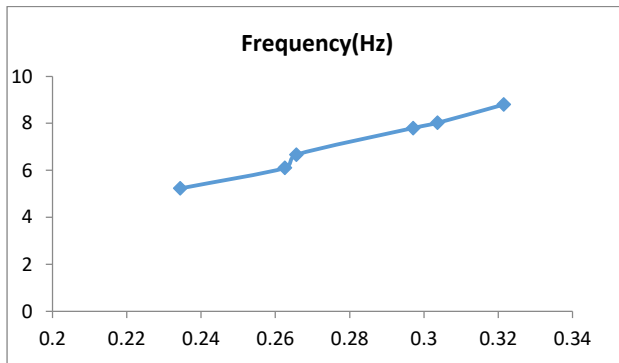


Fig 4: variation of St. with frequency

### Variation of strouhal number for different structural configurations

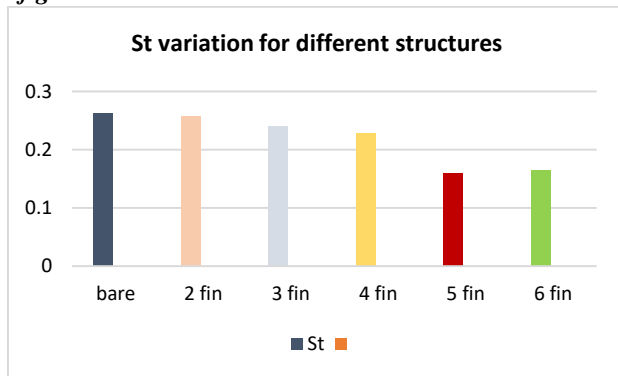


Fig 5: variation of St. for various models

From the figure, it is clear that the value of Strouhal number is minimum for the cylinder with five fin configuration. As the number of fins increased further, the VIV frequency also increases, thereby increasing the strouhal number ,St.

In the downstream or the wake region, due to boundary layer separation and adverse pressure gradient, the fluid particles flow gets reversed. This result in the formation of eddies. There is no vortex shedding occurs at  $Re=40$ . At  $Re=100$ , flow around the cylinder becomes unstable. Vortex shedding still occurs in the wake of finned tubes. The

system of projecting fins was the most effective device for suppressing vortex induced excitations of the cylinder. From this study we can concluded that the cylinder with rectangular fins is an effective device for suppressing vortex induced excitations of the cylinder. As a passive vortex control method, linear array of projecting fins is very effective in suppressing vortex shedding. Also the frequency of vortex shedding reduced drastically by fins of suitable height.

## VII. CONCLUSION

- The vortex shedding frequency of a circular cylinder is found out for different structural configurations in terms of Strouhal number.
- The frequency variation was minimum for cylinder with 5 fins. Hence it is a more stable configuration..
- Increasing the number of fins beyond a certain limit has adverse effect on the VIV reduction property of the finned cylinder configurations.
- As the number of fins increases the VIV suppression capability is reduced beyond a certain limit.
- In this experiment, the addition of fins beyond 5 nos reduced the stability of the structure.

## REFERENCE

1. Bearman, P. W., Brankovic, M., 2006. Measurements of transverse forces on circular cylinders undergoing vortex-induced vibration. Journal of Fluids and Structures 22, 829-836.
2. S.Ozono, 1999, Flow control of vortex shedding by a short splitter plate asymmetrically arranged downstream of a cylinder, Phys. Fluids 11, 2928
3. Durao, D.G, Heitor, M.V, Pereira, J.F 1988: ‘Measurement of turbulent and periodic flows around a square cylinder’, Experiments in Fluids, Vol.6, p. 298-304.
4. Lee KeeQuen (2014), “Investigation on the effectiveness of helical strakes in suppressing VIV of flexible riser”. Applied Ocean Research 44, 82–91
5. Zachary J. Taylor, Gregory A. Kopp, 2014 Effects of leading edge geometry on the vortex shedding frequency of an elongated bluff body at high Reynolds numbers, J. Wind Eng. Ind. Aerodyn. 128 66–75
6. K. Kwon, H. Choi. 1996 ‘Control of laminar vortex shedding behind a circular cylinder using splitter plates’. Phys. Fluids 8 479-486
7. Korkischko I, Meneghini JR. 2010 ‘Experimental investigation of flow-induced vibration on isolated and tandem circular cylinders fitted with strakes’. Journal of Fluids and Structures;26:611–25.

8. K. Kwon, H. Choi. 1996 ‘Control of laminar vortex shedding behind a circular cylinder using splitter plates’. *Phys. Fluids* 8 479-486
9. Shan Huang, Andy Sworn. ‘Hydrodynamic coefficients of two fixed circular cylinders fitted with helical strakes at various staggered and tandem arrangements’. *Applied Ocean Research* 43 (2013) 21–26
10. Shan Huang. 2011 ‘VIV suppression of a two degree of freedom circular cylinder and drag reduction of a fixed circular cylinder by the use of helical grooves’. *Journal of Fluids and Structures* 27 1124–1133
11. T. Zhou, S.F. Mohd. Razali, Z. Hao, 2011 On the study of vortex-induced vibration of a cylinder with helical strakes. *Journal of Fluids and Structures* 27 ,903–917
12. R A. Kumar\*, Chan-Hyun Sohn ,H.L. Gowda 2008 Passive Control of Vortex-Induced Vibrations: An Overview Recent Patents on Mechanical Engineering 2008, 1, 1-11

# Monitoring of Elderly/Blind Patients Health Remotely Through Wearable Sensors

[<sup>1</sup>] Nasreen Taj M.B., [<sup>2</sup>] Firoz Khan, [<sup>3</sup>] Imran Khan, [<sup>4</sup>] Sandeep Telkar R

[<sup>1</sup>][<sup>2</sup>][<sup>3</sup>] Department of IS&E, GMIT, Davangere, India

[<sup>4</sup>]Department of CS&E, KLS VDIT, Haliyal, India

**Abstract**— The paper represents how to monitor health remotely by the use of wearable sensors, mainly for care holders. Serviceable sensors will assist elderly persons for self-sustaining who are living alone in their homes. This approach focusing on the welfare of elderly persons. There is a drastic change in technology and modern style of coping paradigm authorize coexistent acquisition, computing and keep an eye on activities in home automation. The system given specific features can be serviceable gadgets to behold the complete health prime of the patient and an automation application software for relatives will decrease expenses incurred for maintaining health and health practitioner's burden in attentive units. Moreover, it also helpful for relatives to keep an eye on activities of elder person, whenever, they are on the outside from habitation.

**Keywords**— Arduino Uno, Internet of Things, Telegram, Wearable sensors

## I. INTRODUCTION

In frequent years, people give more importance to their work or passion than taking care of their health along with their parent's health. Elderly people and adults sometimes may forget to take medicines at proper time. If this happens multiple times may lead to deterioration of health. In this paper we propose a method to overcome these types of situations by providing reminders to such people regarding their medicines and giving them the instructions on correct time and amount. Here physical and digital reminders are combined to provide help to such people. Aim is to concentrate more on helping elderly people to take their medicine in time with correct dosage.

In today's fast-growing world elderly people and patients need a solution to carry out their daily responsibilities independently without anyone's help. The wireless and IoT technologies advancement offers a solution to make life easier and more beautiful so that elderly people can live a quality and happy life by taking their medications on time.

As the population of aging people are increasing in the society, we need to take care of elderly people but that we cannot do sometimes because of our busy schedules. So, in this paper we aim at providing an independent and quality life to elderly persons who are living alone.

## II. RELATED WORK

Taking care of elderly people is important thing, which makes difficulties for young generation as they are busy with their life and passionate things to do, at the same time they need to take care of elderly people. This leads to

difficulties for young generation who are struggling so here they introduced some of the application through which they can keep an eye on their elderly people health and medications.

In this paper a health monitoring system based on mobile application was proposed. The system proposed the access of patient's location and heart rate status by doctors and patient's relatives. The heart rate signal is measured in the proposed model using pulse sensor and then it is transmitted via Bluetooth wireless connection to smart phone. The proposed system for real-time geolocation tracking utilizes the internal GPS sensor. Then to send the obtained geolocation an alarm mechanism is developed to deliver first aid if some emergency situations arise. A module is added for messaging with the doctor [1].

The main conclusion to be drawn from this study is their system used three health sensors: body temperature sensor, heart pulse sensor and galvanic skin response sensor. By combining Arduino Uno and Raspberry Pi, all three sensors were merged into a single system. The data collected from the sensors is sent to a cloud storage through the Raspberry Pi. The cloud storage is updated continuously in real time. Then by using Android Studio they developed an Android application to access the database and show the health parameters in graphical representation. In order to understand the functioning of the sensors used, a detailed analysis of the signals was then obtained with respect to variations in physical and environmental activities [2].

The aim here is to provide health monitoring with minimal location and time constraint for the elderly [4]. In

this study a cloud-based intelligent and secure Smart home structure for elderly individuals is presented [3].

The major conclusion drawn from the paper is, the system tracks and analyze activity of senior citizen biometric data which includes pulse, weight, and blood pressure. The number of steps the seniors have taken over few weeks were tracked. This data is analyzed to find if whether increase in physical activities by senior citizens has a positive effect on the vital signs of older adults [5].

### III. PROPOSED MODEL



**Fig 1: Proposed model**

In the above fig. 1, LCD (liquid crystal display) is used to display some of the instruction to guide the elder person. Next the touch sensor is used for the instructing the blind elder person like about the things to carry while going out and the touch sensor is attached in the slipper of the blind elder person. Then the temperature sensor is used for the detecting the temperature of the elderly person home is normal or not. Gas sensor is used to detect if any harmful gas is present in the house of the elder person. Then the APR module is used to store voice which are used to instruct the blind elder person. Next Node MCU is used in this project to connect all the device and sensor through Arduino which is of 16 pins. And the last but one the Telegram is used for the send the alert message to the caretaker and blink is used as a database in this project.

## IV. MATERIALS USED

### A. Hardware requirements:

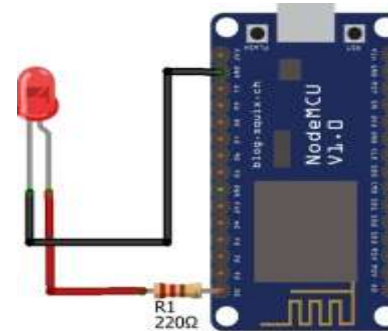
- 1) Arduino Uno



**Fig 2: Arduino Uno**

Arduino Uno (16-bit) shown in fig. 2 is a microcontroller and the platform where many of the sensors can be mounted and the required data can be fetched through those sensors.

- 2) NodeMCU



4) Touch sensors



**Fig 5: Touch sensor**

Touch sensor shown in fig. 5 is a small, simple and a low-cost electronic sensor which is used to detect and record the physical touch.

5) Gas sensors



**Fig 6: Gas Sensor**

Gas sensor shown in fig. 6 is very helpful as a safety measure which detects the gas leaks. The results obtained from these are sent to the microcontroller.

6) Temperature sensors



**Fig 7: Temperature Sensor**

Above fig 6. shows temperature sensor. These sensors measure the temperature and allow them to detect the temperature changes of the surroundings and convert these changes to data form.

7) APR 9600



**Fig 8: APR 9600**

The APR shown in fig. 8 is a low-cost high-performance device in which record/replay of the IC occurs. Even after the power supply is removed from the module, the recorded sound is retained.

**B. Software requirements:**

1) Telegram Bot



**Telegram**

Users can interact with the bots by sending messages. A telegram bot is an application hosted on the server and uses telegram Bot APIs to connect to the messenger clients.

2) Blynk



Blynk is an ideal platform to control arduino and the other devices via the internet. The blynk can be used to read, store and visualize the data and can control the hardware remotely.

3) Embedded C



Embedded C is the extension of C and is usually used in the embedded systems which are integrated together and performs operations.

**V. METHODOLOGY**

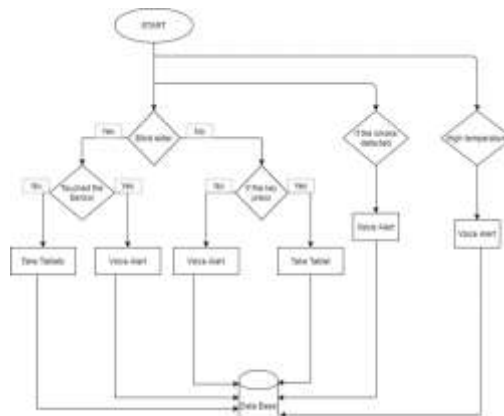


**Fig 9: Flow of the project.**

In this section we are discussing about the flow of the project shown in fig. 9. Here we have blind elder person if it is yes then we have a touch sensor to them to instruct their daily activities like here if the sensor is been sense from the blind elder person then the voice alert will be given to the elder blind person.

If the elder person is not blind then we have a button to be pressed if the elder person press the button after his daily activity is done like for example here after taking his tablet and then it is given for the database if not then it gives a voice alert like please take your tablets.

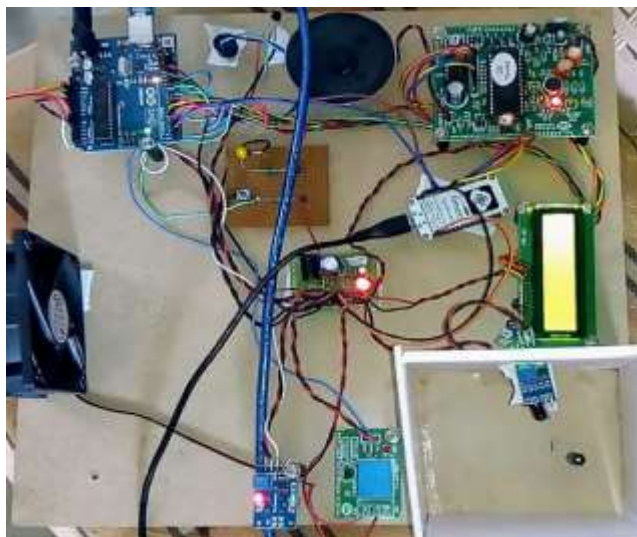
If any smoke is detected in the house of the elder person then for the elder person it gives a voice alert, Even the elder person is blind or non-blind.

Then we find any temperature variations are there in the house of the elder person then for the elder person it gives alert message like temperature is the height. Even the elder person is blind or non-blind also give voice alert.

All the data are been stored in a database here we are using a blynk has a database in this project

## VI. DESIGN AND RESULTS

In this part we are discussing about the design and the outcomes of the “Elderly person monitoring system. This system has two sectors.



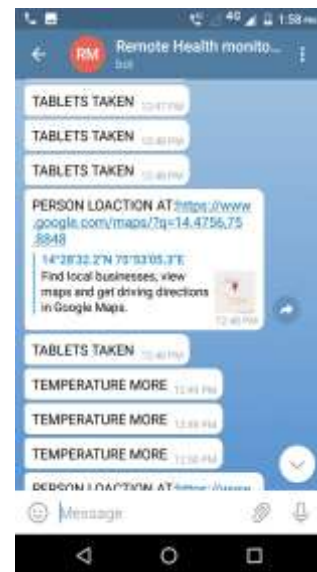
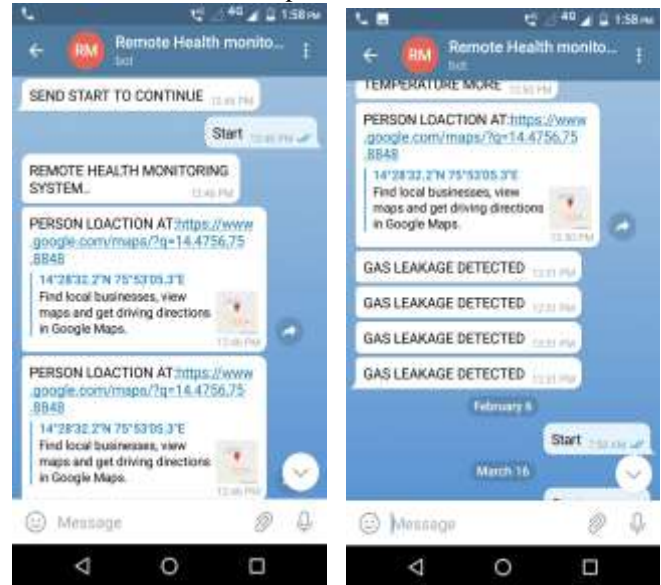
The first part is elder person with visual impaired: In this case we guide the elder person for their daily activity through the voice message or alert

And the second part is for the elder person who is good at their visual impairments: we can guide them easily through the message to telegram or through the LCD

But in some situations, we need to alert the elder person through voice alert message to be given in the both kind of elder persons.

Then here we are sending the updates message of the elder person to their caretaker through the telegram app. Even we share the location of the elder person through this telegram itself so in any emergency it gives a trace of the elder person to the caretaker.

Some of the results snapshots are as follows



## VII. CONCLUSION

To give strength for keep an eye on the everyday activities for elder person, automated application is suitable and appropriate devices due to its high functionality. In this we have used the automated mobile application, automated home, and coping services will decreases the requirements on elder people attentively and effort while computing everyday activities. It gives alerts for emergency and overall activities for elder people. Activities and alerts for any

emergency conditions are created for caretaker and relatives. It reduces the health expenses and burden of health practitioners. Our applications is good integrated with automated home atmosphere and hospital environment.

#### REFERENCES

- [1] Emre Oner Tartan, Cebrair Ciflikli: “An Android application for geolocation based health Monitoring, consultancy and alarm system”, 2018.
- [2] Sumit Paul, Mohd. Hamim, Md. Nafiu Rahman: “IOT based remote health monitoring system for patients and elderly people”, 2019.
- [3] Mohammed Mehedi Hassan, Abdulhameed Alelaiwi, and Md. Zakirul Alam Bhuiyan: “Secured and Dependable connected smart home system for elderly”, 2017.
- [4] H.M. Adam, P.J. Soh: “Development of a Health Monitoring Vest for the Elderly”, IEEE paper 2016.
- [5] Laura Sookhai, Jean F. Coppola and Chris Gaur “Intergenerational Activity Tracker Program: Impact with Health Related Outcomes on Older Adults, IEEE paper, 2015.

# Detection and Identification of Head and Neck Cancer Using Hybrid Image Processing Technique

[<sup>1</sup>] Imran Khan, [<sup>2</sup>] Firoz Khan, [<sup>3</sup>] Nasreen Taj M.B, [<sup>4</sup>] Sandeep Telkar R

[<sup>1</sup>][<sup>2</sup>][<sup>3</sup>] Department of IS&E, GMIT, Davangere, India

[<sup>4</sup>]Department of CS&E, KLS VDIT, Haliyal, India

**Abstract**—Head and Neck cancers are the most common type of cancer in the world and account for 6% of all tumors. Most of head and neck cancers are squamous cell carcinomas that develop in the upper throat as a result of exposure to risk factors. It usually presents itself in an advanced stage in older men. Cancer can start any place in the body. It starts when cells grow abnormally and crowd out normal cells. This makes it difficult for the body to work the way it should. The medical imaging tools play an important role in the early diagnosis of cancer. Medical imaging has emerged as a non-invasive tool for diagnosis of diseases. So it is important to identify cancer and know its stages in order to determining treatment options that may be tailored to needs. Here we are introducing hybrid image processing technique for noise reduction, segmentation and classification to detect and identify stages of cancer in head and neck.

**Keywords**— Head and Neck Cancer, Hybrid Image Processing Techniques

## I. INTRODUCTION

I Head and neck cancer is a disease of abnormal cells multiplying and increasing into a tumour. Cancer cells continue to increase and form new, abnormal cells. Many of them notice their disease when it's too late and the surgery is not simply possible. So finding of head and neck cancer earlier is most important for successful treatment. Diagnosis is mainly based on CT scan images. Cancerous tumour starts in the part of head and neck is called primary head and neck cancer. Following are the types of this head and neck cancer and these are divided into two main types:

1. Small cell cancer
2. Non small cell cancer

The major cause of cancer death is head and neck cancer. Detection of cancer in the early phase can provide more treatment options, less invasive surgery and increases the survival rate. A mass of tissue that originates by a slow development of strange cells is known as a tumor. Tumor cells are those cells that develop, despite the fact that when the body does not require them, and besides as typical old cells, they don't lapse. The malignancy cells present in head and neck causes head and neck growth illness. These cells discovery is critical issue for medicinal specialists. The odds of a compelling treatment will essentially increment with early recognition.

The Computed Tomography (CT) pictures are utilized which are more proficient than X-ray. Tumor cells are identified in head and neck malignancy CT pictures by utilizing marker controlled watershed grouping method. Watershed gives better results compared with other

segmentation algorithms and calculation time is less in watershed segmentation. classification algorithms Support Vector Machine and KNN is used. Evaluation would be done on the basis of correctly classified trial data. MATLAB is broadly utilized programming for the investigation of head and neck disease identification from CT filter pictures. This work concentrates on discovering tumor and its stages. In this Marker-controlled Watershed division is utilized to disengage a head and neck of a CT picture. A graphical user interface is developed to scan all the images and display the features and cancer stage. This system can help in early detection of head and neck cancer.

## II. SYSTEM DESIGN

### 2.1 SYSTEM ARCHITECTURE

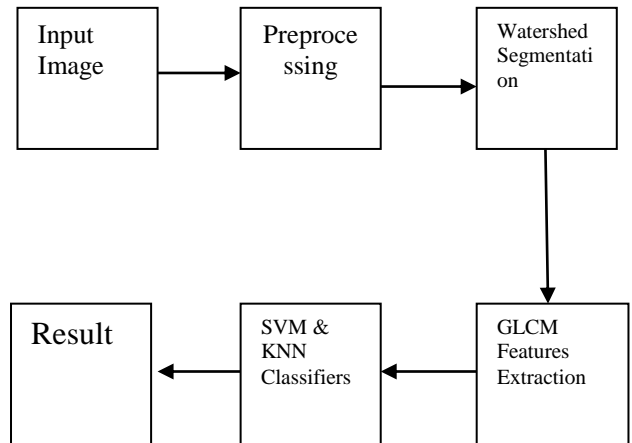


Figure 2.1 System Architecture modules

**The system architecture consist of following modules**

**Input image** :Read in the CT image slice of a particular patient.

**Preprocessing** :Pre-process the CT image slice by using adaptive mean filtering.

**Segmentation** :Segment the pre-processed image using Marker Controlled Watershed segmentation

**Feature extraction** :Extract the features from the binary image by using GLCM algorithm.

**Classifiers** :With the extracted features, identify the stage of the cancer by using SVM and KNN classifiers.

**Result** :Identifies whether the head and neck nodule is affected by cancer or not.

flowchart.0 This are the keypoints which deal with the perfect identification and formulizing the structure.

### III. IMPLEMENTATION

#### 3.1 IMAGE PREPROCESSING

Picture improvement procedures in Picture Preparing Tool kit empower you to expand the flag to clamor proportion and emphasize picture includes by changing the hues. Edge identification calculations let you distinguish question limits in a picture. These calculations incorporate the Sobel, Prewitt, Roberts, Watchful, and Laplacian of Gaussian strategies. The Watchful strategy can identify genuine feeble edges without being tricked by commotion.

A portion of the improvements Strategies are Differentiate Extending ,Commotion separating ,Histogram change.

##### 3.1.1 Adaptive Median Filtering

In our Venture We are making utilization of straight Adaptive Median Filtering. It will directly extends the first advanced estimations of the remotely detected information into new appropriation which is as appeared in figure 3.1.1 .

The above Figures 3.1.1 Show the flow Chart For Preprocessing of an image. At the start the Original image is Converted from RGB To Gray and Then it is resized To required Size. Later For which adaptive Median Filter and Histogram Equalization Techniques are Applied . Finally We get the preprocessed Output.

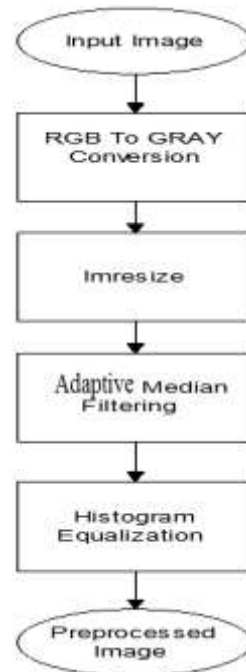


**Figure 3.1.1 flowchart for Image Preprocessing**

#### 3.2. Image Segmentation

*Image segmentation* is the way toward separating a picture into different parts. This is commonly used to recognize objects or other important data in computerized pictures. The objective of division is to improve or potentially change the portrayal of a picture into something that is more significant and simpler to examine.

##### 3.2.1. Marker Controlled Watershed Segmentation

This count considers the information picture as a topographicosurface (where higher pixel regards mean height) and reenacts its flooding from specific seed centers or markers. A typical decision for the markers are the nearby minima of the slope of the picture, yet the technique takes a shot at a particular marker, either chose physically by the client or decided naturally by another calculation. The yield of marker control watershed division yield is as appeared in figure 3.2.1

Figure 3.2.1. Shows The detailed Step By Step flow of watershed segmentation. At the beginning the preprocessed image is Given as input to the watershed segmentation. At beginning the flow starts with two part. In first part the preprocessing of image is Done as shown In figure.

In second Stage the image is transformed into L\*a\*b Colorspace from RGB. For which k-mean Clustering is obtained to find Concavity point splitting. Which is ended with Morphological processing. At the end output of both preprocessing and marker extraction is used to find watershed transform of an image.

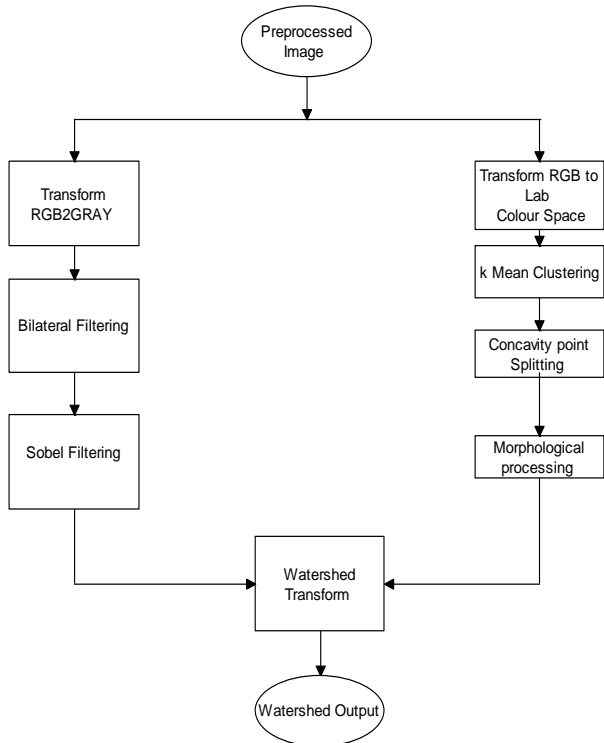


**Figure 3.2.1 Flowchart of Watershed Transform**

#### Pseudocode for Marker-controlled segmentation

```

1: procedure S=SPECTMARKER(M,I)
2: {[R],labels}=ConnectedComponents(M)
3: for k=1:|labels|do
4:   S(k)=R(k)basic spectral marker
5:   a=Activity(I(R(k)))
6:   if a>T5
7:     S(k)=TS_MRF(I(R(k))) update active regions
8:   endif
9: endfor
10: S=kS(k)aggregated marker map
11: endprocedure
    
```

#### Pseudocode for Morphological operations

```

1: procedure M=MORPHMARKER(D)
2: seeds=LocalMinima(-D)list of local minima
3: for k=1:|seeds|do
4:   s=seeds(k)
5:   SE=circle(D(s))-structuring element
6:   M(k)=Dilate(1s,SE)basic marker for s
7: endfor
8: M=kM(k)aggregated marker map
9: endprocedure
    
```

### 3.3 Feature Extraction

In machine learning, feature extraction starts from a basic course of action of measured data and a mass of induced systems (highlights) proposed to be valuable and non-dull, empowering the following learning and theory steps, and once in a while provoking better human understandings. Incorporate extraction is related to dimensionality diminishment. Exactly when the data is too many and it is suspected to be abundance (e.g. a comparable estimation in both feet andometers, or the repetition of pictures presented as pixels), at that point it can be changed into a diminished plan of parts (moreover named a component vector). Choosing a subset of the fundamental segments is called feature extraction. The picked parts are required to contain the essential information from the data, so that they desired task can be performed by using this lessened depiction as opposed to the whole beginning data.

#### 3.3.1. GrayLevel Co-Occurrence Matrix (GLCM)

One of the most commonly used technique to extract textural data of Images is GrayLevelCo occurrenceMatrix (GLCM). The GLCM technique gives sensible surface data of a picture that can be acquired just from two pixels. Dark level co-event frameworks acquainted by Haralick [30] endeavor with portray surface by measurably inspecting how certain dim levels happen in connection to other dim levels. Assume a picture to be broken down is rectangular and has Nx lines and Ny levels. Accept that the dim level showing up at every pixel is quantized into Ng levels.

Let  $L_x = \{1, 2, 3, \dots, N_x\}$  be the spatial space,  $L_y = \{1, 2, 3, \dots, N_y\}$  be the vertical spatial area, and  $G = \{0, 1, 2, \dots, N_g - 1\}$  be the arrangement of Ng quantized dim levels. The set  $L_x \times L_y$  is the arrangement of pixels of the picture requested by their row and column assignments. At that point the picture can be spoken to as an element of co-event framework that doles out some dark level in  $L_x \times L_y$ ;  $I: L_x \times L_y \rightarrow G$ . The dim level moves are ascertained in light of the parameters, dislodging ( $d$ ) and rotation ( $\theta$ ). By utilizing a separation of one pixel and edges quantized to 450 interims, four lattices of flat, first corner to corner, vertical, and second slanting (0, 45, 90 and 135 degrees) are utilized. At that point the unstandardized recurrence in the four primary headings is characterized by Condition 6.3.1(a)

$$\begin{aligned}
 hP(i, j, d, \theta) = & \# \\
 ([k, l], (m, n)) \in & [(L_x \times L_y) \times (L_x \times L_y)] \\
 k - m = 0, |l - n| = d \text{ or } & (k - m = d, l - n = -d)
 \end{aligned}$$

$$orh(k - m = -d, l - n = d) hor(|l - m| = d, l - n = 0)$$

--- (1)

$$or(k - m = d, l - n = d) hor(k - m = -d, l - n = -d)$$

$$I(k, l) h = i, I(m, n) = j$$

where # is the quantity of components in the set, z (k, l) the directions with dark level hi, (m, n) the directions with high level hj. The accompanying Figure 3.3.1 represents the above meanings of a co-event network ( $d=1$ ,  $\theta=00^\circ$ ):

			$0^\circ$	1	2	3	$45^\circ$	1	2	3
3	3	3	1	0	0	2	1	0	0	2
1	3	3	2	0	0	0	2	0	0	0
1	3	2	3	0	1	3	3	0	0	2

(a)

(b)

(c)

Figure 3.3.1(a) An example of GLCM

Despite the fact that Haralick extricated 24 parameters from co-event network, just seven are generally utilized, for example, vitality, entropy, differentiate, neighborhood homogeneity, relationship, group shade what's more, group noticeable quality as given in Conditions (2.2) to (2.8) and is put away in highlight database. In expansion, the principal arrange measurable elements (i.e., mean and standard deviation (StdDev) are utilized to portray the qualities of picture as appeared in Conditions (2.9) to (2.10) individually. The first what's more, second request factual elements are demonstrated as follows:

Vitality measures the quantity of rehashed sets and furthermore measures consistency of the standardized Network

Entropy

$$= \sum_{i,j=0}^{N-1} -\ln(P_{ij})P_{ij} \quad (2)$$

The differentiation highlight is a distinction snapshot of the P lattice and is a standard estimation of the measure of nearby varieties show in a picture. The higher the estimation of differentiation are, the more honed the auxiliary varieties in the picture

Energy

$$= \sum_{i,j=0}^{N-1} -\ln P_{ij}^2 \quad (3)$$

The contrast feature is a distinction snapshot of the P lattice and is a standard estimation of the measure of neighborhood varieties show in a picture. The higher the estimation of complexity are, the more honed the auxiliary varieties in the picture.

$$Contrast = \sum_{i,j=0}^{N-1} P_{ij} (i - j)^2 \quad (4)$$

It quantifies the sameness of the dispersion of components in the GLCM to the corner to corner. The opposite of homogeneity results in the announcement of differentiation.

$$LocalHomogeneity = \sum_{i,j=0}^{N-1} \frac{P_{ij}}{1 + (i - j)^2} \quad (5)$$

where  $P_{ij}$  is the pixel at location (i, j) of the surface picture, N is the quantity of dark levels in the picture,  $\mu = \sum_{i,j=0}^{N-1} i(j=0)^{(N-1)} P_{ij}$  is mean of the surface picture and  $\sigma = \sum_{i,j=0}^{N-1} [(P_{ij} - \mu)^2]$  is difference of the surface picture.

Correlation is the measure of similarity between two images in likeness. The measure is the mean (m), which represents the average intensity

Correlation

$$= \sum_{i,j=0}^{N-1} P_{ij} \frac{(i - \mu)(j - \mu)}{\sigma^2} \quad (6)$$

$$ClusreShade = \sum_{i,j=0}^{N-1} P_{ij}(i - M_x + j - M_y)^2 \quad 3.3.1.(f)$$

Cluster prominence

$$= \sum_{i,j=0}^{N-1} P_{ij}(i - M_x + j - M_y)^4 \quad (7)$$

Where  $M_x = \sum_{i,j=0}^{N-1} i P_{ij}$  and  $M_y = \sum_{i,j=0}^{N-1} j P_{ij}$

$$mean(m) = \sum_{i=0}^{L-1} z_i P(z_i)$$

The measure is the mean which represents the average intensity (m),

Standard Deviation ( $\sigma^2$ )

$$= \sum_{i=0}^{L-1} (x_i - m)^2 P(x_i) \quad (8)$$

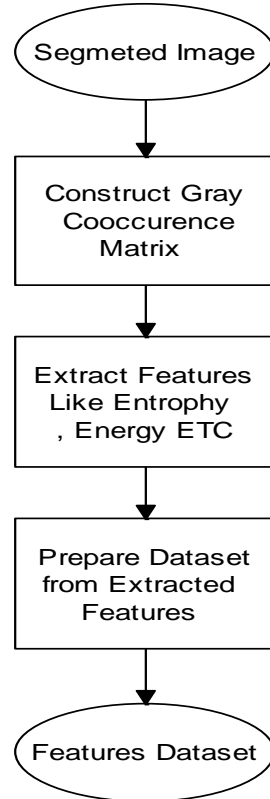


**Figure 3.3.1(b) Flowchart for GLCM**

### 3.4 Classification

Classification /Arrangement is the naming of a pixel or a gathering of pixels in light of its dark esteem. Grouping is standout amongst the frequently utilized techniques for data extraction. In Order, generally numerous elements are utilized for an arrangement of pixels i.e., many pictures of a specific question are required. In Remote Detecting region, this system expect that the symbolism of a particular geographic territory is gathered in numerous districts of the electromagnetic range and that the pictures are in great enlistment.

#### 3.4.1. Support Vector Machines (SVM)

- Used generally for arrangement/Classification (additionally, can be adjusted for relapse and notwithstanding for unsupervised learning applications).
- It meets exactness tantamount to Multilayer perceptrons

#### Definitions of SVM and Margin

Find  $f(x) = (W^T X + b)$  with maximum margin, such that for points closer to the separating hyperplane,  $|W^T X_i + b| \leq h$  (also called the support vectors) and for other points,  $|W^T X_i + b| > 1$  that  $w$  is a vector perpendicular to the hyperplane, so we have:

$$\begin{aligned}
 f(\mathbf{x}) &= f(\mathbf{x}_p + \frac{\mathbf{w}}{\|\mathbf{w}\|} \cdot r) = \mathbf{w}^T \mathbf{x}_p + \mathbf{w}^T \frac{\mathbf{w}}{\|\mathbf{w}\|} r + b \\
 &= \|\mathbf{w}\| \cdot r \quad (\text{since } \mathbf{w}^T \mathbf{x}_p + b = 0) \\
 r &= \frac{f(\mathbf{x})}{\|\mathbf{w}\|}
 \end{aligned}$$

Therefore:

Now, solve for margin length  $\rho$ :

$$\rho = \frac{f(\mathbf{x}_+) - f(\mathbf{x}_-)}{\|\mathbf{w}\|} = \frac{2}{\|\mathbf{w}\|} \quad (10)$$

#### Hypothetical Defense:

The accompanying imbalance could be inferred: some steady

$$h \leq \frac{R^2}{\rho^2} + 1 \quad (11)$$

margin  $h$  speaks to the VC measurement that measures how effective the learning calculation is. It is desirable over utilize the easiest conceivable calculation that gains adequately accurately from the given information.

In this way, we need to limit  $h$ .

Accepting a straightly detachable dataset, the errand of learning coefficients  $w$  and  $b$  of bolster vector machine  $f(\mathbf{x}) = (\mathbf{w}^T \mathbf{x}_i + b)$  decreases to taking care of the accompanying obliged streamlining issue:  $\frac{1}{2} \|\mathbf{w}\|^2$

subject to imperatives:  $y_i(\mathbf{w}^T \mathbf{x}_i + b) \geq 1, \forall i$

This streamlining issue can be comprehended by utilizing the Lagrangian work characterized as:

$$L(\mathbf{w}, b, \alpha) = \frac{1}{2} \mathbf{w}^T \mathbf{w} - \sum_{i=1}^N \alpha_i [y_i(\mathbf{w}^T \mathbf{x}_i + b) - 1],$$

such that  $\alpha_i \geq 0, \forall i$

where  $\alpha_1, \alpha_2, \dots, \alpha_N$  are Lagrange multipliers and  $\alpha = [\alpha_1, \alpha_2, \dots, \alpha_N]^T$ .

The arrangement of the first obliged streamlining issue is controlled by the seat purpose of  $L(w, b, \alpha)$  which must be limited concerning  $w$  and  $b$  and amplified regarding  $\alpha$ .

Comments about Lagrange multipliers:

The arrangement of the first obliged improvement issue is dictated by the seat purpose of  $L(w, b, \alpha)$  which must be limited concerning  $w$  and  $b$  and expanded as for  $\alpha$ . If  $y_i(\mathbf{w}^T \mathbf{x}_i + b) > 1$ , the value of  $\alpha_i$  that maximizes  $L(w, b, \alpha)$  is  $\alpha_i = 0$ .

If  $y_i(\mathbf{w}^T \mathbf{x}_i + b) < 1$ , the value of  $\alpha_i$  that increases  $L(\mathbf{w}, b, \boldsymbol{\alpha})$  is  $\alpha_i = +\infty$ . However, since  $\mathbf{w}$  and  $b$  are trying to decrease  $L(\mathbf{w}, b, \boldsymbol{\alpha})$ , they will be altered in such a way to make  $y_i(\mathbf{w}^T \mathbf{x}_i + b)$  at least equal to +1.

From this brief discussion, the so-called **Kuhn-Tucker Conditions** follow:

$$\alpha_i \{y_i(\mathbf{w}^T \mathbf{x}_{i+b}) - 1\} = 0, \forall i \quad (12)$$

Notation:

Data points  $\mathbf{x}_i$  with  $\alpha_i > 0$  are called the **support vectors**

Optimality conditions:

The essential conditions for the saddlepoint of  $L(\mathbf{w}, b, \boldsymbol{\alpha})$  are

$$\frac{\partial L}{\partial \mathbf{W}_j} = 0, \forall j \quad (13)$$

$$\frac{\partial L}{\partial \alpha \mathbf{W}_i} = 0, \forall i \quad (14)$$

$$\nabla_{\mathbf{w}} L = 0, \quad \nabla_{\boldsymbol{\alpha}} L = 0$$

or, stated a different way,

Solving for the essential conditions results in

$$\mathbf{w} = \sum_{i=1}^N \alpha_i y_i \mathbf{x}_i \quad (15)$$

$$\sum_{i=1}^N \alpha_i y_i = 0 \quad (16)$$

By restoring  $w = \sum_{i=1}^N \alpha_i y_i x_i$  into the Lagrangian function and by using  $\sum_{i=1}^N \alpha_i y_i = 0$  as a new constraint the **dual optimization problem** can be constructed as

Find  $\boldsymbol{\alpha}$  that increases  $\sum_i \alpha_i - \frac{1}{2} \sum_i \sum_j \alpha_i \alpha_j y_i y_j$   
subject to

$$\sum_{i=1}^N \alpha_i y_i = 0, \alpha_i \geq 0,$$

This is a curved quadratic programming issue, so there is a worldwide least. There are various improvements schedules fit for taking care of this enhancement issue. The streamlining can be illuminated in O(N^3) time (cubic with the extent of preparing information) and in direct time in the quantity of characteristics. (Contrast this with neural systems that are prepared in O(N) time)

Bolster Vector Machine: Last Indicator

Given the qualities  $\alpha_1, \alpha_2, \dots, \alpha_N$  acquired by arrangement of the double issue, the last SVM indicator can be communicated from as

$$f(\mathbf{x}) = \mathbf{w}^T \mathbf{x} + b = \sum_{i=1}^N \alpha_i y_i \mathbf{x}_i^T \mathbf{x} + b \quad (17)$$

where

$$\mathbf{b} = \frac{1}{|I_{support}|} \cdot e \sum_{I_{support}} \left( y_i - \sum_{i=1}^N \alpha_i y_i \mathbf{x}_i^T \mathbf{x} + b \right) \quad (18)$$

$I_{support}$  is the arrangement of bolster vectors.

### Vital remarks:

To acquire the expectation, all information focuses from the preparation information are counseled. Since  $\alpha_i \geq 0$  just for the bolster vectors, just bolster vectors are utilized as a part of giving a forecast. Take note of that is a scalar.

**Bolster Vector Machine:** Directly Nonseparable Case  
Up until this point, we have examined the development of bolster vector machines on straightly divisible preparing information. This is an extremely solid suspicion that is farfetched in most genuine applications.

**Solution:** Introducing the slack variables  $\xi_i, i=1, 2, \dots, N$ , to relax the constraint

$$y_i(\mathbf{w}^T \mathbf{x}_i + b) \geq 1 \text{ and } (\mathbf{w}^T \mathbf{x}_i + b) \geq 1 - \xi_i, \xi_i \geq 0$$

In a perfect world, one would lean toward every slack variable to be zero and this would compare to the directly detachable case. Subsequently, the enhancement issue for development of SVM on directly nonseparable information is characterized as:

find  $\mathbf{w}$  and  $b$  that minimize:  $\frac{1}{2} \|\mathbf{w}\|^2 + C \sum_i \xi_i^2$

$$\text{subject to: } y_i(\mathbf{w}^T \mathbf{x}_i + b) \geq 1 - \xi_i, \xi_i \geq 0$$

**Problem:** Support vector machines portrayed with a straight capacity  $f(x)$  (i.e. an isolating hyperplane) have exceptionally constrained representation power. Thusly, they couldn't be extremely helpful in functional characterization issues.

Uplifting news: With a little change, SVM could take care of exceeding nonlinear grouping issues!

### Avocation: Cover's Hypothesis

Assume that informational collection  $D$  is nonlinearly divisible in the first property space. The quality space can be changed into another property space where  $D$  is directly divisible!

**Caveat:** Cover's Hypothesis just demonstrates the presence of the changed property space that could take care of the nonlinear issue. It doesn't give the rule to the development of the quality change!

SVM answer for grouping

Denote  $\Phi: \mathcal{R}^M \rightarrow F$  as a mapping from the first  $M$ -dimensional credit space to the exceptionally dimensional characteristic space  $F$ .

By taking care of the accompanying double issue where  $C > 0$  is an appropriately picked parameter. The additional term maintains each slack variable to be as closed to zero as could be normal in light of the current

situation.

**Doubledissuse:** As in the directly detachable tissue, this improvement tissue can be changed over to its double tissue:

find  $\alpha$  that increases subject to

$$\sum_i \alpha_i - \frac{1}{2} \sum_i \sum_j \alpha_i \alpha_j y_i x^t_j x_j \sum_{i=1}^N \alpha_i y_i = 0 \quad (19)$$

Take note of: The result of presenting parameter C is in obliging the scope of adequate estimations of Lagrange multipliers  $\alpha_i$ . The most proper decision for C will rely on upon the particular informational collection accessible.

Issue: Bolster vector machines spoken to with a straight capacity  $f(x)$  (i.e. an isolating hyperplane) have extremely constrained depictional power. In that capacity, they couldn't be extremely helpful in useful characterization issues.

Uplifting news: With a slight adjustment, SVM could take care of exceedingly nonlinear characterization issues!!

#### **Support: cCover's Hypothesis**

Assume that informational index D is nonlinearly distinct in the first property space. The quality spaces can be changed into another characteristic spaces where D is straightly distinct!

Proviso: Cover's Hypothesis just demonstrates the presence of the changed property space that could take care of the nonlinear issue. It doesn't give the rule to the development of the quality change!

#### **SVM answer for order:**

Indicate  $\Phi: \mathbb{R}^M \rightarrow F$  as a mappings from the first M-dimensional spaces to the very dimensional characteristic spaces F.

By taking care of the accompanying double issue

find  $\alpha$  that maximizes

$$\sum_i \alpha_i - \frac{1}{2} \sum_i \sum_j \alpha_i \alpha_j y_i y_j \Phi(x_i)^T \Phi(x_j) \quad (20)$$

subject to

$$\sum_{i=1}^N \alpha_i y_i = 0 \quad (21)$$

the resulting SVM is of the form

$$f(x) = w^T \phi(x_i) + b = \sum_{i=1}^N \alpha_i y_i \phi(x_i)^T \phi(x) + b \quad (22)$$

**Viable Problem:** Although a SVM are effective in managing profoundly dimensional characteristic spaces, the way that the SVM preparing scales directly with the quantity of properties, and considering a restricted memory space could to a great extent confine the decision of mapping  $\Phi$ . Arrangement: Kernel Trick

It permits registering scalar items (e.g. ) in the first property space. It takes after from Mercer's Theorem:

There is a class of mappings  $\Phi$  that has

the following property:

$$\phi(x_i)^T \phi(y) = K(x, y) \quad (23)$$

where  $K$  is a corresponding kernel function.

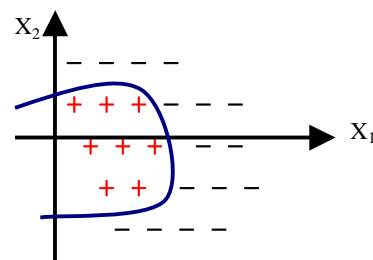
**Examples of kernel function:**

• Gaussian Kernel:  $K(x, y) = e^{-\frac{\|x-y\|^2}{A}}$ , A is a constant

• Polynomial Kernel:  $K(x, y) = (x^T y + 1)^B$ , B is a constant

By introducing the kernel trick:

The dual problem: to find  $\alpha$  that maximizes



$$\sum_i \alpha_i - \frac{1}{2} \sum_i \sum_j \alpha_i \alpha_j y_i x^t_j x_j K(x_i, y_i) \quad (24)$$

subject to  $\sum_{i=1}^N \alpha_i y_i = 0$

The resulting SVM is:

$$f(x) = w^T \Phi(x_i) + b = \sum_{i=1}^N \alpha_i y_i K(x_i, x) + b$$

$$f(x) = w^T \phi(x_i) + b = \sum_{i=1}^N \alpha_i y_i K(x_i, x) + b \quad (25)$$

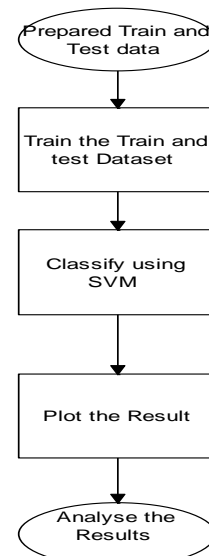


Figure 3.4.1 Flowchart for SVM Classifier

The figures 3.4.1 show the flowchart for the SVM Classifier. From the Results of GLCM Features Prepare the test and train data for SVM Classifier . Later train the prepared trained data and test data into the classifier for classification as shown in flowchart. At the end plot and analyze the result.

#### Pseudo code for svm

```

initialize5I = P i∈I xi/|I| for5every positive bag5BI
REPEAT
    compute5QP solution w, b5for data set5with
    positive5examples {xi : YI = 1}
    compute5outputs fi = hw, xii + b5for all xi in
    positive5bags
    set5XI = xs(I), s(I) = arg5maxi∈I fi for5every I, YI = 1
    WHILE5 (selector5variables s(I) have5changed)
    OUTPUT5 (w, b)

```

#### IV. CONCLUSION

Head and neck cancer is one of the most dangerous diseases in the world. Correct Diagnosis and early detection of head and neck cancer can increase the survival rate. CT scan images are acquired from various hospitals. These images include less noise5as compared to X-ray and MRI images. The CT captured images are processed. The system consist of preprocessing,segmentation ,feature extraction and final classification.The proposed marker controlled watershed segmentation technique separates the touching objects in the image.It provides best identification of the main edge of the image and also avoids over segmentation.Two different classifiers are used for classification purpose.Using both SVM and KNN classifier increases accuracy of detection and reduces false detection.The proposed technique gives very promising results comparing with other used techniques.

#### REFERENCES

- [1] Machine Learning and Integrative Analysis of Biomedical Big Data, Bilal Mirza, WeiWang, JieWang, Howard Choi, Neo Christopher Chung and Peipei Ping, Received: 2 December 2018; Accepted: 21 January 2019; Published: 28 January 2019
- [2] Using deep learning to enhance head and neck cancer diagnosis and classification, Pooja Gupta ; Dr. Avleen Kaur Malhi, 2018 IEEE International Conference on System, Computation, Automation and Networking (ICSCA)
- [3] Removal of Salt and Pepper Noise in Corrupted Image Based on Multilevel Weighted Graphs and IGOWA Operator. QinXu, QiangZhang, DuoHu, and JinpeiLiu, Mathematical Problems in Engineering Volume 2018, Article ID 7975248,

- [4] Medical Image Classification Based on Deep Features Extracted by Deep Model and Statistic Feature Fusion with Multilayer Perceptron. ZhiFei Lai and HuiFang Deng, Computational Intelligence and Neuroscience Volume 2018, Article ID 2061516.
- [5] Selective Feature Fusion Based Adaptive Image Segmentation Algorithm, QianwenLi ,ZhihuaWei ,andWenShen, Advances in Multimedia Volume 2018, Article ID 4724078.
- [6] A Review Paper on Feature Extraction and General Approaches for Face Recognition. Venus Bansal1, Dr. Ajay Kumar Singh, International Journal for Research in Applied Science & Engineering Technology (IJRASET) , Volume 6 Issue I, January 2018- Available at [www.ijraset.com](http://www.ijraset.com).
- [7] A novel feature ranking method for prediction of cancer stages using proteomics data, Ehsan Saghpour, Saeed Kermani, Mohammadreza Sehhati, September 21, 2017

# A Survey on the Role of Emotions in Engineering, Medical and Psychology Domains

[<sup>1</sup>]Imran Khan [<sup>2</sup>] Dr.Mouneshachari S

[<sup>1</sup>] Department of IS&E,GMIT,Davangere, India

[<sup>2</sup>]Department of CS&E,GMIT,Davangere, India

**Abstract**—Since centuries the area psychology is trying to find out the causes and effects of the most interesting and challenging topic “Emotion” which may be connected to most complex and unpredictable organ of human body “Brain”. These days it is becoming region of interest for the research and developments. This paper is tried to minimize the gap between psychology and scientific domains like engineering and medical sciences also to show the evolution of emotion findings since from centuries till today.

**Keywords**— Emotion, Emotion in Psychology and Science, Emotion in Technology, Emotions Classification

## I. INTRODUCTION

The word emotion ostensibly appeared in the year 1570-80 and it is derived from Middle French word esmovoir and in Latin ēmovēre means move the feelings. *What is emotion? is it feeling?* Since sixteen century to today the philosophers, psychologists and researchers have been trying to define the word emotion in various ways. Mandler (1984) stated that “*too many psychologists fail to accept today that there is no commonly, even superficially, acceptable definition of what a psychology of emotion is about*” [34]. Chaplin and Krawiec said that “*one of the difficulties that has stood in the way of an acceptable theory of emotions has been disagreement over definitions*” [14].

Paul R. Kleinginna, Jr., and Anne M. Kleinginna from Georgia Southern College published a paper during 1981, which includes 92 definitions and 9 skeptical statements from a variety of sources in the literature of emotion. These definitions and statements were classified into an outline of 11 categories, on the basis of the emotional phenomena or theoretical issues emphasized [65]. Some of the important definitions later 1981 are listed below.

**Table 1: Definitions of emotion**

Authors	Definition
R.Ezhilarasi, R.I.Minub, 2012 [71]	“Emotions are a key semantic component for human communication. Effective communication between humans is only accomplished when both the meaning and the emotion of the communication are understood by all parties involved”.
Descartes et al. (de	“Emotions are made up of primary

Sousa, 2008) [68]	emotions and are measured in function to a limited number of finite dimensions (ex. level of stimulation, intensity, pleasure or aversion, one's own intention or that of others, etc.)”
Hockenbury & Hockenbury, 2007 [37]	“An emotion is a complex psychological state that involves three distinct components: a subjective experience, a physiological response, and a behavioral or expressive response”.
Scherer, 2005[48]	“In general, emotion can be seen as a sort of process that involves different parts, including subjective feeling, cognition, physical expression, the tendency of action or desires, and the neurological process”.
Frijda, 1986 [59]	“Non-instrumental (discrete, individualized) behaviors, non-instrumental behavioral traits, physiological changes and assessment experiences on the subject, being generated by external or mental events and primarily by the signification of such events”.
Lazarus, 1991[69]	“He highlights that appraisals are necessary and sufficient for emotion. Adding that the notion of coping allows an individual to choose strategies to confront future problems”.
Ortony and Turner,	“Emotions are valence reactions to

1990 [1]	events, agents or objects”.
Greenspan, 1988 [61]	“Emotion is a conscious mental process affecting a major component of the body; it also has a lot of influence on one's thought and action, notably to plan social interaction strategies”.
Kleinginna, P. R. et al., 1981 [49]	“Emotion is a complex phenomenon, with subtle interactions among subjective and objective factors”.

In the book “The Expression of the Emotions in Man and Animals”, Charles Darwin (1872/1965) [18] defended the argument that emotion expressions are evolved and adaptive (at least at some point in the past) and serve an important communicative function. In medicine the emotion is defined as “An intense mental state that arises subjectively rather than through conscious effort and is often accompanied by physiological changes [24]”. In science it is “A psychological state that arises spontaneously rather than through conscious effort and is sometimes accompanied by physiological changes; a feeling [25]”.

## II. STUDY OF EMOTIONS

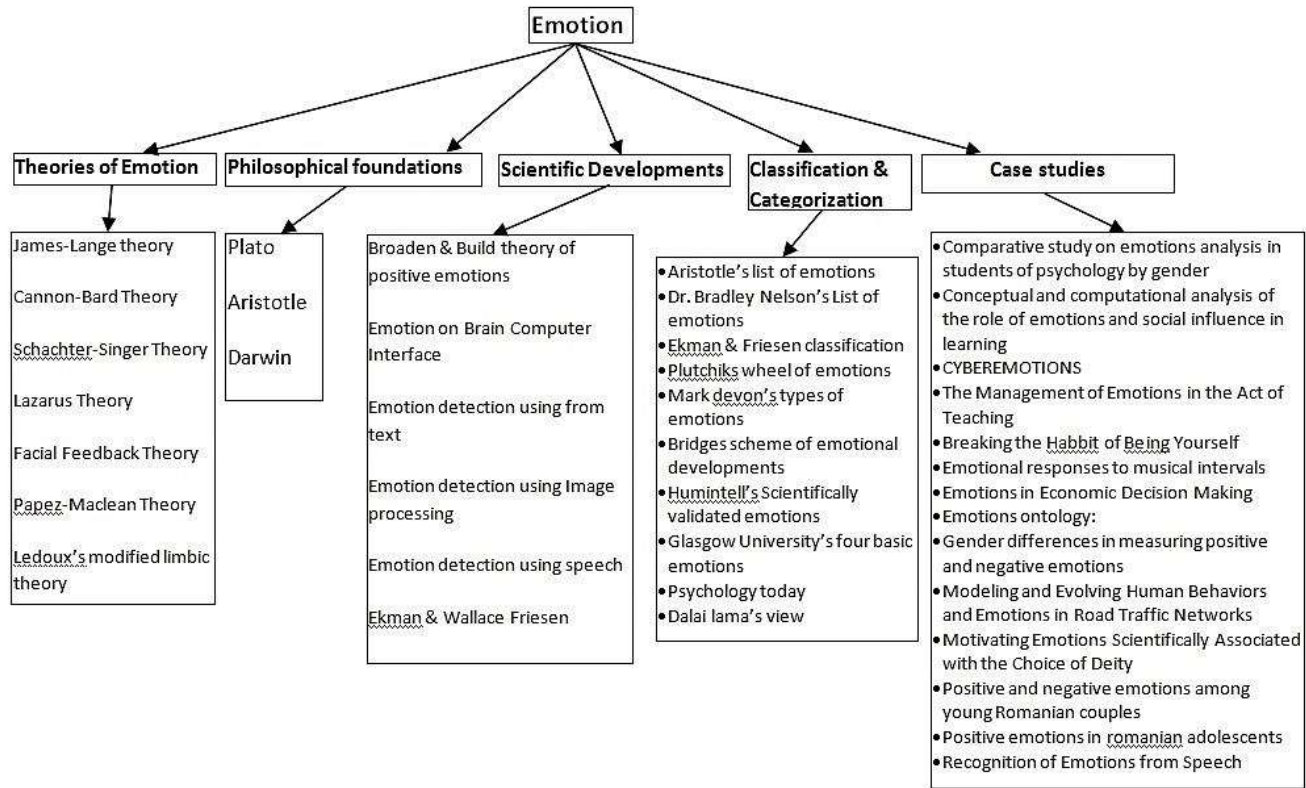


Figure1: Layout of the paper to deal with emotions at various domains and case studies

This paper is mainly emphasizing on the developments of emotion at various domains such as Philosophical, Psychological and Scientific. Also it highlights the number of emotion classification by number of researchers at various domains. Number of applicable case studies have been discussed at the end of the paper before conclusion. Figure1 shows the layout of the study of the emotion in this paper.

### III. THEORIES OF EMOTION

Theories discussed are devised based on the relation

between emotion, cognition and physiological changes.

William James and C G Lange propose an emotion theory during the year 1922 called as **James-Lange theory of emotion** [90] and it argues that “An event causes physiological arousal first and then we interpret this arousal. Only after our interpretation of the arousal we experience emotion. If the arousal is not noticed or is not given any thought, then we will not experience any emotion based on this event”. For example, when you are sitting alone at home late night and when air makes a noise near window behind you and you begin tremble, your heart beats

faster and sometimes your breathing deepens. You observe these physiological changes and keep your body ready for fearful situation and then feel fear.

The **Cannon-Bard theory** argues that “*we experience physiological arousal and emotional at the same time, but gives no attention to the role of thoughts or outward behavior*” [29]. The theory asserts that “*the thalamic region in the brain area responsible for emotional responses to experienced stimuli*” [16]. For example, when you are sitting alone at home late at night and when air makes a noise near window behind you and you begin tremble, your heart beats faster and sometimes your breathing deepens. Here physiological changes and fear experience occurs parallel.

“Cognitive revolution” held during 1962 in the field of psychology, the researchers Schachter and Singer devised a new theory of emotion based on cognitive factors called as Schachter-Singer Theory [78]. According to this theory “an event causes physiological arousal first. You must then identify a reason for this arousal and then you are able to experience and label the emotion.” For example, when you are sitting alone at home late night and when air makes a noise near window behind you and you begin tremble, your heart beats faster and sometimes your breathing deepens. Upon noticing this arousal and you may realize that noise may be by air or any other. This behavior is dangerous and therefore you feel the fear. So this theory depicts the emotion fear based on cognition.

**Lazarus Theory** [69] states that “*a thought must come before any emotion or physiological arousal. In other words, you must first think about your situation before you can experience an emotion*”. For example, when you are sitting along at home late at night and when air makes a noise near window behind you and you may think that it is by black energy and you begin tremble, your heart beats faster and sometimes your breathing deepens at the same time you experience fear.

**Facial Action Coding System** (FACS) is a systematic classification of facial movements by their appearance on the face it is originally developed by a Carl-Herman Hjortsjo [36]. It was later adopted by Paul Ekman and Wallace V. Friesen, and published in 1978 [60]. Ekman, Friesen, and Joseph C. Hager published a significant update to FACS in 2002 [64]. FACS encodes the movements of the each and individual facial muscles by observing even minor difference from the facial appearance [32]. It is commonly used standard classification tool by psychologists and animators while categorizing the emotions based on facial expressions. Basically FACS does the detection of faces in videos, extracts the geometrical features and producing the profiles of each facial movement. For example, when you are sitting alone at home late at night and when air makes a noise near window behind you and you begin tremble, your

heart beats faster and sometimes your breathing deepens and you may clench your teeth or open your eyes bigger then suddenly your brain may interpret these as the emotion of fear.

**Papez-Maclean theory** devised by Papez-Maclean mainly focus on the structure of the brain while dealing with two important emotions such as rage and fear [10] and this theory is based on the functioning of hippocampus, amygdala in limbic system of the brain. This theory says that “the limbic system and hypothalamus stimulate the production of adrenaline, which provokes ANS (Automatic Nervous System), which creates a physiological response (e.g. increased heart rate) and a behavioral response (e.g. increased attention) in readiness to deal with the stimulus”. **LeDoux’s modified limbic theory** is one of the improvised version of Papez-Maclean theory, This theory proposes that “two separate brain circuits involved in emotion: rapid emotional response (thalamus – amygdala) and slower emotional response (thalamus – cortex, thereby affected by higher mental processes)”[45].

#### IV. PHILOSOPHICAL FOUNDATIONS

The essence of philosophical foundation is most required bough for the proper justification of growing leaves of approaches like psychology, biology, neurology, neurophysiology, ontology of emotions and so on. Many philosophers of mind and psychology had proposed most of the recognizable theories of emotion. These theories and thoughts had triggered certain sort of concern to a subject, motivating characteristics behavior and encouraging the social behavior to sort out the meaningful aspect of civilization. This section deals with the contribution by the ancient philosophers – Plato, Aristotle, Spinoza, Descartes, Hobbes and Hume to the world of emotions.

##### *Plato*

Plato’s (428 BCE – 348 BCE) point of views on emotion are based on the analysis of three parts of the soul i.e., feeling-thinking-desiring linkages. According to Plato, Emotion is the base for any medieval, inhibitory and disruptive to the normal and optimal function of mind. Emotion must be under the control for the sake of normal behavior, thoughts and action [92]. In the other angle it can be defined as negative view of emotions, it says that, “emotions usually affect reasoning for the worse” [26]. Plato also designed a model with respect to metaphysics or spiritualism as “the degrading of feelings and emotions to a low status is not just a byproduct of metaphysics; it belongs to metaphysics’ essential constitution” [35]. J Macmurray in his book “Reason and Emotion” makes important standpoints on Plato and observes that the reason for rationality and irrationality is not the feelings it is primarily an affair of emotion and the rationality thinking is the

derivative and secondary one [51]. Again, this is a general consideration but it does not qualify Plato's view in terms of the negativity of emotion. As for more recent authors the more focused point is: "In the tri-partite soul, each part has its own reason, emotion, and desire"[51].

Now, if one agrees that affectivity is various and inherently differentiated, one will welcome Plato's model as all the more useful. If, however, one is inclined to treat the whole of affectivity as one-dimensional, Plato's model will appear to him pretty useless [75].

#### **Aristotle (385 BC - 322 BC)**

Aristotle was a Greek philosopher and scientist born in the Macedonian city of Stagira, Chalkidice, on the northern periphery of Classical Greece. Aristotle prefers to call emotion as pathos [pl. pathe], pathe are the responses found in the animals in the beginning to the outside world like a perceptions. Pathe are the origin for actions and Aristotle treated them as movements of sort. This declares that pathe is a component of a soul which informs a body for actions. Aristotle discuss the different ways and solutions to the control of pathe for the rational influence and voluntary action [6]. Aristotle ethical write-ups are regarded as Nichomachean Ethics. These ethics characterizes pathe as the "feelings accompanied by pleasure or pain, listing appetite, anger, fear, confidence, envy, joy, love, hatred, longing, emulation, and pity as examples" [7]. Also the pathe are the reason for appetite and provokes the actions in different faces. Aristotle brought a distinctive thought corresponding to fail to act well. Weak-willed individual recognizes well doing without actually doing it. "Aristotle, however, appears to have thought of them more as exercising a cognitive interference that disrupts our completion of the practical syllogism than as an external force overturning our otherwise smoothly operating reason" [79].

#### **Darwin**

Darwin strongly believed that the adaptation to new environment and circumstances may mould mind and instinct become influenced in originating new expression of emotions. His one of the book "The Expression of the Emotions in Man and Animals" during 1872 has grabbed the minds of entire science and technology researches and it emphasizes manly on how the emotions of man and animals are correlated or analogous as a supporting theory that the man and animals derived from the same ancestors [89]. "Certain complex actions are of direct or indirect service under certain states of the mind, in order to relieve or gratify certain sensations, desires, etc.; and whenever the same state of mind is induced, however feebly, there is a tendency through the force of habit and association for the same

movements to be performed, though they may not then be of the least use[62]". These action may be suppressed by willness or through constant use complex movements may be facilitated i.e., "the conducting power of the nervous fibres increases with the frequency of their excitement"[43]. Darwin called these movements as inherited and instinctive also he gave many examples like horrid sight, shaking of head or shutting of the eyes."

#### **V. SCIENTIFIC DEVELOPMENTS**

Murdock [6] has created a list of common denominator of cultures and human nature, which was expanded by Tiger and Fox (1971)[87], Hockett(1973), and D E Brown(1991). This list is later developed in anthropology, psychology and linguistics. These were held during the 20th century as a identification of universals.

Ralph B et. al. in the paper Universal Development of Emotion Categories in Natural Language says that "no matter whatever the language is and language never defines the type of emotion during communication" and the this study has been made "*to determine whether the need to communicate about emotion-eliciting events was sufficiently alike so that the encoding sequence progressed similarly across languages*" [72].

#### *The Broaden-and-Build Theory of Positive Emotions*

Language learning has become supportive area for the studies of emotions, because it involves acquisition at first and second languages. The process of emotion embedding in the second language may or may not differ. Thus far, "*affect has been considered as a core component of individual differences having a close bearing on second language learning*" says Ellis [22]. Affect also claims the degree of motivation and values says Schumann [80]. This affect can also be regarded as emotion.Forgas [27] and Fredrickson [9] proved that the tendency of the multi-component response generated by the group of opinions which will have both positive and negative responses is a short-live one but have a definite cause. Fredrickson [9] says "*emotions begin with an individual's situational appraisal of an antecedent event thereby a cascade of response tendencies are triggered in the form of expressive or display behaviors*" also he states that "*certainly, moments in people's lives characterized by experiences of positive emotions – such as joy, interest, contentment, love, etc. – are moments in which they are not plagued by negative emotions, such as anxiety, sadness, anger and the like*". The main component of emotion is the assessment and analysis of the current situation and connected them to earlier incidences as given by Solomon and Stone [73]. Negative emotions took major role in the studies of emotions during nineteen hundreds. The negative emotions such as fear, anxiety, sadness and anger received little attention in the study of emotions [9][53]. So the positive emotions effect

more in the acquisition of second language [66]. Many studies have shown that the second language learning and its acquisition is emotionally driven task. The Broaden and build theory [9] on positive emotions was proposed by Fredrickson based on the findings done by Isen and he says that "*broad, flexible cognitive organization and ability to integrate diverse material*" [4]. This theory is mainly emphasizes on positive psychology.

#### **A Framework for Automatic Human Emotion Classification Using Emotion Profiles**

Emotion profile is the highest level of confidence quantified based on utterance assigned to the emotion class. Here the classification of the utterance-level is composed of four binary Support Vector Machine (SVM) classifiers, one for each emotions sadness, happiness, anger and neutrality. Utterance is defined as one sentence for each speaker turn or the entire speaker turn. These Emotion Profiles are used at the intermediary level to implement emotion classification from vocal and motion capture activities [23]. Emotions contain varieties of multiple affective classes [15][58]. It is challenging task for any science and technological methods for estimation of emotions based on naturalistic expressions. For example, in [41], the author explains a scene in which evaluators view on a clip of woman learning that her father remain in jail. The four evaluators labels four different emotions by seeing this clip as sadness, despair, disappointment and anger [41]. Sometimes it is very difficult to recognize the type of emotion by seeing natural expression which has a lack of emotion purity. Hence this lack of emotion can be captured and considered while estimation and classification of emotions. SVM for the Emotion Profiles based classification can be replaced by KNN or LDA classification methods but the strengths of SVM is its relative insensitivity to the selection of the base classifier. The type of interaction can be declared based on the human current emotional state. Hence, its detection, recognition and classification has made more required for human computer applications [81]. The paper [12] highlights the different strategies followed by researchers to detect emotion from text and speech [2] along with its limitations and further enhancements. Ekman and Wallace Friesen devised a FACS i.e., Facial Action Coding System in 1978 it is like a atlas of the human face expressions represents the detailed description of facial movements. Later they used for studying thousands of emotions. [63]. Richard Lazarus a psychologist has introduced a concept called "*Themes Central Relational*" in order to analyze and study the emotions when communicating with others. [70].

#### **VI. CLASSIFICATION AND CATEGORIZATION OF EMOTIONS**

The classification and categorization of emotions must be based on philosophical, psychological and scientific

perspectives. Aristotle has defined [38] Anger, Mildness, Love, Enmity (hatred), Fear, Confidence, Shame, Shamelessness, Benevolence, Pity, Indignation, Envy, Emulation, Contempt. Dr. Bradley Nelson has made many shades of emotions [11] like Abandonment, Anger, Anxiety, Betrayal, Bitterness, Blaming, Conflict, Confusion, Creative Insecurity, Crying, Defensiveness, Depression, Despair, Discouragement, Disgust, Dread, Effort Undeceived, Failure, Fear, Forlorn, Frustration, Grief, Guilt, Hatred, Heartache, Helplessness, Hopelessness, Horror, Humiliation, indecisiveness, Insecurity, Jealousy, Lack of Control, Longing, Lost, Love Unreceived, Low Self-Esteem, Lust, Nervousness, Overjoy, overwhelm, Panic, Peeved, Pride, Rejection, Resentment, Sadness, Shame, Shock, sorrow, Stubbornness, Taken for Granted, Terror, Unsupported, Unworthy, Vulnerability, Wishy Washy, Worry, Worthless. One of the most popular classification of emotions is Ekman and Friesen classification. They have been proposed universal and standard emotional expressions, they are happiness, sadness, anger, disgust, surprise and fear [21, 28, 57, 31, 41] as shown in the following figure 2.



**Figure 2: The six universal standard emotional expressions**

Robert Plutchik is a well known psychologist and proposed a psycho-evolutionary theory of emotion. Also this theory establishes the relationship between emotions. Majorly he identifies eight basic or primary emotions i.e., Joy, Trust, Fear, Surprise, Sadness, Anticipation, Anger, and Disgust. This circumplex model is a result of gradual development in the area of Evolutionary Psychology. It is the work since 1921 when a social psychologist William McDougall proposes the similarity analysis between color and emotions and says "*the color sensations present, like the emotions, an indefinitely great variety of qualities shading into one another by imperceptible gradients...*". The first circumplex model was designed by Harold Schlosberg in 1941 later it was improved by Robert Plutchiks as shown in figure 3. Mark Devon proposes five types of emotions [52] i.e., conceptions, sensations, reflexes, involuntary expressions and voluntary expressions as shown in figure 4.

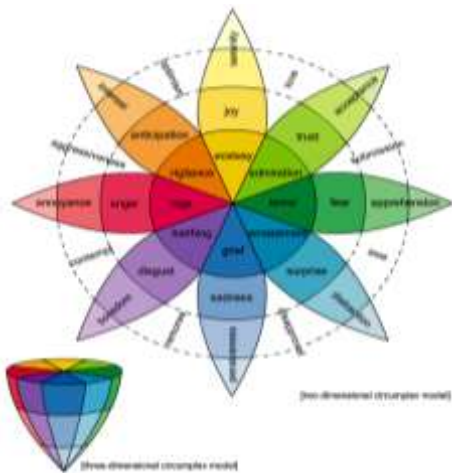


**Figure 3 : Plutchik Model of Emotions Classification**

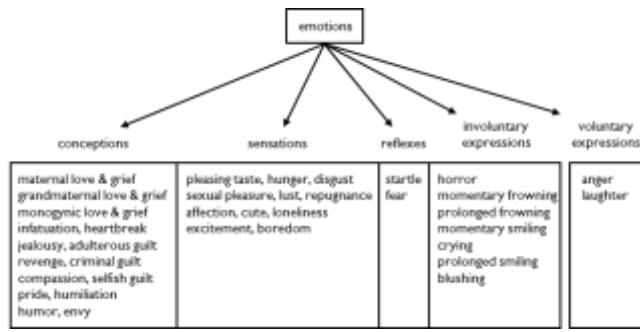


**Figure 4: Mark Devon's five types of emotions**

Conceptions, sensations, reflexes and involuntary expressions are biological adaptations. They are transmitted to the next generation through reproduction. They are universal to the species. Voluntary expressions are cultural adaptations. They are transmitted to the next generation through interaction. They vary by culture. Bridge during 1932 proposes the differentiation of emotions [47] during the first 24 months of any birth as shown in figure 5. Birth time the baby will have excitement emotion. Gradually branches to distress in the 1st month then to delight after 2 months and so on [47].

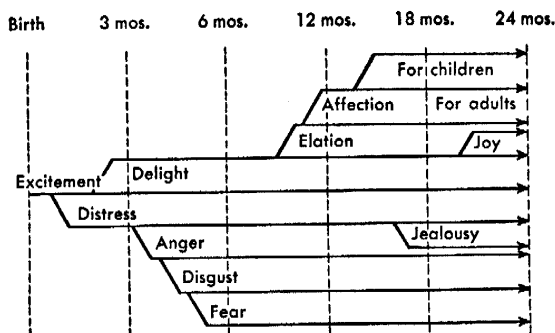


**Figure 5: Bridges scheme of emotional developments**

Humintell's scientifically validated, emotion recognition training tools features images of individuals portraying the 7 basic emotions: Anger, Contempt, Fear, Disgust, Happiness, Sadness and Surprise. Basic emotions are emotions that have been scientifically proven to have a certain facial expression associated with it [39].

## VII. CASE STUDIES

Understanding and Comparing study on emotions analysis in students of psychology by gender is tried to examine any gender differences in analysis and emotion recognition. The results showed that two of emotions, fear and contempt, have significant differences in their recognition which can lead to possible directions of research on these two and the reasons these differences between males and females, studying psychology. This study is made based on Paul Ekman theory, there are seven basic emotions [21] which are universal: happiness, sadness, anger, fear, surprise, contempt, disappointment. So, emotional spectrum analysis should not be viewed as one by itself, but simply as an expression of emotional experiences and their individual transformations. In conclusion, analysis of the data in the paper supports the idea that emotions play an important role in social interactions, mediating the relationship of the individual. The future psychologists who are preparing to become professional persons must know how well they can use recognition of emotions in their work and how well they can rely on it. The clients of psychologists can be sometimes insincere, so being a good psychologist suppose having this skill. An early training assure better skills in time [31].

Another study Conceptual and computational analysis of the role of emotions and social influence in learning [42] investigate more on learning process which may be active or reflective by the analysis of emotions of own and social environment. This work has been done in two phases as conceptual and computational phases. Conceptual phase includes the analysis of cognitive, affective and social neuroscience on the roles of emotions where as computational phase includes computation of learning process. Neural mechanisms of both the person's own emotions and emotions of others are observed to study the learning process. This study has observed the strengthening of learning process by considering effects of emotions and social interactions. Also this study uses the insights for learning and teaching done by Immordino-Yang & Fischer in Cognitive, Affective and Social Neuroscience. Junghyun Ahn et. al. introduces “Cyberemotions – Collective emotions in cyberspace” is an emerging phenomena to detect and analyze the emotional elements in the ICT (Information Communication Technologies) services. This study has proven that “*the data on the cyberspace not only includes factual also contains the emotional elements*” by developing state-of-the-art sentiment analysis algorithms.

This project works in three different layers i.e., data, theory and ICT output [46].

The paper “*The Management of Emotions in the Act of Teaching*” [50] mainly focus on embedding the emotion in process of teaching and observation of outcome at different systems irrespective of country and culture. The performance is analyzed versus the traditional teaching process. Hascher Tina explores that “the students’ feelings and frames of mind may be influenced by simple teaching methods, at least in the short run” [33]. Dispenza and Joe proves that emotion is the element or the action source for further thoughts and it becomes action. For this they conducted a classroom experiments between teacher and student’s. They prove that “*Any final stage of a communication process (OUTPUT) is a part of the INPUT of the next stage*”. This research reveals that positive emotion generated ensures the learners understanding. Also the negative emotions are useful to ensure the learners attention and capacities [19]. The paper [67] tried to replicate some of the earlier studies as follows a) “musical pieces in a major mode with fast tempo will be perceived as happy and slow pieces in a minor mode will be perceived as sad” [84], b) “250 ms of musical stimulation will be sufficient for the distinction between happy and sad music” [40], and c) “consonance represents a measure of pleasantness” [85] [77].

Also recent investigations have shown that musical elements may cause arousal of specific emotional responses [13]. Creation of specific acoustics for a particular musical stimuli is a major part of this [67] work by observing and analyzing the acoustic properties. As it has been stated by Rabin (1998) [54], the study of human behavior has to be integrated into economics, and the tractable and parsimonious psychological findings should not be ignored by the economic research. Kahneman (2003) [17] says that incorporating psychological aspects of the intuitive agent into economic theory might be challenging, but this challenge seems to be quite successful. According to Peterson (2009) [55], behavioral economics studies judgments and decision making focusing on psychological aspects. Elster (1998) [44] claims that economic theory is mostly interested in the interaction between emotions and other motivations, like self-interest [3]. EmotionsOnto is a ontology of emotion, emotion description and its detection and it is introduced by Rosa Gil et. al. in the year 2015 [76] to understand basic and fundamental components required to design and develop emotion-aware applications to reduce learners’ or students’ drop outs in Massive Online Open Courses (MOOCs) or proliferating the collection of emotion related data in social networking sentiment analysis. Studies have observed around 90% of drop outs in the MOOCs [20]. Hence the sentiment analysis is more required tool to

decrease the drop outs in MOOCs environment [55]. The paper [57] brings the experimental analysis of the gender differences in the self perception of Romanian high school students with respect to positive and negative emotions. This study has proved that the positive emotion self-perception in school girls aged 16 to 18 is more significant than the school boys ( $7.43 > 6.25$ ;  $p=0.05$ ). Negative emotion self-perception is also significant higher than the school boys ( $5.40 > 4.41$ ;  $p<0.05$ ). Earlier research on positive and negative emotions with gender difference has shown that “*Gender differences were also found for negative deactivating emotions suggesting that girls reported less hopelessness and boredom than boys*” [8]. “*Related pursuit of pride is related with aspiration of normative goals*” [88].

The paper [30] studies the behavioral modeling and its decision making by the analysis of artificially generated multi-agent environment and demonstrates that “models of steady state that do not account for behavioral modeling under-estimate risk and the differences are significant”. Mainly this model is used for understanding the behaviors of an agent in dynamically changing environment and its decision making, then these understandings are compared and tested using the collision-avoidance physics-based model and a rational cognitive model. In the other angle of the study strongly agrees that the choice of the deity plays major role in the motivating the emotions in human being rather than genetics, traditions, cultural and geographical environments. This study mainly focuses on the finding out the scientific ism in reason, emotion and its belief aspects [86]. The paper [83] says that “confirmed and enforced alexithymia mainly upon men” while exploring the positive and negative emotions of young Romanian couples in terms of their method of expressiveness. The observations have shown that the Romanian specific tradition and heritage is very popular and unique hence young Romanian couples face difficulties in expressing and recognizing the emotions even though knowing its benefits. “*The positivity ratio predicts only the global evaluation of personal values, but not the other dimensions of irrational thinking*” says the paper [5] while studying the hypothesis “whether or not positivity ratio (the ratio between positive and negative emotions) can predict irrational thinking” and “*the influence of positive emotions on creative thinking and adolescents' attitudes concerning change*”.

Findings in this study also suggest fostering change in psychotherapy [5]. The paper [82] conducts an experiment to capture the emotion specific detail by the analysis of the speech. Here author has used GEU-SNEC (GEU Semi Natural Emotion Speech Corpus) database and it is collected by recording the bollywood actors / actresses. Mainly they have tried to capture the emotions like sad, anger, happy and neutral. Linear Prediction Analysis is used to estimate LP

residual, which gives rise to the characteristics of emotional elements in the speech. Also Gaussian Mixture Model (GMM) is used for LP residual analysis. Performance of the emotion recognition in speech has given up to 50-60%.

### VIII. CONCLUSION

Since emotion is one the most tedious and unpredictable component of human being, its studies and developments of the tools will be more cumbersome and challenging. Hence knowing the developments of emotion and its related issues in the research and developments since from the centuries till today is very much required for the further developments. Hence this paper has tried to highlight the importance, developments at various fields like psychology, scientific, music and so on of the emotion.

### REFERENCES

- [1] A. Ortony, T. Turner, 1990 What's basic about basic emotions, *Psychological review* 97 3 315331.
- [2] Agnes Jacob, P. Mythili, A socio friendly approach to the analysis of emotive speech, *International Conference on Communication Technology and System Design* 2011, *Procedia Engineering* 30 (2012) 577 – 583.
- [3] Agnes Virlics, Emotions in Economic Decision Making: a Multidisciplinary Approach, *Procedia - Social and Behavioral Sciences* 92 ( 2013 ) 1011 – 1015.
- [4] Alice M. Isen, "An Influence of Positive Affect on Decision Making in Complex Situations: Theoretical Issues With Practical Implications", *JOURNAL OF CONSUMER PSYCHOLOGY*, 11(2), 75–85, 2001.
- [5] Alina Vulpe, Ion Dafinoiu, "Positive emotions' influence on attitude toward change, creative thinking and their relationship with irrational thinking in romanian adolescents", *Procedia - Social and Behavioral Sciences* 30 (2011) 1935 – 1941.
- [6] Angela Chew, Aristotle's Functional Theory of the Emotions, *Institute of Philosophy SAS, Organon F* 16 (2009), No. 1, 5 – 37.
- [7] Aristotle Translated by W. D. Ross, *Nichomachean Ethics*, Web edition by eBooks@Adelaide, <https://ebooks.adelaide.edu.au/a/aristotle/nicomachean/index.html>.
- [8] Athanasios Mouratidis, Maarten Vansteenkiste, Willy Lens, Georgios Sideridis, "The Motivating Role of Positive Feedback in Sport and Physical Education: Evidence for a Motivational Model", *Journal of Sport & Exercise Psychology*, 2008, 30, 240-268.
- [9] Barbara L. Fredrickson, The broaden-and-build theory of positive emotions, *The Royal Society*, 2005.
- [10] Beglinger, L. J., Haut, M. W., Parsons, M. W. (2006). The role of the Mammillary bodies in memory: A case of amnesia following bilateral resection. [Article]. *European Journal of Psychiatry*, 20(2), 88-95.
- [11] Bradley Nelson, *The Emotion Code*, Definitions of Emotions.
- [12] C.H. Wu, Z.J. Chuang and Y.C. Lin, "Emotion Recognition from Text Using Semantic Labels and Separable Mixture Models", *ACM Transactions on Asian Language Information Processing (TALIP)*, vol. 5, issue 2, Jun. 2006, pp. 165-183, doi:10.1145/1165255.1165259.
- [13] CAROL L. KRUMHANSL, An Exploratory Study of Musical Emotions and Psychophysiology, *Canadian Journal of Experimental Psychology*, 1997, 51:4, 336-352.
- [14] Chaplin, J. P., & Krawiec, T. S. Systems and theories of psychology (4th ed.). New York: Holt, Rinehart & Winston, 1979, (p.422).
- [15] D. Seppi, A. Batliner, B. Schuller, S. Steidl, T. Vogt, J.Wagner, L. Devillers, L. Vidrascu, N. Amir, and V. Aharonson, "Patterns, prototypes, performance: Classifying emotional user states", in Proc. InterSpeech, 2008, pp. 601–604.
- [16] Dalgleish, T. (2004). "The emotional brain". *Nature Reviews Neuroscience* 5 (7): 582–589. doi:10.1038/nrn1432. PMID 15208700.
- [17] Daniel Kahneman, "Maps of Bounded Rationality: Psychology for Behavioral Economics", *The American Economic Review*, 93(5), pp. 1449-1475, December 2003.
- [18] Darwin, C. (2007) [1872]. *The expression of the emotions in man and animals*. New York: Filiquarian. ISBN 0-8014-1990-5.
- [19] Dispenza, Joe, (2014),"Breaking the Habit of Beeing Yourself: How to loose Your Mind and Create a New One", Curtea Veche Publishing, Bucharest;
- [20] Diyi Yang, Tanmay Sinha, David Adamson, Carolyn Penstein Rose, "Turn on, Tune in, Drop out": Anticipating student dropouts in Massive Open Online Courses, 2013
- [21] Ekman P (1970), Universal Facial Expressions of Emotions, *California Mental Health Research Digest*, Vol. 8, Autumn 1970, Number
- [22] Ellis, R. (1994). The study of second language acquisition. Oxford, Oxford University Press.
- [23] Emily Mower, Maja J Mataric',Shrikanth Narayanan, 2011, A Framework for Automatic Human Emotion Classification Using Emotion Profiles, *IEEE Transactions on Audio, Speech and Language Processing*, Vol 19, No. 5, 1057-1070.
- [24] Emotion. (n.d.). The American Heritage® Stedman's Medical Dictionary. Retrieved July 12, 2015, from Dictionary.com website: <http://dictionary.reference.com/browse/emotion>
- [25] Emotions. (n.d.). The American Heritage® Science Dictionary. Retrieved July 12, 2015, from

- Dictionary.com website: <http://dictionary.reference.com/browse/emotions>
- [26] EVANS, D., The search hypothesis of emotion in: Emotion, Evolution, and Rationality . Ed. by D.Evans & P. Cruse, Oxford: Oxford University Press, 2004, p. 179 – what is the first sentence of the paper.
- [27]Forgas, Joseph P.,On mood and peculiar people: Affect and person typicality in impression formation., Journal of Personality and Social Psychology, Vol 62(5), May 1992, 863-875.
- [28] Fredrickson, B. L., Mancuso, R. A., Branigan, C., & Tugade, M. M. (2000). The Undoing Effect of Positive Emotions. Motivation and Emotion, 24(4), 237-258.
- [29] Friedman, B.H. (2010). "Feelings and the body: The Jamesian perspective on autonomic specificity of emotion". Biological Psychology 84: 383–393. doi:10.1016/j.biopspsycho.2009.10.006.
- [30] George Leu, Neville J. Curtis, Hussein Abbass, "Modeling and Evolving Human Behaviors and Emotions in Road Traffic Networks", Procedia - Social and Behavioral Sciences 54 ( 2012 ) 999 – 1009.
- [31] Georgeta Pârisoara, Ion Ovidiu Pârisoara, Cristina Marina Sandu, (2015), "Comparative study on emotions analysis in students of psychology by gender", Procedia - Social and Behavioral Sciences 180 ( 2015 ) 1638 – 1642.
- [32] Hamm, J., Kohler, C. G., Gur, R. C., Verma, R. (2011). "Automated Facial Action Coding System for dynamic analysis of facial expressions in neuropsychiatric disorders". Journal of Neuroscience Methods 200 (2): 237–256. doi:10.1016/j.jneumeth.2011.06.023. PMC 3402717. PMID 21741407.
- [33] Hascher, Tina, (2005), Emotionen im Schulalltag: Wirkungen und Regulationsformen, in Zeitschrift für Pädagogik, Vol. 5/2005, Belz Publishing;
- [34] Hearst, E. (1979) The First Century of Experimental Psychology. Hillsdale, NJ: Erlbaum.
- [35] HELLER, A. A Theory of Feelings [1979]. Lanham: Rowman & Little field Publishers, Inc.,2009, p. 1
- [36] Hjortsjö, CH (1969). Man's face and mimic language
- [37] Hockenbury, D. H. & Hockenbury, S. E. (2007). Discovering psychology. New York: Worth Publishers.
- [38] <http://spot.colorado.edu/~hauserg/ArEmotList.htm>
- [39] <http://www.humintell.com/2010/06/the-seven-basic-emotions-do-you-know-them/>
- [40] Isabelle Peretz\*, Lise Gagnon, Bernard Bouchard, "Music and emotion: perceptual determinants, immediacy and isolation after brain damage", Cognition 68 (1998) 111–141.
- [41] J. Martin, R. Niewiadomski, L. Devillers, S. Buisine, and C. Pelachaud, "Multimodal complex emotions: Gesture expressivity and blended facial expressions", Int. Humanoid Robot., vol. 3, no. 3, pp. 269–292,2006.
- [42] Jan Treur, Arlette van Wissen, (2013), Conceptual and computational analysis of the role of emotions and social influence in learning, Procedia - Social and Behavioral Sciences 93 ( 2013 ) 449 – 467.
- [43] Joh Muller, Elements of Physiology, Vol II, London, Printed for Taylor and Walton, 1842, referred from free ebook[https://play.google.com/books/reader?id=\\_CM9AAAAYAAJ&printsec=frontcover&output=reader&hl=en&pg=GBS.PR27](https://play.google.com/books/reader?id=_CM9AAAAYAAJ&printsec=frontcover&output=reader&hl=en&pg=GBS.PR27).
- [44] Jon Elster, "Emotions and Economic Theory", Journal of Economic Literature, Vol. 36, Issue1 (Mar. 1998), 47-74.
- [45] Joseph LeDoux(2003), The Emotional Brain, Fear, and the Amygdala, Cellular and Molecular Neurobiology, Vol. 23, Nos. 4/5, October 2003.
- [46] Junghyun Ahn, Anna Borowiec, Kevan Buckley, Di Cai, Anna Chmiel, Agnieszka Czaplicka, Grzegorz D abrowski, Antonios Garas, David Garcia, Stéphane Gobron, Robert Hillmann, Janusz Holyst, Arvid Kappas, Dennis Küster, Marija Mitrovic, Georgios Paltoglou, Hannes Pirker, Stefan Rank, Frank Schweitzer, Julian Sienkiewicz, Marcin Skowronek, Paweł Sobkowicz, Daniel Thalmann, Mike Thelwall, Mathias Theunis, Matthias Trier, Elena Tsankova, Paweł Weronski, "CYBEREMOTIONS – Collective Emotions in Cyberspace", Procedia Computer Science 7 (2011) 221–222.
- [47] K. M. B. Bridges, (1932). Emotional development in early infancy. Child Development, 1932, 3, 324-341.
- [48] K. R. Scherer, 2005 What are emotions? and how can they be measured?, Social Science Information 44 4 695729.
- [49] Kleinginna, P. R., Jr. and Kleinginna, A. M.; A categorized list of emotion definitions, with a suggestion for a consensual definition. Motivation and Emotions, 5, 345-379 (1981).
- [50] Laura Goran, Gabriel Negoescu, "Emotions at Work. The Management of Emotions in the Act of Teaching", Procedia - Social and Behavioral Sciences 180 ( 2015 ) 1605 – 1611.
- [51] MACMURRAY, J. Reason and Emotion, London: Faber & Faber Limited, 1935, p. 26.
- [52] Mark Devon, The origin of Emotions, Version 1.0, ISBN 1-4196-2745-7, Printed in Charleston, South Carolina, USA.
- [53] Martin E. P. Seligman, Mihaly Csikszentmihalyi, Positive Psychology:An Introduction, January 2000 ° American Psychologist, Voh 55. No. 1. 5 14 DOI: 10.1037//0003-066X.55.1.5
- [54] Matthew Rabin, "Psychology and Economics", Journal of Economic Literature, Vol. 36, No.1 (Mar. 1998), 11-46.
- [55] Miaomiao Wen, Diyi Yang, Carolyn Penstein Rosé, "Sentiment Analysis in MOOC Discussion Forums:

- What does it tell us?", Proceedings of the 7th International Conference on Educational Data Mining (EDM 2014).
- [56] Michael Bang Petersen, "Public Opinion and Evolved Heuristics: The Role of Category-Based Inference", *Journal of Cognition and Culture* 9 (2009) 367–389.
- [57] Mihaela Chraif, Mihai Anitei, "Gender differences in measuring positive and negative emotions self-perception among Romanian high school students-a pilot study", *Procedia - Social and Behavioral Sciences* 76 ( 2013 ) 181 – 185.
- [58] N. Sebe, I. Cohen, T. Gevers, and T. Huang, "Emotion recognition based on joint visual and audio cues", in *Proc. Int. Conf. Pattern Recognition*, 2006, pp. 1136–1139.
- [59] N.H. Frijda, "The Laws of Emotion.", *American Psychologist*, 43 (1988) 349-358.
- [60] P. Ekman and W. Friesen. *Facial Action Coding System: A Technique for the Measurement of Facial Movement*. Consulting Psychologists Press, Palo Alto, 1978.
- [61] P. Greenspan, 1988 *Emotions & reasons: an inquiry into emotional justification*, Routledge.
- [62] Paul Ekman, *Darwin and Facial Expression: A Century of Research in Review*, 2006, ISBN: 1-883536-88-x, ISBN-13: 978-1-883536-88-6.
- [63] Paul Ekman, Wallace V Friesen, *Facial Signs of Emotional Experience*, *Journal of Personality and Social Psychology*, 1980, Vol 39, No. 6, 1125-1134.
- [64] Paul Ekman, Wallace V. Friesen, and Joseph C. Hager, *Facial Action Coding System: The Manual on CD ROM*. A Human Face, Salt Lake City, 2002.
- [65] Paul R. Kleinginna, Jr., and Anne M. Kleinginna, *A Categorized List of Emotion Definitions, with Suggestions for a Consensual Definition*, *Motivation and Emotion*, VoL 5, No. 4, 1981.
- [66] Peter MacIntyre, Tammy Gregersen, *Emotions that facilitate language learning: The positive-broadening power of the imagination*, *Studies in Second Language Learning and Teaching*, Adam Mickiewicz University, Kalisz, SSLLT 2 (2). 193-213.
- [67] Petros Papavasiliou, Argiro Vatakis, "Emotional responses to musical intervals with specific acoustical properties and the effect of the induced emotions in duration perception", *Procedia - Social and Behavioral Sciences* 126 ( 2014 ) 237 – 238.
- [68] R. de Sousa, 2008 *Emotion*, in E. N. Zalta (ed.), *The Stanford Encyclopedia of Philosophy*, fall 2008 edn.
- [69] R. S. Lazarus, 1991 *Emotion and Adaptation*, Oxford University Press, New York.
- [70] R. S. Lazarus, *FROM PSYCHOLOGICAL STRESS TO THE EMOTIONS" A History of Changing Outlooks*, *Annu. Rev. Psychol.* 1993. 44:1 21.
- [71] R.Ezhilarasi, R.I.Minub,"Automatic Emotion Recognition and Classification", *INTERNATIONAL CONFERENCE ON MODELLING, OPTIMISATION AND COMPUTING*, Procedia Engineering 38, 21 – 26, 2012.
- [72] Ralph B. Hupka, Alison P. Lenton, and Keith A. Hutchison, (1999), *Universal Development of Emotion Categories in Natural Language*, *Journal of Personality and Social Psychology*, Vol 77, No. 2, 247-278.
- [73] Robert C Solomon and Lori D Stone, On "Positive" and "Negative" Emotions, *Journal for the Theory of Social Behavior* 32:4, 0021-8308.Blackwell Publications, 2002.
- [74] Robert Plutchik, *The Nature of Emotions*, *American Scientist*, Volume 89, pp 344-350.
- [75] Robert Zaborowski, Some remarks on Plato on emotions, Jun-Dec 2012/ISSN 1676-5818.
- [76] Rosa Gil, Jordi Virgili-Gomá, Roberto García, Cindy Mason, "Emotions ontology for collaborative modelling and learning of emotional responses", *Elsevier Computers in Human Behavior*, 2015.
- [77] Sammler D, et al., Syntax in a pianist's hand: ERP signatures of "embodied" syntax processing in music, *Cortex* (2012), <http://dx.doi.org/10.1016/j.cortex.2012.06.007>.
- [78] Schachter, S. & Singer, J. E. (1962). Cognitive, Social, and Physiological Determinants of Emotional State. *Psychological Review*, 69(5), 379-399.
- [79] [79] Schmitter, Amy M., "17th and 18th Century Theories of Emotions", *The Stanford Encyclopedia of Philosophy* (Spring 2014 Edition), Edward N. Zalta (ed.).
- [80] Schumman, J. (1997). *The neurobiological Affect in Language*. Boston: Blackwell.
- [81] Seungchan Lee, Younghak Shin, Soogil Woo, Kiseon Kim and Heung-No Lee, "Review of Wireless Brain-Computer Interface Systems", Chapter 11, Computer and Information Science, Human-Computer Interaction, "Brain-Computer Interface Systems - Recent Progress and Future Prospects", book edited by Reza Fazel-Rezai, ISBN 978-953-51-1134-4, Published: June 5, 2013 under CC BY 3.0 license.
- [82] Shashidhar G Koolagudi, Swati Devliyal, Bhavna chawla, Anurag Barthwal, and K. Sreenivasa Rao, "Recognition of Emotions from Speech using Excitation Source Features", *Procedia Engineering* 38 (2012) 3409 - 3417.
- [83] Simona Herb, Maria Nicoleta Turliuc, Roxana Dumitru, "Positive and negative emotions among young Romanian couples what, how and why to express them", *Procedia - Social and Behavioral Sciences* 187 ( 2015 ) 470 – 474.
- [84] Ste'phanie Khalfa\*, Peretz Isabelle, Blondin Jean-Pierre, Robert Manon, "Event-related skin conductance responses to musical emotions in humans", *Neuroscience Letters* 328 (2002) 145–149.

- [85] Stefan Koelsch,\* Thomas Fritz, D. Yves v. Cramon, Karsten Mu'ller, Angela D. Friederici, "Investigating Emotion With Music:An fMRI Study",Human Brain Mapping 27:239 –250(2006).
- [86] Sukran Karatas, "Motivating Emotions Scientifically Associated with the Choice of Deity", Procedia - Social and Behavioral Sciences 185 ( 2015 ) 225 – 233.
- [87] Tiger, L., & Fox, L.R. (1989). The imperial animal. New York: Holt.
- [88] Urdan, T., & Mestas, M. (2006). The goals behind performance goals. Journal of Educational Psychology, 98(2), 354-365.
- [89] Ursula Hess, Pascal Thibault, Darwin and Emotion Expression, American Psychologist, Vol. 64, No. 2, 120–128 DOI: 10.1037/a0013386, 2009.
- [90] Walter B Cannon (December 1927). "The James-Lange Theory of Emotions: A Critical Examination and an Alternative Theory". The American Journal of Psychology 39: 106–124. doi:10.2307/1415404.
- [91] WARD H. GOODENOUGH, George Peter Murdock: A Biographical Memoir, NATIONAL ACADEMY OF SCIENCES WASHINGTON D.C., 1994.
- [92] ZHU, J. & THAGARD, P., Emotion and Action in: Philosophical Psychology 15, 2002, p. 20.

# Comparison of CNN and Contour Algorithm for Number Identification Using Hand Gesture Recognition

[<sup>1</sup>] Adarsh Pathak, [<sup>2</sup>] Faraz Ahmed Khan

[<sup>1</sup>][<sup>2</sup>] B.Tech, Computer Science Engineering, Medi-Caps University, Indore, India

**Abstract**— This paper compares the performance of two methods for hand gesture recognition for number identification. The image is captured employing a web camera system and undergoes many process stages before recognition of the numbers. Some of these stages include capturing the images, noise elimination, application of the CNN and contour algorithm to predict the number. Once the hand is placed in the region of interest the CNN algorithm predicts the number and gives output in the frame using deep learning techniques, whereas the contour algorithm creates the boundary of the hand and predict the number using the convexity hull defects algorithm and gives the output in the frame. The proposed methods of CNN and Contour achieved the accuracy of 91.2% and 93.8% respectively.

**Keywords**— Contour, Convexity Hull, Convolutional Neural Network (CNN), Hand Gesture Recognition

## I. INTRODUCTION

Gestures are a type of nonverbal communication within which visible bodily actions are accustomed to communicating vital messages, either in situ of a speech or along and in parallel with spoken words. Gestures embrace the movement of the hands, face, or different elements of the body. Physical non-verbal communication like strictly communicative displays, proxemics, or displays of joint attention differs from gestures, that communicate specific messages. With the assistance of those hand gestures, we can determine numbers, characters, etc using numerous algorithms that have numerous applications. With advances in computer vision technology, hand gesture communication is seeing loads of application in human-computer interaction. This paper presents a way to compare the performance of two algorithms for number identification using hand gesture recognition. Some modern systems use a hand gesture, mostly number of fingers raised within the region of Interest to perform various operations such as Play, Pause, seek forward, seek back word in a video player (for instance VLC media player) [1]. Other applications employing a vision system for hand gesture recognition are developed for multimedia system device management [2]. In recent years, several analysis groups have adopted machine-learning strategies to train models for classification, such as support vector machine [3], convolutional neural network (CNN) [4], recurrent neural network [5] and so on.

## II. LITERATURE REVIEW

Deepak K. Ray, et al. [1]: explains the use of hand

gesture recognition for controlling the VLC media player options such as play, pause etc. with the help of raised fingers detected.

S.G.Rayo [2]: explains the use of hand gesture recognition for managing multimedia devices using machine learning techniques.

T.-N. Nguyen, et al. [3]: shows the performance of support vector machines for classification problems such as hand gesture recognition for character and number identification.

Hung-Yuan Chung, et al. [4]: shows the performance of CNN for hand gesture recognition with the help of tracking of hand by kernelized correlation filters (KCF) algorithm.

Chigozie Enyinna Nwankpa, et al. [6]: explains the performance of CNN on various activation functions by comparing their accuracy and learning rates for the same dataset.

Guifang Lin, Wei Shen [7]: explains the performance of CNN by using the improved ReLU by varying hyperparameters.

Yanan Xu1, et al. [9]: explains the contour and convexity defects algorithm for hand gesture recognition by calculating the ratio of convex hull and contour area.

## III. PROPOSED METHOD

The project is divided into two algorithms first, the Convolutional Neural Networks (CNN) and the second is the Contour algorithm. In the first algorithm, the image is captured using the webcam and the dataset is created (Figure 1). After the creation of the dataset for all gestures, the model is trained. After the completion of training, the

prediction is performed using CNN and output is displayed on the screen. In the second algorithm the image is taken at runtime using the webcam and contour and convex hull are formed and with the help of convexity defects, the output is predicted and displayed on the screen.

#### A. Convolutional Neural Networks (CNN)

Convolutional Neural Networks are made of neurons which consists of weights and biases that can be learned. Every neuron receives many inputs, takes a weighted sum, pass it through the activation function and gives an output.

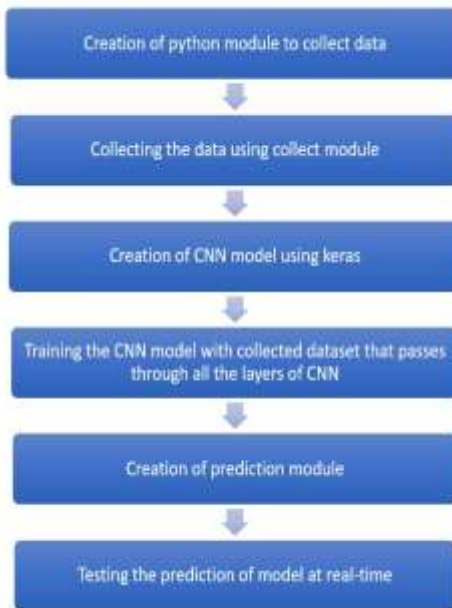


**Figure 1: Process Flow of CNN Algorithm**

There are four layers in Convolutional Neural Networks:

1. Convolution,
2. Activation Function Layer,
3. Pooling and
4. Full Connectedness (Fully Connected Layer).

#### 1) Convolution Layer

Convolution is used in image processing to classify images. This layer converts the images into a pixel matrix where the pixel is represented in the form of 1's and -1's (1 for image present in pixel and -1 for absence of image in pixel). The calculation in this layer takes place by multiplying the pixel value to the feature pixel and taking the summation and dividing by the total number of pixels in the feature [8].

#### 2) Activation Function Layer

Activation Functions are functions used in Neural Networks to compute the weighted sum of inputs and biases, which decides if a neuron can be fired or not [6]. It

manipulates the conferred knowledge through some gradient process typically gradient descent to produce output for the Neural Network, that contains the parameters within the knowledge. In this project the ReLU activation function and adam optimizer is used for image classification these are the most efficient [7].

$$RELU(x) = \begin{cases} 0 & \text{if } x < 0 \\ x & \text{if } x \geq 0 \end{cases}$$

#### 3) Pooling Layer

In this layer, the matrix which is given by the activation function layer is converted into a smaller size. In this layer the calculation takes place by selecting the reduced size of the matrix (generally 2 or 3). This reduced matrix is moved across the original matrix and the maximum value of the matrix is taken [8].

#### 4) Fully Connected Layer

This is the last layer of CNN. The input of this layer is the reduced matrix given by the pooling layer. In this layer, the matrix is converted into a flattened matrix like a list. The pattern of 1's and 0's of the flattened matrix is compared with the flattened matrix of the trained image matrix. The matching of both the matrix is compared with the probability and the output is given for the most probable input match [8].

#### B. Contour Algorithm

##### 1) Contour

The contour of the hand is defined as when the boundary pixels of the given gestures is connected to form a close figure of the hand space. Once we get the contour, it is used for further calculations in the algorithm for prediction of the gesture [9]. In Figure 2 we can see that the blue line around the hand gesture given through the webcam is the required contour.



**Figure 2: Contour Boundary of the Hand**

## 2) Convex Hull

The convex hull of hand gesture is the polygon formed by joining the end points of contour of the hand gesture [9], as shown in figure 3, the polygon formed by red curve boundary is the convex hull of hand gesture and green curve boundary is contour of the hand.

 **Contours**

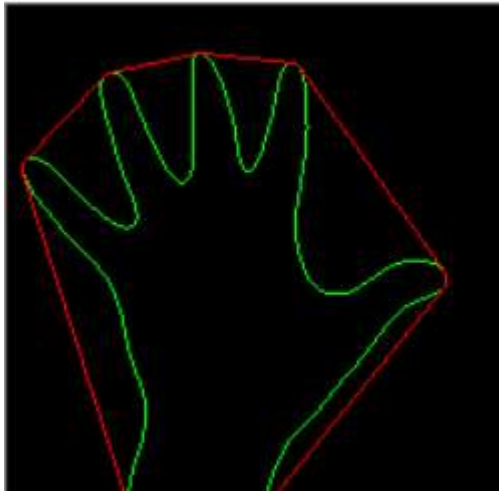


**Figure 3: Convex hull Boundary (Red) of Hand**

## 3) Convexity Defects

The convexity defect is defined as the difference in the area between the convex hull and contour. The area which is inscribed in the convex hull but not in the contour is defined as the convexity defect of the hand gesture [9]. In figure 4, the red spots are placed in the convexity defects that lie in between the contour area and hull area. In figure 4 as the number of fingers increases the red spots also increase with the formula of “no. of fingers - 1”, therefore if the number of fingers is 5 then the number of convexity defects are 4.

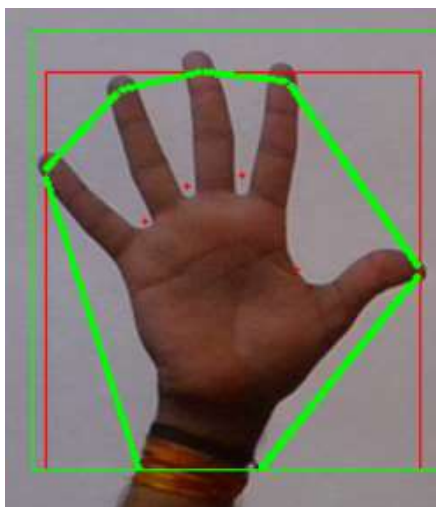


**Figure 4: Convexity defects of hand gesture at run time**

When the hand is placed in the Region of Interest (ROI), the contour and the convex hull is formed. The fingertips are identified. The angle is calculated between the contour and convex hull of the hand. If the angle is acute Convexity Defect is identified and red spots are placed in the defects (Figure 5). With the help of these red spots, the output is predicted and displayed on the screen (Table 1).



**Figure 5: Process Flow of Contour Algorithm**

No. of Convexity Defects	0	1	2	3	4
Predicted Output	One	Two	Three	Four	Five

**Table 1: Convexity Defects with corresponding output**

## IV. RESULTS AND DISCUSSION

The web camera captures the images of the hand gesture at the run time in both algorithms. After the hand is placed in the Region of Interest both the algorithms are initiated. In the CNN algorithm, the Region of Interest captures the images at the frames per second(fps) speed of the camera and convert them into an array and processes it through all the four layers of CNN and the hand gesture is detected and the desired number is predicted and displayed on the screen, whereas in Contour algorithm when the hand is put in the region of interest contour and the convex hull of the hand are formed and convexity defects are calculated. With the help of the number of convexity defects, the desired number is predicted and displayed on the screen. Figure 6 shows the

predicted number with the ROI using CNN algorithm whereas Figure 7 shows the predicted number with the ROI using the Contour algorithm.

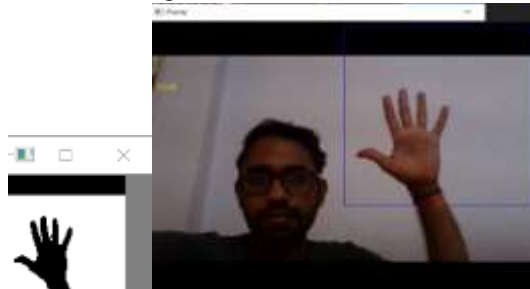
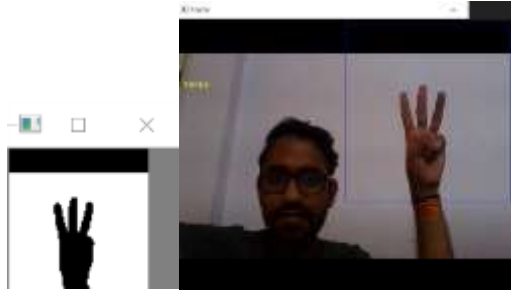


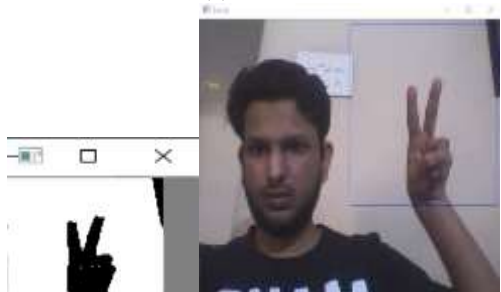
Figure 6: (a) Five



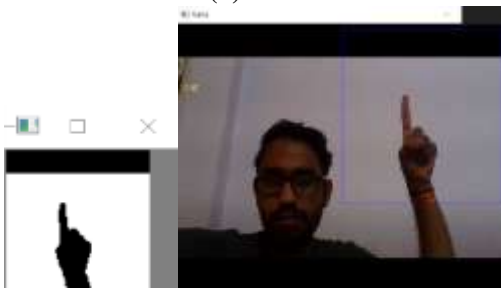
(b) Four



(c) Three



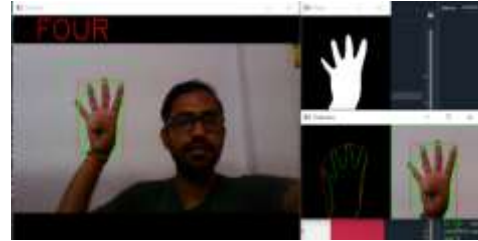
(d) Two



(e) One



Figure 7: (a) Five



(b) Four



(c) Three



(d) Two



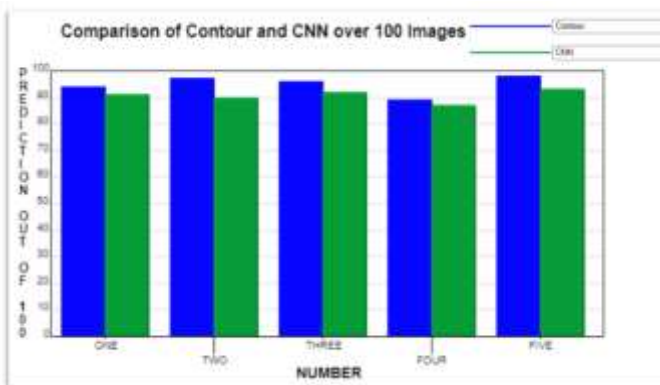
(e) One

Figure 8 and Table 2 shows the correct predictions of CNN and Contour algorithms over 100 images. The accuracy of CNN comes out to be around 91.2% and that of Contour is 93.8% which was calculated manually for every gesture by:

$$\text{Accuracy} = (\text{no. of correct predictions}) / (\text{no. of times (100) prediction done})$$

	One	Two	Three	Four	Five
Correct output by CNN out of 100 images	91	90	92	87	93
Correct output by Contour out of 100 images	94	97	96	99	98

**Table 2: Comparison of CNN and Contour over 100 images**



**Figure 8: Comparison of correct predictions of CNN and Contour over 100 images**

## V. CONCLUSION AND FUTURE WORK

The comparison presented in this paper between CNN and Contour algorithm shows that in less number of gestures the Contour algorithm has better accuracy than CNN whereas in more number of gestures the CNN has much better accuracy than Contour. The accuracy of CNN for less number of gestures can be improved by increasing the size of dataset. This project is working on the image currently, further development can lead to detecting the motion of the video sequence and assigning it to a meaningful sentence with TTS assistance. This project can also be further compared with various machine learning algorithms.

## REFERENCES

- [1] Deepak K. Ray, Mayank Soni, Prabhav Johri, Abhishek Gupta, "Hand Gesture Recognition using Python", International Journal on Future Revolution in Computer Science & Communication Engineering ISSN: 2454-4248 Volume: 4 Issue: 6.
- [2] S.G.Rayo, "Hand Gestures and Hand Movement Recognition for Multimedia Player Control", February 2008, unpublished thesis.
- [3] T.-N. Nguyen, D.-H. Vo, H.-H. Huynh, and J. Meunier, "Geometry-based static hand gesture recognition using support vector machine," In Proc. The 13th International Conference on Control Automation Robotics & Vision, Singapore, December 10–12, 2014.
- [4] Hung-Yuan Chung, Yao-Liang Chung, Wei-Feng Tsai, "An Efficient Hand Gesture Recognition System Based on Deep CNN," 2019 IEEE International Conference on Industrial Technology (ICIT).
- [5] T. Koizumi, M. Mori, S. Taniguchi, and M. Maruya, "Recurrent neural networks for phoneme recognition," In Proc. The Fourth International Conference on

Spoken Language Processing, PA, USA, October 3–6, 1996.

- [6] Chigozie Enyinna Nwankpa, Winifred Ijomah, Anthony Gachagan, and Stephen Marshall, "Activation Functions: Comparison of Trends in Practice and Research for Deep Learning", arXiv:1811.03378v1 [cs.LG] 8 Nov 2018.
- [7] Guifang Lin, Wei Shen, "Research on convolutional neural network based on improved Relu", 8th International Congress of Information and Communication Technology.
- [8] <https://www.edureka.co/blog/convolutional-neural-network/> (Date of access: 23rd March 2021)
- [9] Yanan Xu1, Dong-Won Park and GouChol Pok "Hand Gesture Recognition Based on Convex Defect Detection", International Journal of Applied Engineering Research ISSN 0973-4562 Volume 12, Number 18 (2017) pp. 7075-7079.

